

**mTORC2 in Dendritic Cells Restrains mTORC1-regulated Metabolic Activity and Their T Cell Stimulatory Function in Transplantation**

by

Alicia Rose Watson

B.S., State University of New York at Fredonia, 2012

Submitted to the Graduate Faculty of  
the School of Medicine in partial fulfillment  
of the requirements for the degree of  
Doctor of Philosophy

University of Pittsburgh

2018

UNIVERSITY OF PITTSBURGH

School of Medicine

This dissertation was presented

by

Alicia Rose Watson

It was defended on

October 17, 2018

and approved by

Marie C. DeFrances, M.D., Ph.D, Department of Pathology

Alejandro Soto-Gutierrez, M.D., Ph.D, Department of Pathology

Hēth R. Turnquist, Ph.D, Department of Immunology

Greg M. Delgoffe, Ph.D, Department of Immunology

Dissertation Director: Angus W. Thomson, Ph.D, D.Sc, Department of Surgery

Copyright © by Alicia Rose Watson

2018

## **mTORC2 in Dendritic Cells Restrains T Cell Stimulatory Function in Transplantation and mTORC1-regulated Metabolic Function**

Alicia Rose Watson, Ph.D.

University of Pittsburgh, 2018

Mechanistic target of rapamycin (mTOR) complexes (C) 1 and 2 play important roles in determining the differentiation and function of immune cells. While suppression of mTORC1 antagonizes dendritic cell (DC) maturation and suppresses graft rejection, the role of mTORC2 in DC in determining host responses to transplanted tissue is undefined. Utilizing an innovative mouse model in which mTORC2 was deleted specifically in CD11c<sup>+</sup> DC (TORC2<sup>DC-/-</sup>), we show that transplantation of minor histocompatibility (m-Ag) antigen (HY)-mismatched skin grafts from TORC2<sup>DC-/-</sup> donors into wild-type recipients results in accelerated rejection, characterized by enhanced CD8<sup>+</sup> T cell responses in the graft and regional lymphoid tissue. Augmented CD8<sup>+</sup> T cell responses were also observed in skin grafts from TORC2<sup>DC-/-</sup> B6 donors into major histocompatibility (MHC) mismatched BALB/c recipients, and in a delayed-type hypersensitivity model in which mTORC2 was absent in cutaneous DC. These responses could be ascribed to an increased T cell stimulatory phenotype of TORC2<sup>DC-/-</sup> and not to enhanced lymph node homing of the cells. These findings suggest mTORC2 in skin DC plays an important role in initiation of rejection and restrains effector CD8<sup>+</sup> T cell responses. In addition, we describe a novel metabolic regulatory role of mTORC2 in DC, whereby mTORC2 restrains glycolytic bias and mitochondrial dysfunction by regulating mTORC1-driven metabolic function. These studies have implications for understanding the impact of conventional and new generation mTOR inhibitors that target mTORC2 in the multiple clinical contexts, including transplantation and cancer therapeutics.

## Table of Contents

Preface.....	xv
<b>1.0 Introduction.....</b>	<b>1</b>
<b>1.1 Dendritic Cell (DC) Biology.....</b>	<b>1</b>
1.1.1 Function.....	1
1.1.2 Activation and maturation .....	2
1.1.3 Antigen (Ag) acquisition, processing, and presentation .....	3
1.1.4 DC subsets.....	4
<b>1.2 DC activation of adaptive immune responses .....</b>	<b>6</b>
1.2.1 Lymph node (LN) homing .....	6
1.2.2 T cell activation.....	7
1.2.3 T cell polarization .....	8
<b>1.3 Organ Transplantation .....</b>	<b>10</b>
1.3.1 Pharmacological immunosuppressants .....	10
1.3.2 Cell therapy in transplantation .....	12
1.3.3 Limitations of current immunosuppressive regimens .....	13
<b>1.4 mTOR Signaling in DC .....</b>	<b>14</b>
1.4.1 mTORC1.....	14
1.4.1.1 Upstream activators.....	14
1.4.1.2 Regulation of cell growth .....	15
1.4.1.3 Regulation of immune function .....	15
1.4.1.4 Regulation of metabolism.....	15

1.4.2	mTORC2.....	16
1.4.2.1	Upstream activators and downstream targets .....	16
1.4.2.2	Regulation of immune function .....	17
1.4.3	Interplay between mTORC1 and mTORC2.....	18
1.5	Metabolic Regulation of Dendritic Cell Function.....	19
1.5.1	Aerobic glycolysis .....	19
1.5.2	Lipid metabolism .....	20
1.5.3	Metabolic targeting in transplantation.....	22
1.6	DC-Specific mTORC2 Knockout Mouse Model.....	23
1.7	Murine Models of Transplantation.....	23
1.7.1	Skin grafting .....	23
1.7.1.1	Major histocompatibility (MHC) mismatch model.....	24
1.7.1.2	Minor histocompatibility Ag (m-Ag) mismatch models.....	24
1.7.2	Heterotopic heart transplantation .....	25
2.0	Statement of the Problem .....	27
3.0	mTORC2 Deficiency in Passenger DC Accelerates Graft Rejection .....	29
3.1	Introduction .....	29
3.2	Methods .....	30
3.2.1	Mice.....	30
3.2.2	Heterotopic heart transplantation and rejection grading .....	31
3.2.3	Skin grafting and rejection grading.....	33
3.2.4	Immunohistochemistry and immunofluorescence .....	33

3.2.5	Mixed leukocyte reaction (MLR), skin-resident leukocyte isolation, and flow cytometry .....	34
3.2.6	Statistical analyses .....	35
3.3	Results.....	36
3.3.1	TORC2 <sup>DC-/-</sup> cervical HHT donors have decreased graft function over time and increased cell infiltrate as compared to Ctrl HHT donors.....	36
3.3.2	HY-mismatched skin grafts from TORC2 <sup>DC-/-</sup> donors exhibit more severe rejection.....	37
3.3.3	HY-mismatched skin grafts from TORC2 <sup>DC-/-</sup> donors elicit enhanced CD8 <sup>+</sup> T cell graft infiltration as compared to WT Ctrl donors .....	41
3.3.4	HY-mismatched skin grafts from TORC2 <sup>DC-/-</sup> donors exhibit enhanced CD8 <sup>+</sup> PD-1 <sup>+</sup> T cell infiltrate compared with grafts from WT donors .....	43
3.3.5	Skin grafts from TORC2 <sup>DC-/-</sup> donors elicit enhanced CD8 <sup>+</sup> T effector cell responses in regional LN and augmented IFN $\gamma$ and IL-2 production in response to donor Ag stimulation .....	45
3.3.6	MHC-mismatched skin grafts from TORC2 <sup>DC-/-</sup> donors do not exhibit significantly accelerated rejection but do show evidence of rejection earlier than grafts from Ctrl donors.....	47
3.3.7	MHC-mismatched skin grafts from TORC2 <sup>DC-/-</sup> donors do not elicit enhanced CD8 <sup>+</sup> T cell infiltration compared with grafts from WT Ctrl donors .	49
3.3.8	MHC-mismatched skin grafts from TORC2 <sup>DC-/-</sup> donors elicit enhanced number of CD8 <sup>+</sup> and CD8 <sup>+</sup> PD-1 <sup>+</sup> T cells in draining LN compared with grafts from WT donors .....	51

3.3.9	MHC-mismatched skin grafts from TORC2 <sup>DC-/-</sup> donors elicit enhanced proliferation of CD8 <sup>+</sup> T cells in draining LNs and augmented IFN $\gamma$ and Granzyme-B production in response to donor Ag .....	53
3.3.10	Skin graft rejection is not affected in TORC2 <sup>DC-/-</sup> recipients .....	55
3.3.11	OVA <sub>tg</sub> skin grafts in TORC2 <sup>DC-/-</sup> recipients do not exhibit enhanced T cell infiltrates.....	57
3.4	Discussion .....	61
4.0	DC-Specific mTORC2 Deletion Augments Cell-Mediated Delayed Type Hypersensitivity (DTH) Responses.....	65
4.1	Introduction .....	65
4.2	Methods .....	66
4.2.1	Mice.....	66
4.2.2	DTH assay .....	66
4.2.3	Immunohistochemistry and Immunofluorescence .....	66
4.2.4	Statistical analyses .....	67
4.3	Results.....	67
4.3.1	TORC2 <sup>DC-/-</sup> mice exhibit enhanced cutaneous DTH responses .....	67
4.4	Discussion .....	69
5.0	Cutaneous DC Deficient in mTORC2 Do Not Display Defects in Migration or Lymph Node Homing.....	70
5.1	Introduction .....	70
5.2	Methods .....	71
5.2.1	Mice.....	71

5.2.2	<i>In vivo</i> migration assay.....	71
5.2.3	Flow cytometry .....	71
5.2.4	Statistical analyses .....	72
5.3	Results.....	72
5.3.1	TORC2 <sup>DC-/-</sup> mice do not exhibit alterations in skin DC migration, but display a more pro-stimulatory DC phenotype than WT Ctrl mice.....	72
5.4	Discussion .....	74
6.0	mTORC2 Restrains mTORC11-Regulated Metabolic Function in DC .....	76
6.1	Introduction .....	76
6.2	Methods .....	78
6.2.1	Mice.....	78
6.2.2	Bone marrow-derived DC generation .....	78
6.2.3	Extracellular flux assay.....	79
6.2.4	ATP production assay .....	80
6.2.5	Mitochondrial staining and flow cytometry .....	80
6.2.6	Golgi staining and confocal microscopy .....	80
6.2.7	Transmission electron microscopy (TEM).....	81
6.2.8	NanoString gene profiling.....	81
6.2.9	Quantitative PCR .....	82
6.2.10	Statistical analyses .....	82
6.3	Results.....	83
6.3.1	TORC2 <sup>DC-/-</sup> have augmented glycolytic activity, glycolysis-dependent ATP production and viability compared to Ctrl DC .....	83

6.3.2 TORC2 <sup>DC-/-</sup> have increased spare respiratory capacity (SRC), mitochondrial biomass and mitochondria that fail to depolarize following LPS stimulation.....	85
6.3.3 TORC2 <sup>DC-/-</sup> display more compact Golgi stacks with less perinuclear localization as compared to Ctrl DC.....	88
6.3.4 Inhibition of mTORC1 activity in TORC2 <sup>DC-/-</sup> leads to loss of their enhanced spare respiratory capacity and glycolysis .....	90
6.3.5 TORC2 <sup>DC-/-</sup> exhibit a distinct gene expression profile from Ctrl DC .....	92
6.4 Discussion .....	94
7.0 Final Discussion and Biomedical Relevance .....	99
7.1 mTORC2 Restrains DC Function and mTORC1 Regulated Metabolic Control	99
7.2 mTORC2 Targeting in Transplantation and Cancer Immunotherapy .....	102
7.3 Future Directions.....	104
Appendix .....	106
Bibliography .....	113

## List of figures

Figure 1. Overview of mitochondrial metabolism.....	21
Figure 2. TORC2 <sup>DC-/-</sup> cervical HHT donors have decreased graft function over time and increased cell infiltrate as compared to Ctrl HHT donors. ....	37
Figure 3. HY-mismatched skin grafts from TORC2 <sup>DC-/-</sup> donors exhibit more severe rejection. ..	39
Figure 4. HY-mismatched skin grafts from TORC2 <sup>DC-/-</sup> donors exhibit vacuolar damage and diskeratosis at POD 7, and reduced CD3 <sup>+</sup> cell numbers and more severe collagen degradation at POD 14 compared to grafts from WT donors.....	40
Figure 5. HY-mismatched skin grafts from TORC2 <sup>DC-/-</sup> donors elicit enhanced CD8 <sup>+</sup> T cell infiltration compared with grafts from WT Ctrl donors. ....	42
Figure 6. HY-mismatched skin grafts from TORC2 <sup>DC-/-</sup> donors exhibit enhanced CD8 <sup>+</sup> PD-1 <sup>+</sup> T cell infiltrate compared with grafts from WT donors. ....	44
Figure 7. HY-mismatched skin grafts from TORC2 <sup>DC-/-</sup> donors elicit enhanced numbers of CD8 <sup>+</sup> T cells in draining LNs and augmented IFN $\gamma$ and IL-2 production in response to donor Ag stimulation.....	46
Figure 8. MHC-mismatched skin grafts from TORC2 <sup>DC-/-</sup> donors do not exhibit significantly accelerated rejection but do show evidence of rejection earlier than grafts from Ctrl donors. ....	48
Figure 9. MHC-mismatched skin grafts from TORC2 <sup>DC-/-</sup> donors do not elicit enhanced CD8 <sup>+</sup> T cell infiltration compared with grafts from WT Ctrl donors.....	50
Figure 10. MHC-mismatched skin grafts from TORC2 <sup>DC-/-</sup> donors elicit enhanced number of CD8 <sup>+</sup> and CD8 <sup>+</sup> PD-1 <sup>+</sup> T cells in draining LN compared with grafts from WT donors. ....	52

Figure 11. MHC-mismatched skin grafts from TORC2 <sup>DC-/-</sup> donors elicit enhanced proliferation of CD8 <sup>+</sup> T cells in draining LNs and augmented IFN $\gamma$ and IL-2 production in response to donor Ag (B6) stimulation. ....	54
Figure 12. Skin graft rejection is not affected in TORC2 <sup>DC-/-</sup> recipients. ....	56
Figure 13. OVA <sub>Ag</sub> skin grafts in TORC2 <sup>DC-/-</sup> recipients do not elicit augmented T cell infiltration into the graft. ....	58
Figure 14. OVA <sub>Ag</sub> skin grafts in TORC2 <sup>DC-/-</sup> recipients do not enhance T cell numbers in the regional LNs and, in response to donor antigen, these T cells do not produce increased IL-2 or IL-4 compared to WT recipients. ....	59
Figure 15. TORC2 <sup>DC-/-</sup> B6 mice show no significant differences in immune cell populations compared with WT B6 Ctrl mice. ....	60
Figure 16. TORC2 <sup>DC-/-</sup> mice exhibit enhanced delayed-type hypersensitivity responses .....	68
Figure 17. TORC2 <sup>DC-/-</sup> mice do not exhibit enhanced skin DC migration to regional LN, but display reduced B7-H1 (PD-L1) expression on DC compared with WT control mice .....	73
Figure 18. TORC2 <sup>DC-/-</sup> have augmented glycolytic activity, glycolysis-dependent ATP production, and viability as compared to Ctrl DC .....	84
Figure 19. Quiescent non-stimulated TORC2 <sup>DC-/-</sup> display augmented viability following LPS stimulation, but no difference in initial glycolytic function following stimulation as compared to Ctrl DC. ....	85
Figure 20. TORC2 <sup>DC-/-</sup> have increased SRC, mitochondrial biomass, and mitochondria which fail to depolarize following LPS stimulation .....	87
Figure 21. TORC2 <sup>DC-/-</sup> display more compact Golgi stacks with less perinuclear localization as compared to Ctrl DC .....	89

Figure 22. Inhibition of mTORC1 in TORC2<sup>DC-/-</sup> leads to loss of their enhanced spare respiratory capacity and glycolysis ..... 91

Figure 23. TORC2<sup>DC-/-</sup> exhibit a distinct gene expression profile from Ctrl DC..... 93

Figure 24. Proposed signaling mechanism of mTORC1 regulation by mTORC2 ..... 98

## Preface

First and foremost, I would like to thank my mentor Dr. Angus Thomson. Aside from being patient, supportive, and encouraging of me pursuing new avenues of investigation for his lab, he also showed me what a mentor should be—and for that I will always be grateful. I would also like to thank past and present lab members, especially Dalia Raich-Regué, for teaching me how to be an immunologist, and Helong Dai for being my partner in crime and most-valued surgeon scientist for these past few years. My committee members have provided critical insights into these studies over the years, and have also fostered my growth as a scientist. Finally, I would like to acknowledge my family away from the lab—my fiancée Rachel, who has been my rock through all of this, and our veritable zoo of adopted animals for all of their uncertified emotional support.

## 1.0 Introduction

### 1.1 Dendritic Cell (DC) Biology

#### 1.1.1 Function

Dendritic cells (DC) are specialized immune cells that function as the bridge between innate and adaptive immunity. Arising from either myeloid or lymphoid progenitors in the bone marrow, DC reside in tissues and ingest pathogens, cellular debris, and intact cells. DC process and present the digested products as peptide antigens (Ag) to adaptive immune cells within lymphoid tissues. DC are critical professional Ag-presenting cells (APC) for adaptive T cell responses, as DC are the only cell type which can activate naïve T cells<sup>1</sup>.

DC can instigate both inflammatory and regulatory adaptive responses. For example, DC presenting exogenous Ag in the context of bacterial infection will elicit inflammatory cluster of differentiation 4 (CD4)<sup>+</sup> T helper (Th) and CD8<sup>+</sup> cytotoxic T cell (CTL) responses which will ultimately clear the infection by destroying any cells which are displaying the cognate Ag of their T cell receptor (TCR). Conversely, DC can activate regulatory T cells (T<sub>reg</sub>) which serve to dampen inflammatory T cell responses following clearance of exogenous Ag, or DC presenting endogenous Ag processed from “self” can prevent T cell killing of self cells, as seen in various autoimmune disorders<sup>2</sup>.

### 1.1.2 Activation and maturation

DC can be activated by many different danger signals, which fall under two categories: pathogen-associated molecular patterns (PAMPs) and danger-associated molecular patterns (DAMPs). PAMPs and DAMPs will be recognized by various pattern recognition receptors (PRRs) on DC, and initiate their differentiation and maturation into immunogenic APCs<sup>3</sup>.

PAMPs recognized by DC PRRs can come from bacteria, viruses, fungi, and protozoa, and can be nucleic acids, lipoproteins, glycoproteins, and membrane components. PRRs that recognize PAMPs include toll-like receptors (TLRs), retinoid acid-inducible gene 1 (RIG-1) receptors, and nucleotide-binding oligomerization domain (NOD)-like receptors. Activated PRRs will activate intracellular signaling cascades ultimately leading to the production of cytokines, chemokines/chemokine receptors, cell adhesion molecules, and co-stimulatory molecules which will allow the DC to migrate to lymphoid tissues and direct the adaptive immune response against the invading pathogen<sup>3</sup>.

Unlike PAMPs, DAMPs are endogenously derived molecules, which can arise from tissues that are stressed or damaged in response to sterile traumas such as ischemic injury or cancer. DAMPs can be proteins such as high mobility box group 1 (HMGB1), cytoplasmic S100 proteins, and heat shock proteins (HSPs), or non-proteins such as nucleic acids or adenosine triphosphate (ATP). DAMPs are recognized by DC via TLRs or the receptor for advanced glycation end products (RAGE). Following DAMP activation of DC, mitogen-activated protein kinases (MAPKs), nuclear factor kappa-light-chain-enhancer of activated B cells (NF- $\kappa$ B), and the phosphoinositide 3 kinase/protein kinase B (PI3K/Akt) signaling pathways will become activated, all of which are potent mediators of inflammatory cell death/survival responses and will induce cytokine, chemokine, and co-stimulatory molecule expression similar to PAMPs<sup>3</sup>.

### 1.1.3 Antigen (Ag) acquisition, processing, and presentation

DC activation leads to the upregulation of cell adhesion molecules and chemokine receptors which will allow the DC to migrate to lymphoid tissue, as well as co-stimulatory molecules and cytokines which will ultimately assist in shaping adaptive T cell responses. However, DC must also acquire, process, and present Ag peptide to T cells to initiate their activation.

DC acquire exogenous cell-associated Ag via phagocytosis. This process involves the uptake of particulates within the cell membrane envelope, followed by a sequence of fusion and fission events between the plasma membrane and intracellular vesicles to form phagosomes, which will ultimately fuse with lysosomes, culminating in phagolysosome formation. This sequence of events occurs in progressively more acidic conditions with acidic pH-optimum cathepsin proteases, which will lead to digestion of the exogenous Ag<sup>4,5</sup>. DC can also acquire soluble exogenous Ag via receptor-mediated endocytosis, such as mannose receptor-mediated endocytosis of mannoseylated proteins<sup>6</sup>, which will be degraded similarly to phagocytosed Ag. Finally, DC can degrade endogenous Ag following translocation to the endoplasmic reticulum (ER) from the cytosol by the Transporter associated with Ag Processing (TAP) via proteolysis in the proteasome. The proteasome is a barrel-shaped structure consisting of a 20S core capped on each end by a 19S multi-subunit complex which has unfoldase activity to allow proteins to enter the barrel structure and be cleaved by the proteolytic  $\beta$  subunits of the 20S core<sup>7</sup>.

Following Ag acquisition, DC will process Ag into peptide for presentation on major histocompatibility complexes (MHC, in mice; human leukocyte Ag [HLA], in humans). The traditional view of Ag presentation was that intracellularly synthesized Ag (such as from viruses, tumors, or “self”) were processed for MHC Class I (MHCI) presentation via proteasomes, while exogenous Ag was processed for MHC Class II (MHCII) presentation via lysosomes. However,

it is now appreciated that unlike other APC, DC also frequently “cross-present” Ag; i.e. exogenous Ag acquired by DC can be processed and loaded onto MHCI, and endogenous Ag can be processed and loaded onto MHCII. Cross-presented Ag can be acquired from apoptotic cells<sup>8</sup>, necrotic cells<sup>9</sup>, and live cells<sup>10</sup>. Ag cross-presentation is vital for instigating CTL responses against exogenous pathogens<sup>11</sup>.

#### **1.1.4 DC subsets**

Since Ralph Steinman first identified the population of stellate splenocytes he named “dendritic cells” in 1973<sup>12</sup>, not only has the biological relevance of these cells been established, but many different subsets of DC have been identified. These subsets, while all sharing the ability to stimulate T cell activation, differ in their localization and immune function, and include classical DC (cDC), plasmacytoid DC (pDC), and monocyte-derived DC (moDC).

cDC can reside in both lymphoid and non-lymphoid tissue (such as the skin), with lymphoid cDC characterized by CD8 $\alpha$  expression<sup>13,14</sup> and non-lymphoid cDC being characterized by CD103 expression<sup>15,16</sup>. Additionally, heterogeneous populations of CD11b<sup>+</sup> cDC can reside in both lymphoid and non-lymphoid tissues, with CD11b<sup>+</sup> cDC being the most abundant DC population in all lymphoid tissues except the thymus. Development of both CD8 $\alpha$ <sup>+</sup> and CD103<sup>+</sup> cDC (but not CD11b<sup>+</sup> cDC) is orchestrated by the transcription factors inhibitor of DNA binding 2 (Id2), nuclear factor interleukin 3 regulated (NFIL3), basic leucine zipper ATF-like 3 transcription factor (BATF3), and interferon regulatory factor 8 (IRF8)<sup>17-21</sup>. Functionally, CD8 $\alpha$ <sup>+</sup> and CD103<sup>+</sup> cDC are superior cross-presenters of exogenous Ag on MHCI to CD8<sup>+</sup> T cells<sup>22,23</sup>. In addition, TLR stimulation of CD8 $\alpha$ <sup>+</sup> and CD103<sup>+</sup> cDC induces production of the inflammatory cytokine active heterodimeric interleukin 12 (IL-12p70)<sup>24</sup>. Development of

CD11b<sup>+</sup> cDC is regulated by the transcription factors Relb, neurogenic locus notch homolog protein 2 (NOTCH2), recombining binding protein suppressor of hairless (RBP-J), IRF4, and IRF8<sup>25-29</sup>. The exact functions of the heterogeneous population of CD11b<sup>+</sup> cDC have yet to be well defined, but they have been shown to induce more CD4<sup>+</sup> T cell immune responses in comparison with CD8<sup>+</sup> cDC<sup>30</sup>.

pDC can be found in peripheral tissues and circulating blood, and their development is regulated by immunoglobulin transcription factor 2 (ITF-2), which suppresses Id2 expression necessary for cDC development<sup>31,32</sup>. Functionally, pDC are uniquely capable of rapidly producing copious amounts of type I interferons in response to viral infection<sup>33,34</sup>.

moDC originate from monocyte progenitors generated from inflammation within lymphoid and non-lymphoid tissues<sup>35</sup>. Although similar phenotypically to cDC, moDC also express the monocyte markers CD64 and Fc-gamma receptor 1 (FcγR1). While monocytes have long been used to generate ex vivo DC from peripheral blood and bone marrow in the presence of IL-4 and granulocyte-macrophage-colony stimulating factor (GM-CSF)<sup>36</sup>, the in vivo equivalent of these cells is ill defined.

DC can also be localized to specific organs, such as Langerhans cells (LC) and dermal DC within the skin. LC are a population of epidermis-restricted mononuclear phagocytes, which express langerin (CD207). LC express MHCII and are capable of stimulating T cells in a mixed leukocyte reaction (MLR), and were thought to be prototypical of tissue-resident DC which could migrate to draining lymph nodes (dLN) and prime naïve T cell responses<sup>37</sup>. However, gene expression profiling and cell lineage tracing point to LC being more closely related to tissue-resident macrophages, as does the lack of direct evidence that LC can prime naïve T cell responses in vivo<sup>38-40</sup>. Dermal DC comprise of LC migrating to cutaneous dLN, as well as four

cDC populations: CD103<sup>+</sup>CD207<sup>+</sup>, CD103<sup>-</sup>CD207<sup>+</sup>, CD207<sup>-</sup>CD11b<sup>+</sup>, and CD103<sup>-</sup>CD207<sup>-</sup>CD11b<sup>-</sup><sup>41</sup>. While the exact function of each of these subsets is currently unknown, they do share similar function and gene expression to other CD11b<sup>+</sup> cDCs, as well sharing efficient MHCII Ag presentation and a dependence on C-C chemokine receptor type 7 (CCR7)-mediated migration to cutaneous LN<sup>23,41,42</sup>.

## **1.2 DC Activation of Adaptive Immune Responses**

### **1.2.1 Lymph node (LN) homing**

The key function of DC is to present Ag to T cells in order to elicit adaptive immune responses. DC constitutively acquire Ag and travel to peripheral lymphoid tissue via lymphatic vessels, where they can present “self” or “non-self” Ag to T cells, contributing to peripheral tolerance or instigating an inflammatory response, respectively<sup>43</sup>. Non-inflammatory DC will enter primary, secondary, and tertiary LN directly from non-lymphoid tissue; however, inflammatory DC will enter the primary LN proximal to the site of inflammation. The inflammatory DC are then positioned to interact with naïve T cells entering the LN from high endothelial venules (HEV) in the paracortical T cell zone. While the inflammatory DC do not migrate beyond the primary LN, the T cells they activate will divide and egress from primary to tertiary LN and beyond to the site of inflammation<sup>44</sup>.

Upon activation, DC undergo a number of changes, which program them to mobilize from the site of Ag uptake to the T cell zone of the dLN. In the skin, fibroblasts, keratinocytes, and DC will produce tissue necrosis factor  $\alpha$  (TNF $\alpha$ ) and IL-1 family cytokines, which are

essential in the reduction of E-cadherin expression. Abrogating E-cadherin dissociates LC from keratinocytes, and coincides with upregulation of the chemokine CCR7<sup>45,46</sup>. TNF $\alpha$  also increases the expression of the CCR7 ligands CCL21-Ser (serine) and CCL21-Leu (leucine) in the lymphatic vessels. In addition, activated LC produce matrix metalloproteases (MMP), which degrade basement membranes and collagen, and permit LC to migrate through the epidermal basal membrane and the dermis, in conjunction with C-X-C motif chemokine ligand 12 (CXCL12) and cognate CCR4 signaling<sup>47,48</sup>. Upon entering the LN, DC will localize to the subcapsular zone before migrating to the paracortical T cell zone<sup>44</sup>.

### **1.2.2 T cell activation**

Once DC migrate into the T cell zone, they will present Ag to T cells, ultimately leading to T cell polarization and clonal expansion, such that each T cell is specific for the same MHC-Ag complex. This can be endogenously processed Ag presented on MHCI, exogenously processed Ag presented on MHCII, or cross-presented endogenous Ag on MHCII/exogenous Ag on MHCI. MHC-peptide presented by DC provides the first of three signals (Signal 1) required for T cell activation when it is bound by cognate T cell receptor (TCR), with TCRs on CD8<sup>+</sup> T cells recognizing MHCI-Ag and TCRs on CD4<sup>+</sup> T cells recognizing MHCII-Ag. MHC-Ag recognition occurs in the polymorphic  $\alpha$  and  $\beta$  chains of the TCR, while the non-polymorphic CD3 complex of the TCR drives the signaling cascades required for activation<sup>2</sup>.

The second signal for T cell activation (Signal 2) is provided by co-stimulatory/inhibitory molecules on DC binding their respective ligands/receptors on the T cell. The T cell co-stimulatory/inhibitory receptors can either be members of the immunoglobulin (Ig) superfamily, or the TNF receptor superfamily. One such interaction is the binding of constitutively expressed

CD28 (Ig superfamily) on T cells to the ligands CD86 and CD80 on the DC. This initiates a signaling cascade that will ultimately drive Akt activity and promote cell survival/inhibit cell death pathways within the T cell<sup>49</sup>. In addition to activating T cells, co-stimulatory signaling between T cells and DC will also further activate DC, such as CD40L on T cells engaging CD40 on DC driving IL-12 cytokine production by DC<sup>50</sup>. This crosstalk will elicit cytokine production by DC necessary for the third signal of T cell activation (Signal 3), which is integral for T cell lineage polarization.

### **1.2.3 T cell polarization**

Upon activation, CD4<sup>+</sup> T cells differentiate into functionally distinct effector (Th) cell populations or T<sub>reg</sub>, which is dependent on the co-stimulatory/inhibitory Signal 2 and cytokine Signal 3 provided by DC; CD8<sup>+</sup> T cells generally have less plasticity and will differentiate into CTLs or memory T cells. There are three major Th subsets: Th1, Th2, and Th17, although other subsets such as Th9, Th22, and T follicular helper cells (T<sub>fh</sub>) have also been identified. Th cells play a central role in immune responses by helping B cells produce antibodies (Ab), inducing macrophage activity, and recruiting neutrophils<sup>51</sup>, basophils, and eosinophils to sites of inflammation/injury<sup>52</sup>.

Th1 polarization is initially induced by DC production of the cytokines IL-12, type I interferons (IFN) and IFN $\gamma$ , with IFN $\gamma$  also acting to inhibit Th2 cell proliferation<sup>53</sup>. Additionally, IFN $\gamma$  also induces the activation of T-bet, the main regulator of Th1 differentiation<sup>54</sup>. Functionally, Th1 cells mediate responses to intracellular pathogens, and have also been identified to induce some autoimmune diseases. The principally release the cytokines IFN $\gamma$  and IL-2<sup>52</sup>.

While DC are not thought to produce the Th2 polarizing cytokine IL-4<sup>55</sup>, there is evidence that DC presenting OX40-ligand and Jagged 1 promote Th2 polarization<sup>56</sup>. Conversely, CD103<sup>+</sup> DC producing IL-12 have recently been shown to suppress Th2 responses<sup>57</sup>. It has also been postulated that Th2 is the “default” Th programming, occurring in the absence of Th1 and Th17 polarizing stimuli<sup>58</sup>. While the exact roles DC play in Th2 induction are not yet clear, it is known that IL-4 and IL-2 are essential cytokines in Th2 polarization, through the upregulation of the transcription factor GATA binding protein 3 (GATA3)<sup>59</sup>. Functionally, Th2 cells mount immune responses against extracellular pathogens such as helminthes, as well facilitate tissue repair by secreting IL-4 and IL-13, which are integral for the production of collagen I and III<sup>60</sup>.

Th17 polarization is driven by the cytokines transforming growth factor  $\beta$  (TGF $\beta$ ), IL-6, IL-21, and IL-23, with TGF $\beta$  and IL-6 being responsible for initial polarization and IL-23 being crucial for robust Th17 responses. TGF $\beta$  and IL-21 act synergistically to induce expression of the transcription factor retinoic acid receptor-related orphan receptor  $\gamma$ -t (ROR $\gamma$ t), which drives expression of the signature Th17 cytokine IL-17<sup>61</sup>. Functionally, Th17 cells mount immune responses against bacteria and fungi and recruit neutrophils via their IL-17 production, creating a general state of tissue inflammation<sup>62</sup>. Th17 cells are also thought to be critical to the development of autoimmunity<sup>61</sup>.

Unlike effector Th cells and CTLs, Treg serve to suppress, rather than antagonize, immune responses. While thymic DC can contribute to Treg generating during T cell development to induce central tolerance against self Ag, they can also induce Treg in the periphery to control immune responses to non-self Ag. While many subsets of Treg have been identified, their generation by DC is largely mediated by IL1-, IL-27, TGF $\beta$ , indoleamine 2,3-dioxygenase (IDO), retinoic acid, and vitamin D3. Forkhead box P3<sup>+</sup> (Foxp3<sup>+</sup>) Treg are one of

the subpopulations of Treg that are critically important for maintaining immune tolerance and preventing autoimmunity<sup>63</sup>. Functionally, Treg can suppress immune responses by producing inhibitory cytokines such as IL-10 and TGF $\beta$ , cytolysis of effector T cells, IL-2 cytokine deprivation of effector T cells, and suppressing DC maturation via cytotoxic T-lymphocyte antigen-4 (CTLA4) engagement of CD80/86 or lymphocyte-activated gene 3 (LAG3) engagement of MHCII<sup>64</sup>.

### **1.3 Organ Transplantation**

#### **1.3.1 Pharmacological immunosuppressants**

Organ transplantation is a life-saving procedure for patients with organ failure. Historically, there had been many unsuccessful attempts to transplant various organs from both other humans and animals to patients with organ failure, the first of which was xenotransplantation of goat and pig kidney into to patients performed by Mathieu Jaboulay in 1906<sup>65</sup>. While Jaboulay did develop the basic vascular anastomosis technique that was critical for successful organ transplantation, he (nor anyone at the time) did not understand the importance of immune tolerance of transplanted organs.

There are now currently many pharmacological agents used in transplantation to both induce and maintain tolerance. These include: the calcineurin inhibitors (CNIs) cyclosporine and tacrolimus; the mechanistic target of rapamycin (mTOR) inhibitors rapamycin (RAPA, or sirolimus) and RAPAlogs such as everolimus; mycophenolic acid, a guanosine nucleotide synthesis inhibitor; and biological agents such as antibody (Ab)-based therapies like basiliximab

(anti-CD25) and alemtuzumab (anti-CD52), and fusion proteins like belatacept. These agents are usually given as a combination regimen, along with anti-inflammatory steroids<sup>66</sup>.

CNIs inhibit T cell proliferation by preventing T cell activation. The rate-limiting step in T cell activation following TCR ligation is activity of the serine-threonine phosphatase calcineurin. Cyclosporine inhibits this phosphatase by complexing with cyclophilin. Tacrolimus inhibits calcineurin by complexing with the 12 kDa FK506 binding protein (FKBP12). Generally, tacrolimus is a more potent immunosuppressant than cyclosporine<sup>67</sup>.

RAPA and RAPAlogs inhibit mTOR, a central nutrient-sensing kinase that regulates cell growth, proliferation, protein synthesis and ribogenesis. Therefore, RAPA is able to inhibit cell proliferation/activation responses such as T cell proliferation in response to IL-2. It is important to note that the effects of RAPA are not restricted to lymphocytes<sup>68</sup>.

MPA prevents the de novo synthesis of the guanosine nucleotide by inhibiting its requisite enzyme, inosine monophosphate dehydrogenase. This effectively blocks cell proliferation by preventing nucleotide synthesis. MPA is lymphocyte-specific, as lymphocytes are the only cell type to not have alternate guanosine synthesis pathways. MPA is not as potent an immunosuppressant as CNIs or RAPA<sup>69</sup>.

Ab-based therapies are often used as induction therapies, i.e. perioperatively or prophylactically. While anti-thymocyte globulins (ATG) was commonly used in induction therapies, it has since fallen out in favor of monoclonal Abs that can target more specific lymphocyte populations. Basiliximab targets the IL-2 receptor (CD25), which is only expressed on activated T cells, while alemtuzumab specifically targets active, circulating T and B cells<sup>70</sup>. Contrary to Ab induction therapies, fusion proteins like belatacept are showing promise as maintenance immunosuppressants. Belatacept is composed of the Fc fragment of IgG1 and the T

cell co-inhibitory molecule extracellular domain of cytotoxic T-lymphocyte associated protein 4 (CTLA-4), and acts to block T cell activation specifically<sup>71</sup>.

### **1.3.2 Cell therapy in transplantation**

Another approach being developed to induce/maintain transplant tolerance is cell-based therapy. The basic principle of this approach is to administer cells with regulatory properties to transplant recipients in order to promote a regulatory host immune response. To date, clinical trials for cell therapy in transplantation have included administration of bone marrow hematopoietic stem cells, mesenchymal stem cells, and regulatory immune cells.

While different transplant centers have varying specific protocols for hematopoietic stem cell therapy, generally bone marrow chimerism is achieved through a conditioning regimen of irradiation to deplete recipient lymphocytes followed by stem cell infusion. Post-transplant, pharmacological immunosuppressants are used and eventually the patient is weaned from these drugs. Groups at Stanford, Northwestern, and Massachusetts General Hospital have used this general regimen with varying amounts of success in terms of maintaining chimerism following both HLA-matched and mismatched kidney transplant<sup>72</sup>.

Mesenchymal stem cells (isolated from adipose tissue, bone marrow, or umbilical cord) are not used to induce chimerism, but rather to function in vascular repair and inflammation reduction. These stem cells have been demonstrated to have immunomodulatory functions on T cells, B cells, DC, and natural killer cells, and have shown promise as either a replacement for anti-IL-2 induction therapy or as a way to minimize pharmacological immunosuppressant dosing<sup>73</sup>.

As regulatory immune cells (such as T<sub>reg</sub>) are known to be important for restraining inflammatory immune responses, groups have also tried to expand the populations of these regulatory cells in order to shift recipient immunity to a more regulatory nature. For example, the ONE Study includes eight transplant centers from around the world (including the US) and will measure the effect of T<sub>reg</sub> administration to random patients on an identical immunosuppression protocol<sup>74</sup>.

### **1.3.3 Limitations of current immunosuppressive regimens**

Current immunosuppressive regimens prevent acute rejection effectively, with around only 10-15% of deceased donor kidney transplants rejecting within one year of transplantation<sup>75</sup>. However, these regimens do not effectively prevent chronic/long-term rejection—only 54% of transplanted kidneys are functional 10 years post-transplant<sup>76</sup>. With a shortage in suitable organs available for transplant (there are currently 75,000 active waiting list patients in the US<sup>77</sup>), there is a real need to improve the long-term efficacy of immunosuppressants in transplant.

In addition, there are also many adverse side effects ascribed to current immunosuppressants. Immunosuppression in general can increase the risk of infection (especially cytomegalovirus) and malignancy. CNIs can induce nephrotoxicity, neurotoxicity, and diabetes. MPA may cause gastric distress. While mTOR inhibitors have lower nephrotoxicity and incidence of diabetes than CNIs, they can impair wound healing, as well as cause fatal alveolar inflammation in the lungs. mTOR inhibitors are usually used as an alternative to CNIs in patients with renal failure or in patients that develop malignancies<sup>66</sup>.

## 1.4 a TOR Signaling in DC

### 1.4.1 mTORC1

mTOR complex 1 (mTORC1 or TORC1) is one of the complexes the serine-threonine kinase mTOR is known to function in. mTORC1 consists of mTOR, regulatory-associated protein of mTOR (Raptor), DEP domain-containing mTOR-interacting protein (Deptor), mammalian lethal with SEC13 protein 8 (mLST8), and proline-rich Akt substrate of 40kDa (PRAS40)<sup>78</sup>. Canonically, RAPA specifically inhibits mTORC1.

**1.4.1.1 Upstream activators** mTORC1 activity is dependent on nutrient availability, in particular amino acids such as leucine. Nutrient availability acts in synch with growth factors such as insulin to induce intracellular signaling upstream of mTORC1. Specifically, growth factors will activate PI3K and its downstream target Akt. Akt will then phosphorylate tubersclerosis complex (TSC) 2. TSC2 is a guanosine triphosphate (GTP)-ase activating protein (GAP) homolog which when heterodimerized with TSC1 exerts GAP activity on Ras homolog enriched in brain (Rheb). These phosphorylation events inhibit the GAP activity of TSC1/2, thus allowing GTP-bound Rheb to activate mTORC1 through a currently unknown mechanism. In contrast, nutrient deprivation will inhibit mTORC1 activity. This can be attributed in part to the differential phosphorylation of TSC2 by AMP-activated protein kinase (AMPK) and glycogen synthase kinase 3 (GSK3). In this way, Akt and AMPK exert opposing effects on mTORC1 activity<sup>79</sup>.

**1.4.1.2 Regulation of cell growth** Activated mTORC1 positively regulates cell growth by promoting anabolic protein synthesis and lipogenesis and inhibiting anabolic processes. mTORC1 positively regulates protein synthesis through its downstream effectors eukaryotic initiation factor 4E (eIF4E)-binding protein 1 (4E-BP1) and p70 ribosomal S6 kinase 1 (S6K1), which increase messenger ribonucleic acid (mRNA) synthesis and cap-dependent translation. Also downstream of mTORC1 are sterol regulatory element binding protein 1 (SREBP1) and peroxisome proliferator-activated receptor- $\gamma$  (PPAR $\gamma$ ), transcription factors that positively regulate lipid homeostasis<sup>80</sup>.

**1.4.1.3 Regulation of immune function** It is also now becoming appreciated that mTORC1 integrates signals from the immune microenvironment to dictate DC maturation and function. As RAPA has been shown to inhibit macropinocytosis in APCs, it has been suggested that mTORC1 may regulate Ag uptake by DC. Administration of RAPA to bone marrow-derived DC also inhibits their maturation, as marked by decreased expression of co-stimulatory molecules and decreased cytokine production. Monocyte-derived DC generated in the presence of RAPA also do not fully mature, and have regulatory properties correlated with their decreased overall cytokine production. Interestingly, both bone marrow-derived and peripheral DC stimulated with LPS in the presence of RAPA have enhanced IL-12 production as a result of increased GSK3 activity. However, only peripheral DC have enhanced Th1/Th17 polarizing capacity in these conditions<sup>81</sup>.

**1.4.1.4 Regulation of metabolism** Aside from its function in cell growth and immunomodulation, mTORC1 is also regarded as a master regulator of cell metabolism.

mTORC1 alters the physical interaction of PPAR $\gamma$  co-activator 1 (PGC1- $\alpha$ ) and yin-yang 1 (YY1), which together transcriptionally regulate both mitochondrial biogenesis and metabolism<sup>79</sup>. In DC specifically, it has recently been demonstrated that commitment to aerobic glycolysis upon TLR stimulation is dependent on the PI3K/mTORC1 signaling pathway driving the expression of inducible nitric oxide synthetase (iNOS) and hypoxia-inducible factor 1 (HIF-1  $\alpha$ )<sup>82</sup>.

## 1.4.2 mTORC2

mTOR complex 2 (mTORC2 or TORC2) is the other complex the serine-threonine kinase mTOR is known to function in. mTORC2 consists of mTOR, rapamycin-insensitive companion of mTOR (Rictor), Deptor, protein observed with Rictor (Protor), mLST8, and mammalian stress-activated MAP kinase-interacting protein 1 (mSIN1). Canonically, mTORC2 is insensitive to RAPA<sup>83</sup>.

**1.4.2.1 Upstream activators and downstream targets** To date, the upstream regulators of mTORC2 are not defined. Unlike mTORC1, Rheb is not an upstream activator of mTORC2. Furthermore, how or even if mTORC2 is regulated by extracellular cues is unknown. It has been demonstrated that insulin can activate mTORC2, but only if the complex contains two specific SIN isoforms<sup>84</sup>. There is also evidence that in human embryonic kidney (HEK) 293 T cells mTORC2 can be directly activated by phosphatidylinositol 3,4,5-trisphosphate (PtdIns(3,4,5)P<sub>3</sub>)<sup>85</sup>. In yeast, TORC2 has been shown to be regulated in part by cell membrane tension, and there have been some studies suggesting this may also be the case in mammalian cells, as cell stretching induces mTORC2-dependent phosphorylation of Akt on the Ser473 site.

However, this is controversial as in addition to cell membrane localization, mTORC2 has also been described as being localized to the mitochondrial membrane, the endoplasmic reticulum (ER), and the lysosome<sup>86</sup>.

Active mTORC2 is known to phosphorylate multiple protein kinase (PK) A, PKC, and PKG family kinases, including Akt, PKC $\alpha$ , and serum/glucocorticoid regulated kinase 1 (SGK1). However, elucidating the complete downstream effector pathways of mTORC2 has remained difficult, as these phosphorylation events don't impact kinase activity so much as substrate specificity. Nonetheless, it has been demonstrated that deletion/knockdown of Rictor (which prevents mTORC2 assembly and this abolishes its activity) in DC may decrease phosphorylation of FOXO1 at the Ser256 site<sup>87</sup> and GSK3 $\beta$  at the Ser9 site<sup>88</sup>.

**1.4.2.2 Regulation of immune function** Unlike mTORC1, a specific pharmacological inhibitor of mTORC2 has not yet been identified. This, in conjunction with mTORC2 only having been identified in 2007, has led to a paucity of knowledge regarding the specific biological functions of this complex. Using small interfering RNA (siRNA) against Rictor, Brown et al. showed mTORC2 negatively regulates inflammatory responses in DC<sup>87</sup>. More recently, our lab generated a transgenic mouse model in which Rictor is deleted specifically in CD11c<sup>+</sup> cells (TORC2<sup>DC-/-</sup> mice)<sup>89</sup>, and using this model we have made great advancements in understanding the immunological function of mTORC2 in DC.

TORC2<sup>DC-/-</sup> generated from bone marrow display decreased PD-L1 and increased CD86 expression, indicating an enhanced inflammatory phenotype. TORC2<sup>DC-/-</sup> also produce more IL-6, IL-12p70, IL-23, and TNF $\alpha$  inflammatory cytokines than wild-type (WT) DC after stimulation with lipopolysaccharide (LPS), a TLR4 agonist. In addition, TORC2<sup>DC-/-</sup> are more stimulatory

than WT DC, inducing more T cell proliferation, as well as enhanced Th1/Th17 inflammatory effector T cell polarization<sup>88</sup>. Finally, intratumoral injection of TORC2<sup>DC-/-</sup> has been demonstrated to delay B16 melanoma growth progression due to the enhanced ability of these DC to activate CD8<sup>+</sup> T cell responses<sup>90</sup>. Taken together, mTORC2 clearly has a role in restraining inflammatory DC responses.

### **1.4.3 Interplay between mTORC1 and mTORC2**

Given mTORC1 is downstream of Akt, and mTORC2 phosphorylates Akt at the Ser473 site, it would follow that mTORC2 could be a positive regulator of mTORC1 activity. However, this becomes more complex when taking into account that mTORC1 inhibits its own activity via a feedback loop mediated by S6K activity on insulin receptors and insulin receptor substrate 1 (IRS-1) and insulin-dependent PI3K signaling may be an activating factor for mTORC2 as well. In addition, it has been reported that phosphorylation of Akt on Ser473 may not be required for phosphorylation of TSC2 by Akt, which would place mTORC1 activity outside of mTORC2 regulation. Finally, it has been suggested that mTORC2 may not be the only kinase capable of phosphorylating Akt on Ser473<sup>84</sup>. As more is learned about the upstream activators and complete downstream signaling pathways of mTORC2, the nature/existence of crosstalk between the two mTOR complexes may become more clear.

## 1.5 Metabolic Regulation of Dendritic Cell Function

### 1.5.1 Aerobic glycolysis

Aerobic glycolysis, also known as Warburg metabolism, was first described as an unconventional metabolic process observed in cancer cells, whereby they would convert glucose to lactate in the presence of oxygen, as opposed to non-malignant cells in which glucose is converted into pyruvate and lactose conversion occurs in the absence of oxygen<sup>91</sup>. However, it is now appreciated that non-malignant cells may also utilize aerobic glycolysis; this observation in immune cells has led to the development of a new field of scientific study, immunometabolism.

Like other cells, quiescent DC utilize oxidative phosphorylation (OXPHOS) to meet their relatively low bioenergetic demands. However, activation leads to changes in these bioenergetic and biosynthetic needs. Therefore, successful DC activation is underpinned by metabolic regulation. It is now appreciated that upon TLR ligation, DC increase their reliance on aerobic glycolysis<sup>92</sup>. The initial “switch” of this process occurs within minutes of TLR agonism, and is dependent on the TANK (TRAF family member-associated NF-kappa-B activator)-binding kinase 1 (TBK1)/Inhibitor of nuclear factor kappa-B kinase subunit epsilon (IKK $\epsilon$ )/Akt pathway, which in turn increases the association of the glycolytic enzyme hexokinase-II (HK-II) to the mitochondria. Functionally, this glycolytic switch permits DC to utilize glucose as a carbon source to increase pyruvate production, as pyruvate is the end product of glycolysis. In turn, pyruvate is utilized in the citric acid cycle (also known as the Krebs’s cycle and the tricarboxylic acid [TCA] cycle), leading to an increase in spare respiratory capacity (SRC) as well as cytosolic acetyl-CoA. The ultimate consequence of this enhanced aerobic glycolysis/TCA cycle by DC

appears to be *de novo* fatty acid synthesis, which most likely is crucial in supporting Golgi/endoplasmic reticulum (ER) expansion to facilitate protein synthesis and export<sup>93,94</sup>.

Following the initial glycolytic switch, DC also “double-down” and commit to increased glycolytic metabolism; after 12 hours of stimulation through TLRs, DC almost exclusively use aerobic glycolysis metabolically. In bone marrow-derived DC (BMDC), this has been demonstrated to be a survival mechanism. Activation of the PI3K/mTORC1 signaling pathway following TLR ligation of DC promotes the expression of iNOS and HIF-1 $\alpha$ . Nitric oxide (NO) produced by iNOS competes with oxygen along the electron transport chain (ETC), effectively inhibiting the cell from using oxidative OXPHOS to generate adenosine triphosphate (ATP). Meanwhile, HIF-1 $\alpha$  promotes the expression of glucose transporters, which permit DC to increase glycolytic activity and thereby meet ATP demands<sup>82</sup>.

### **1.5.2 Lipid metabolism**

DC utilize both catabolic and anabolic lipid metabolism in the form of fatty acid oxidation (FAO) and fatty acid synthesis (FAS), respectively. Quiescent DC utilize FAO to drive OXPHOS, with mitochondrial fatty acid  $\beta$ -oxidation being reduced upon DC activation<sup>92</sup>. Upon activation, DC will use FAS, which as described above is most likely critical for Golgi/ER expansion and subsequent protein synthesis and transport. FAS in TLR-stimulated DC also leads to increased lipid storage in the form of lipid droplets<sup>95</sup>. While in other cell types these neutral lipid stores can be used catabolically or anabolically, it is not yet clear what their function is in DC.

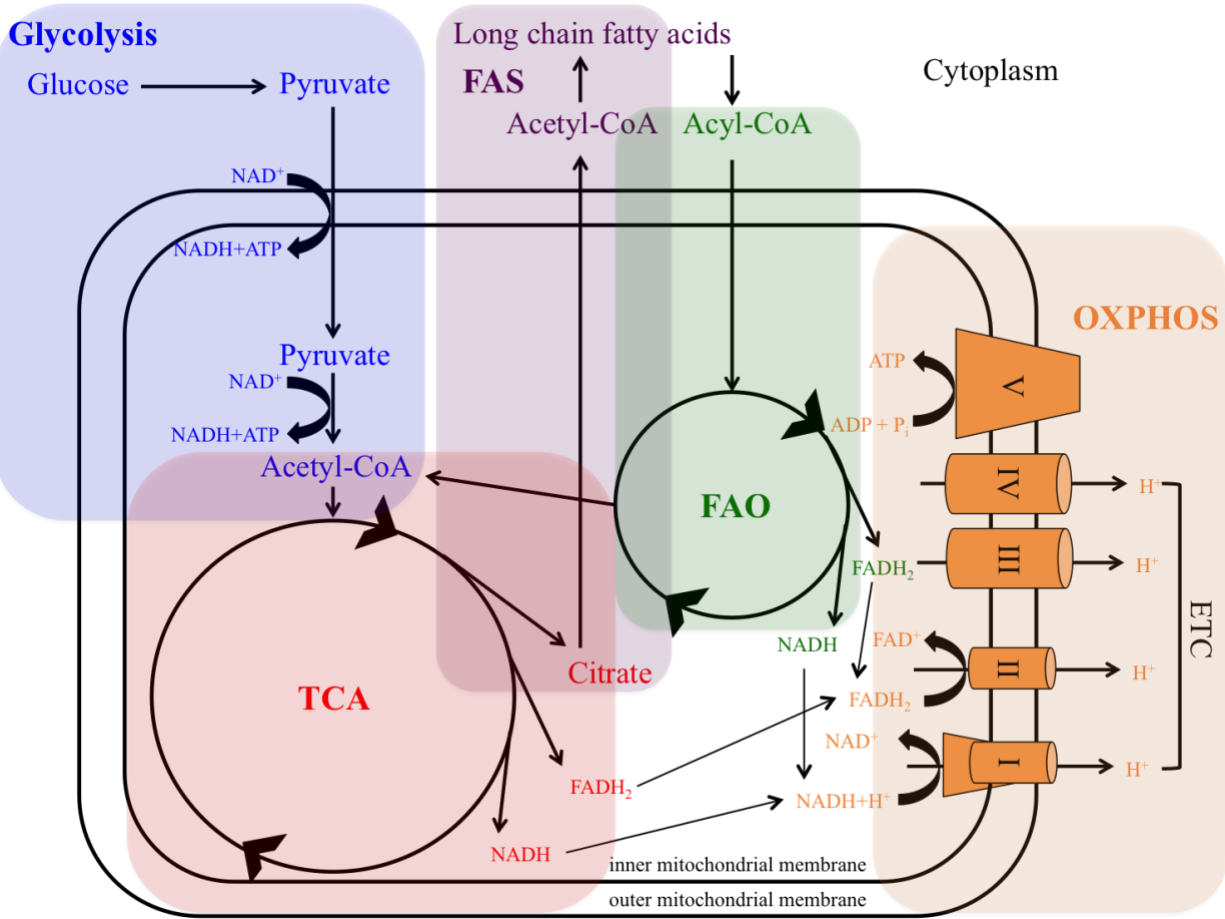


**Figure 1. Overview of mitochondrial metabolism.**

The metabolic pathways involved in DC regulation are intertwined and have end products and intermediates that feed into other pathways. Outlined here are glycolysis (blue), the TCA (red), FAO (green), FAS (purple), and OXPHOS (orange). Acetyl-CoA from glycolysis feeds the TCA; citrate intermediate from the TCA leads to FAS. The long-chain fatty acids from FAS are broken down in FAO, which produces acetyl-CoA to feed the TCA. The co-enzymes NADH and FADH<sub>2</sub> produced by the TCA and FAO act as electron donors for the ETC which creates an proton gradient across the mitochondrial membrane, powering ATP synthase (complex V) and driving OXPHOS.

### 1.5.3 Metabolic targeting in transplantation

As more information is uncovered regarding the metabolic programs not just DC, but other immune cells utilize, metabolic targeting in a variety of disease states is being actively investigated. This approach is especially attractive as leukocytes have different metabolic profiles depending on their activation status; therefore, metabolic inhibitors may have cell specificity based on the bioenergetic demands of the target population. To date, there have been studies in which metabolic pathways were targeted in both bone marrow and solid organ transplantation<sup>96</sup>.

In the case of development of graft-versus-host disease (GVHD) following bone marrow transplant, high level Ag engagement by pathogenic donor T cells demands large amounts of ATP which these cells produce via FAO-mediated OXPHOS. Indeed, targeting FAO with the inhibitor etomoxir in a murine model of GVHD suppressed proliferation and induced apoptosis of pathogenic donor CD8<sup>+</sup> T cells while not impacting normal graft reconstitution<sup>97</sup>.

In solid organ transplantation, donor-reactive lymphocytes are not persistently encountering donor Ag; therefore, their metabolic profile is characterized not by FAO but by enhanced aerobic glycolysis. However, as metabolic pathways feed into each other the future of metabolic inhibitor use in transplantation is most likely with a combination therapy. The glycolytic inhibitor 2-deoxyglucose (2-DG), in combination with the ETC complex I inhibitor metformin and the glutamine uptake/TCA cycle inhibitor 6-diazo-5-oxo-l-norleucine (DON), has been shown to effectively inhibit both CD4<sup>+</sup> and CD8<sup>+</sup> T cell proliferation and allograft rejection in mouse models of full-MHC mismatch heart and skin transplant. In addition, this therapy promoted T<sub>reg</sub> generation as T<sub>reg</sub> are more reliant on lipid metabolism<sup>98</sup>.

## 1.6 DC-Specific mTORC2 Knockout Mouse Model

As no specific pharmacological inhibitor for mTORC2 has yet been identified, studies of this complex must either rely on siRNA knockdown of a mTORC2-specific protein vital for complex assembly (i.e. Rictor), or transgenic approaches such as gene knockout in the well-established Cre-lox system. Our lab has developed a C57/BL6 background transgenic mouse model in which the *Rictor* gene is selectively deleted in CD11c<sup>+</sup> DC.

To generate these mice, we crossed *Rictor* loxP-flanked mice provided by Drs. Lee and Boothby of the University of Vanderbilt School of Medicine<sup>99</sup> with B6.Cg-Tg(*Itgax-cre*)1-1Reiz/J (CD11c-Cre) mice purchased from The Jackson Laboratory (Bar Harbor, ME). The CD11c-Cre mice harbor a bacterial artificial chromosome (BAC) transgene that expresses Cre recombinase in control of the CD11c promoter and enhancer regions within the BAC transgene. In this system, Cre recombination is detectable in 95% of CD11c<sup>+</sup> DC residing in both lymphoid and non-lymphoid tissues, and about 50-80% of pDC<sup>100</sup>. The genotype of these mice (herein referred to as TORC2<sup>DC/-</sup>) was confirmed by polymerase chain reaction (PCR) and confirmed by Western blot<sup>88</sup>.

## 1.7 Murine Models of Transplantation

### 1.7.1 Skin grafting

Skin grafts are the oldest form of organ transplantation, having been recorded to have taken place since the 6<sup>th</sup> Century BCE by the ancient Hindu physician Sushruta in one of the first works on

surgery and medicine, the *Sushruta Samhita*. In fact, the forehead flap rhinoplasty he describes is still used by plastic surgeons today<sup>101</sup>. The mouse model of full-thickness skin grafting has been employed for almost 100 years, decades before Nobel-Prize winner George Snell identified “histocompatibility genes” in mice and Peter Medawar revealed the rules of acceptance by autologous skin grafts and rejection of heterologous skin grafts in mice and rabbits<sup>102-104</sup>. In this model, recipient T cells are activated by DC from the donor graft presenting self-Ag (direct pathway), recipient DC presenting donor Ag on self-MHC (indirect pathway), and recipient DC presenting intact donor MHC-Ag (semi-direct pathway)<sup>105</sup>. The donor skin can either be prepared from the tail of the donor or from lateral thoracic skin (herein referred to as full-thickness skin grafts), with the latter providing a more robust model of rejection due to the higher density of LC and dermal DC present within this type of graft<sup>106</sup>. Graft failure can be monitored subjectively as the percentage of the graft that becomes necrotic and objectively by measuring graft shrinkage.

**1.7.1.1 Major histocompatibility (MHC) mismatch model** Full MHC mismatch skin grafts in mice involves grafting skin from a mouse of one strain background onto that of a different strain background. For these studies, the MHC mismatch model employed utilized skin isolated from either wild-type control (herein referred to as Ctrl) or TORC2<sup>DC-/-</sup> mice with a C57BL/6 background (herein referred to as B6) grafted onto mice with a BALB/c background. These strains are both MHC1 and MHCII disparate, with C57BL/6 mice being haplotype b and BALB/c mice being haplotype d.

**1.7.1.2 Minor histocompatibility Ag (m-Ag) mismatch models** MHC-matched skin grafts that contain minor histocompatibility mismatches can also be used as a model of rejection. In this

model, however, rejection takes longer and in some cases, depending on the m-Ag mismatch, may not reject. For these studies, one of the m-Ag mismatch model used was skin isolated from male Ctrl or TORC2<sup>DC-/-</sup> mice with a B6 background and grafted onto female mice with a B6 background. Rejection in this model is mediated by the expression of male H-Y Ag on the donor skin, and is referred to herein as HY-mismatch<sup>107</sup>. This model allowed us to assess the function of mTORC2 in DC in direct Ag presentation.

The other mode of m-Ag mismatch utilized in these studies was skin from ovalbumin-expressing mice on a B6 background onto either Ctrl or TORC2<sup>DC-/-</sup> mice with a B6 background. Rejection of this model is driven by the expression of chicken-derived ovalbumin on the donor skin<sup>108</sup>. This model allowed us to assess the function of mTORC2 in DC in indirect Ag presentation.

### **1.7.2 Heterotopic heart transplantation**

Heterotopic heart transplantation (HHT) in mice is a vascularized model of rejection that is less robust than skin grafting but more challenging to perform. Unlike orthotopic heart transplantation in which the recipient heart is replaced, in HHT the recipient heart remains in place, with the transplanted heart being placed in a different location. The two most common types of HHT are the cervical and abdominal models. In the abdominal HHT model, the donor thoracic aorta is anastomosed end-to-side to the recipient infrarenal abdominal aorta, and the donor pulmonary artery is anastomosed to the recipient inferior vena cava. In the cervical HHT model, the donor thoracic aorta is anastomosed to the recipient common carotid artery, and the donor pulmonary artery is anastomosed to the recipient external jugular vein. Graft failure is

monitored subjectively as a beating score; this is graded from 0-4, with 0 indicating the graft has stopped beating and 4 indicating the graft is beating strongly.

For these studies, we utilized the cervical HHT method, as this method is less invasive than the abdominal HHT procedure and the transplanted heart is more accessible in regards to monitoring beating strength<sup>109</sup>. The model used was the m-Ag HY-mismatch model, in which the donor heart was isolated from male Ctrl or TORC2<sup>DC-/-</sup> mice with a B6 background and grafted onto female mice with a B6 background.

## 2.0 Statement of the Problem

Currently in the United States, there are 75,000 total waiting list candidates for life-saving organ transplantation. However, from 2014-2015, only 2,577 of these surgeries were performed, with 21 people dying every day due to an incredible shortage of transplantable organs. This shortage is exacerbated by the number of transplant recipients whose grafts fail due to chronic rejection and need to be replaced—for example, within 10 years only 54% of transplanted kidneys are still functioning, and annually over 20% of kidney transplants are re-transplantations. In order to increase the transplantable organ pool, there is clearly a critical need to improve immunosuppressive regimens of transplant recipients. In order to drive development of more effective immunosuppressants, a more detailed understanding of how the targets of current drugs mediate graft rejection/tolerance is necessary.

One immunosuppressant currently used to prevent graft rejection is rapamycin. Rapamycin is an allosteric inhibitor of the mTOR, a nutrient sensor with serine-threonine kinase activity that regulates cell growth, metabolism, and proliferation, as well as immune cell function. mTOR is known to function in two discrete complexes: rapamycin-sensitive mTORC1 and rapamycin-insensitive mTORC2. The function of mTORC1 in DC has been studied extensively using the immunosuppression pro-drug RAPA. RAPA inhibition of mTORC1 in DC prevents DC maturation, leading to decreased T effector cell proliferation and increased T<sub>reg</sub> differentiation. While little was known previously about the function of RAPA-insensitive mTORC2 in DC, we have shown recently that functional mTORC2 deletion specifically in DC leads to both an enhanced pro-inflammatory DC phenotype and Th1/Th17 allogeneic T cell polarization and proliferation. Additionally, intratumoral delivery of mTORC2-deficient DC

delays melanoma progression in a CD8<sup>+</sup> T cell-dependent manner. However, the mechanisms underlying these enhanced DC functions remains undefined. In addition, how selective targeting of mTORC2 impacts transplant outcome has not been investigated.

It is also now appreciated that metabolic programming, in part regulated by mTOR, is a key regulator of immune cell function; namely mTORC1 activity promotes aerobic glycolysis, which is necessary for T cell and DC activation and promotes cytokine/co-stimulatory molecule production and survival in these cells. Indeed, recent studies have employed glycolytic inhibitors to prevent effector T cell differentiation and prevent graft rejection in mouse models of skin and heart transplantation. However, the role mTORC2 may have in regulating DC metabolism has yet to be defined.

Given the inflammatory phenotype of mTORC2-deficient DC, we hypothesized deletion of mTORC2 in DC would accelerate graft rejection and lead to enhanced recipient effector T cell responses. We also posited that the inflammatory phenotype of mTORC2-deficient DC may be the result of an altered metabolic program, wherein aerobic glycolysis was enhanced in these cells. To address these hypotheses, we utilized several different model of acute rejection in which TORC2<sup>DC-/-</sup> mice were used as graft donors or recipients. We also generated BMDC from these mice for metabolic analyses. The results of these studies demonstrate a clear role for mTORC2 in linking DC function and metabolism, and will have implications for understanding the impact of conventional and new generation mTOR inhibitors on immune cell function in the context of transplantation and other disorders.

### **3.0 a TORC2 Deficiency in Passenger DC Accelerates Graft Rejection**

#### **3.1 Introduction**

There is evidence that mTOR controls T helper (Th) Th cell differentiation through selective activation of signaling by mTORC1 and mTORC2<sup>110</sup>, that mTORC1 and mTORC2 selectively regulate CD8<sup>+</sup> T cell differentiation<sup>111</sup> and that mTORC2 controls CD8<sup>+</sup> T cell memory differentiation<sup>112</sup>. While it has been reported that selective mTORC1 disruption in mouse peritoneal macrophages reduces inflammation<sup>113</sup> and that mTORC1 deficiency in intestinal dendritic cells (DC) enhances CD86 expression and suppresses IL-10 production<sup>114</sup>, we have shown<sup>88</sup> that deletion of mTORC2 in bone marrow (BM)-derived DC leads to an enhanced pro-inflammatory phenotype. These DC lacking mTORC2 promote allogeneic Th1/Th17 polarization and proliferation in vitro, as well as augmented antigen (Ag)-specific Th1/Th17 responses in vivo<sup>88</sup>. However, how the absence of mTORC2 activity specifically in DC might impact their function, host T cell responses and graft survival in transplant recipients has not been investigated.

Here, we utilized mice in which Rictor, an essential component of mTORC2<sup>83</sup>, was knocked out specifically in conventional CD11c<sup>+</sup>DC (TORC2<sup>DC-/-</sup>)<sup>89</sup>. To determine how deletion of mTORC2 in DC impacts direct Ag presentation and transplant outcome, we utilized a cervical HHT model and full-thickness skin transplant model in which donor tissue from either B6 male (M) Ctrl or TORC2<sup>DC-/-</sup> mice was transplanted to B6 female (F) mice. We also utilized a full MHC-mismatch skin transplant model, in which skin from either B6 Ctrl or TORC2<sup>DC-/-</sup> mice

was grafted onto BALB/c mice, to determine if donor Ag-specific T cell precursor frequency affected the impact of mTORC2 deletion in donor DC. In addition, we also investigated how mTORC2 deletion in DC impacts indirect Ag presentation and transplant outcome utilizing an established model of indirect Ag presentation-mediated acute rejection<sup>115</sup> in which skin from global transgenic (tg) OVA-expressing B6 mice was grafted onto either B6 Ctrl or TORC2<sup>DC-/-</sup> mice. Here, we demonstrate that TORC2<sup>DC-/-</sup> donors, but not recipients, leads to accelerated graft failure and more severe rejection, characterized by enhanced CD8<sup>+</sup> T cell activation and inflammatory cytokine production.

## 3.2 Methods

### 3.2.1 Mice

Male and female B6.CD11c-CreRictor<sup>fl/fl</sup> (herein referred to as TORC2<sup>DC-/-</sup>) mice were generated by crossing C57BL/6 (B6; H2<sup>b</sup>) mice in which Rictor was flanked by loxP restriction digest sites (generously provided by Drs Keunwook Lee and Mark Boothby, Vanderbilt University School of Medicine) with B6 mice expressing Cre recombinase on the CD11c promoter (CD11c-Cre; The Jackson Laboratory). The genetic background of crossed mice was verified by PCR genotyping; CD11c-Cre- littermates were used as negative controls. C57BL/6-Tg(CAG-OVA)<sup>916Jen/J</sup> (herein referred to as OVA<sup>+</sup>) mice were generously provided by Drs. D. M. Rothstein and F. G. Lakkis (University of Pittsburgh). Female BALB/cByJ mice (herein referred to as BALB/c) were purchased from The Jackson Laboratory. All studies were performed

according to an Institutional Animal Care and Use Committee-approved protocol (16058226) and in accordance with National Institutes of Health (NIH) guidelines.

### **3.2.2 Heterotopic heart transplantation and rejection grading**

Recipient mice were anesthetized with Ketamine/Xylazine. Fur was removed by shaving and the surgical area was sterilized with Betadine and 70% ethanol. The mice were covered with sterile gauze and placed in the supine position, with the head opposite the surgeon. The head was immobilized with a rubber band holding the upper incisor teeth of the animal to the operating board. A midline incision was made over the right side of the neck from the sternum to the lower mandible. The right external jugular vein (EJV) was dissected and mobilized. The right carotid artery (CA) was exposed and mobilized as far as possible, without causing transection of the sternomastoid muscle. The proximal portion of the CA and the EJV were then occluded with plastic microhemostat clamps. Both of the distal portions of the CA and EJV were ligated with 8-0 silk. The vessels that were close to the distal ties were cut. Then the proximal ends were irrigated with heparinized normal saline (HNS). The right CA is then passed through a plastic cuff (outside diameter, 0.6 mm; inside diameter, 0.35-0.45 mm). By pulling the divided CA with forceps, the proximal end of the CA was everted over the cuff and fixed to it with a circumferential ligature of 9-0 silk. The right EJV was passed through a plastic cuff (outside diameter, 0.80 mm; inside diameter 0.55-0.65mm). The edge of the EJV was pulled so that the proximal end of the vein is everted over the cuff. The edge of the vein was then fixed to the cuff, using a circumferential ligature of 9-0 silk.

Donor mice were anesthetized with Ketamine/Xylazine and the surgical area was sterilized with Betadine and 70% ethanol. A midline abdominal incision was made, and HNS (0.5 ml) was injected into the inferior vena cava (IVC). After 1 min, the IVC was ligated proximally with 8-0 silk, a bilateral thoracotomy performed, and the anterior chest wall pulled in a cranial direction. The thymus was removed and the superior vena cava (SVC) of the intrathoracic space was transected and ligated with 8-0 silk. The aorta (A) was then isolated and irrigated with 0.2ml HNS. The A was then proximally transected. The pulmonary artery (PA) was freed from the surrounding tissue and transected as distally as possible. The PA was then proximally transected. Both the A and PA are protected carefully for later usage. The lungs, pulmonary vein, trachea and esophagus were then carefully dissected and ligated with 7-0 silk. The donor heart was harvested and placed in ice-cold Ringer's lactate solution until transplantation.

The A of the donor heart was covered over the end of the CA and fixed to the arterial cuff with a circular ligature of 9-0 silk. The donor PA was covered over the end of the EJV and fixed to the venous cuff with a circular ligature of 9-0 silk. The clamp on the EJV was released, followed by release of the clamp on the CA. Within approximately 1 min, the donor's heart develops a sinus rhythm, and the incision was closed with the 5-0 Vicryl absorbable sutures.

To minimize pain and distress, animals were given a first dose of Buprenex (0.05 mg/kg s.c.) at the end of surgery and then every 12h for the next 2 days. Graft survival was monitored by daily palpation and graded on a 0-4 scale. Rejection was defined as complete loss of palpable heart beating (score 0).

### **3.2.3 Skin grafting and rejection grading**

Skin transplantation was performed according to the technique described by Billingham et al<sup>116</sup>, with some modifications<sup>117</sup>. Recipient mice were anesthetized using ketamine and xylazine. Full-thickness grafts from lateral thoracic skin, cut into circular pieces (~2.25 cm<sup>2</sup> in area), were grafted onto the lumbar region of recipients using 6-0 sutures. The recipients were then wrapped in sterile bandages. To minimize pain and distress, animals were given a first dose of Buprenex (0.05 mg/kg s.c.) at the end of surgery and then every 12h for the next 2 days.

Skin grafts were grossly assessed every day after the removal of bandages on post-operative day (POD) 7, with graft failure defined as >80% loss of visible viable tissue. H&E-stained slides of skin grafts were assessed at POD 14 for the presence of vacuolar/follicular damage, diskeratosis, lichenoid infiltrate/interface dermatitis, vasculitis and thrombi. Banff rejection scores were determined by a 'blinded' dermatopathologist and based on established criteria<sup>118,119</sup>, with scores ranging from 0 (no rejection) to 4 (severe rejection).

### **3.2.4 Immunohistochemistry and immunofluorescence**

For immunohistochemistry, skin grafts were harvested on either POD 7 or 14 and fixed for 24h in 4% v/v paraformaldehyde (PFA). H&E, CD3 (Abcam; Cambridge, MA; clone # ab16669), CD4 (Abcam; ab183685) and Alcian blue staining was performed by the research histology core of the McGowan Institute for Regenerative Medicine, University of Pittsburgh. Quantitative analysis of immunohistochemical staining was performed using the FIJI ImageJ IHC Toolbox plug-in (NIH).

For immunofluorescence, skin grafts were resected on POD 7, fixed in 4% v/v PFA for 24h and embedded in OCT. Slides were stained for CD8 (eBioscience; Waltham, MA clone# 53-6.7; 14-0081-85) or Ly6G/C (eBioscience; RB6-8C5; 14-5931-81) and counterstained with DAPI. Images were recorded at the Center for Biological Imaging, University of Pittsburgh, using an Olympus Provis fluorescent microscope (Ly6G/C) or an Olympus Fluoview 1000 confocal microscope (CD8).

### **3.2.5 Mixed leukocyte reaction (MLR), skin-resident leukocyte isolation, and flow cytometry**

Cells were harvested from the draining axillary LN of skin graft recipient mice on POD 5 or 7 as indicated and T cells isolated via negative immunomagnetic bead selection. The T cells were either 1.) Analyzed via flow cytometry following surface staining with mAb against CD3 (eBioscience clone# 17A2), CD4 (eBioscience RM4-5), CD8 (eBioscience 2.43), PD-1 (eBioscience J105) and intracellular staining for Foxp3 (BioLegend; San Diego, CA FJK-16s), with data acquired using a Fortessa flow cytometer (BD Biosciences, San Jose, CA) and analyzed using FlowJo (Tree Star, Ashland, OR) or 2.) Labeled with carboxyfluorescein succinimidyl ester (CellTrace CFSE) according to the manufacturer's instructions (Invitrogen; Carlsbad, CA) and co-cultured with functionally mature splenic DC (1:10 DC: T cell ratio) isolated via immunomagnetic bead selection from donor-matched mice (either male B6, female B6, or OVA<sub>tg</sub> as indicated) that had been injected i.p. with 10 $\mu$ g of fms-like tyrosine kinase 3 ligand per day for 10 d prior to DC isolation<sup>120</sup>. After 3 days of culture, IFN $\gamma$ , IL-2, IL-4, and Granzyme-B levels in supernatants were determined by via enzyme-linked immunosorbent assay (ELISA) as per the manufacturer's instructions (BioLegend, eBioscience (Granzyme-B)).

Cells were isolated from the skin grafts of recipient mice on POD 7 via a collagenase digestion. Grafts were incubated in 1mL of digestion media (Iscove's Modified Dulbecco's Media (IMDM; ThermoFisher 12440079), 1mg/mL Collagenase D, 1mg/mL DNase. 10mg/mL Hyaluronidase, and 0.1% BSA) for 45m at 37°C in a 6-well plate. 10mM EDTA was then added to each sample, and incubated at room temperature for 5m. Tissues were then rinsed with cold PBS + 0.2% BSA + 2mM EDTA, and crushed in a 70µm cell strainer to isolate graft-resident cells. Cells were then preincubated with Mouse BD Fc Block purified anti-mouse CD16/CD32 mAb (BD Biosciences; San Jose, CA; clone# 2.4G2) for 5m on ice preceding viability staining performed according to manufacturer's instructions (Zombie Aqua Fixable Viability Kit 423101, BioLegend; San Diego, CA) and surface staining for CD45.2 (eBioscience; Waltham, MA; clone# 104), (CD3 (eBioscience 17A2), CD4 (eBioscience RM4-5), CD8 (eBioscience 2.43), and PD-1 (eBioscience J105). Data were acquired using a Fortessa flow cytometer (BD Biosciences, San Jose, CA) and analyzed using FlowJo (Tree Star, Ashland, OR).

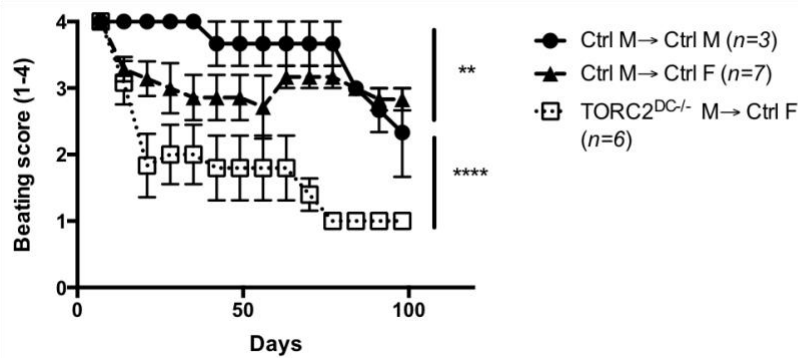
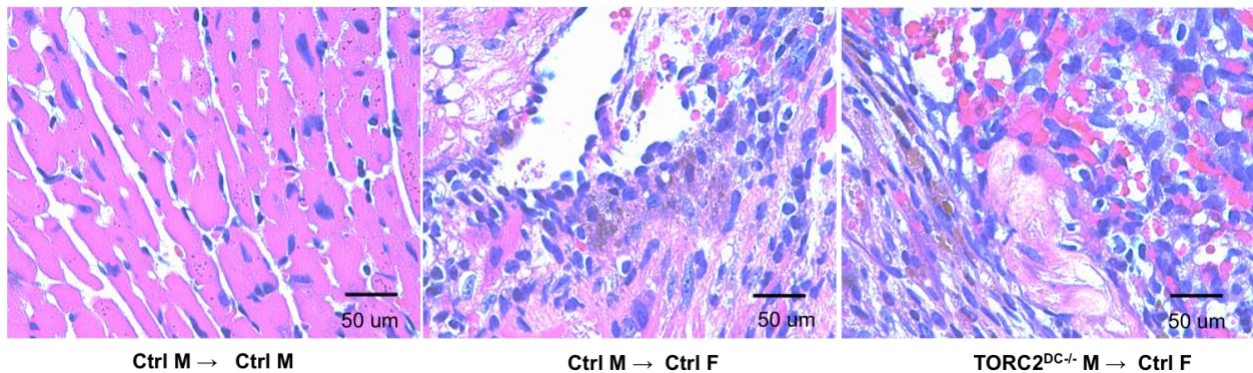
### **3.2.6 Statistical analyses**

Results are expressed as means  $\pm$  1SD. Significances of differences between groups were determined via either Log-rank test (survival curves), Student's 't'-test, or one-way ANOVA Tukey's multiple comparisons test (GraphPad Prism) as indicated with  $p < 0.05$  considered significant.

### 3.3 Results

#### 3.3.1 TORC2<sup>DC-/-</sup> cervical HHT donors have decreased graft function over time and increased cell infiltrate as compared to Ctrl HHT donors

To determine if DC-specific mTORC2 deletion in donor organ would accelerate rejection, we transplanted hearts from either B6 M Ctrl or M TORC2<sup>DC-/-</sup> into B6 F mice heterotopically and assessed graft survival by monitoring beating score and looking at cellular infiltration into the graft at post-operative day (POD) 100 (Figure 2). While none of the grafts failed within the 100 day monitoring period, H&E staining of the grafts at POD100 revealed increased cell infiltrate in the TORC2<sup>DC-/-</sup> donor group. From these data, we determined DC-specific mTORC2 deficiency may impact transplant outcome, but a model in which there were more DC within the donor tissue may be more appropriate for addressing our hypothesis.

**A****B**

**Figure 2. TORC2<sup>DC-/-</sup> cervical HHT donors have decreased graft function over time and increased cell infiltrate as compared to Ctrl HHT donors.**

Hearts from B6 Ctrl M or B6 TORC2<sup>DC-/-</sup> M were transplanted heterotopically into B6 F and monitored for 100 days, then harvested for H&E staining. **(A)** Beating score of the transplanted hearts over 100 days, with 4 denoting strong beating and 0 denoting cessation of beating. **(B)** H&E staining of the heart grafts at POD 100.

### 3.3.2 HY-mismatched skin grafts from TORC2<sup>DC-/-</sup> donors exhibit more severe rejection

As skin contains a more robust population of resident DC, we next determined if donor DC-specific mTORC2 deletion impacted the survival of full-thickness skin transplants. We grafted trunk skin from either WT control B6 males (Ctrl M) or TORC2<sup>DC-/-</sup> B6 males (TORC2<sup>DC-/-</sup> M)

onto WT B6 males or females (Ctrl F). Ctrl M→ Ctrl M grafts were maintained intact up 60 days after which the experiment was terminated, while TORC2<sup>DC-/-</sup> M→ Ctrl F grafts failed significantly more rapidly than Ctrl M→ Ctrl F grafts (median graft survival times [MST] of 22.5 and 17 days, respectively; **Figure 3A**). Grafts from TORC2<sup>DC-/-</sup> M donors were reduced significantly in size at various times post-transplant compared with those from Ctrl M donors (**Figure 3B**). Inspection of the grafts at POD 14 showed evidence of necrosis in the TORC2<sup>DC-/-</sup> M→ Ctrl F grafts (**Figure 3C**). While prior to transplant, TORC2<sup>DC-/-</sup> donor skin showed no morphological differences in the epidermis, dermis or hair follicles compared with normal Ctrl skin (**Figure 3D**), Banff scoring at POD 14 showed more severe rejection in the TORC2<sup>DC-/-</sup> M→ Ctrl F compared with the Ctrl M→ Ctrl F grafts (**Figure 3E**), as evidenced by (1) vacuolar damage, (2) diskeratosis, (3) interface dermatitis, (4) acantholysis, (5) vasculitis, and (6) thrombi (**Figure 3F**). While there was some vacuolar damage and interface dermatitis in the Ctrl M→ Ctrl M grafts, both the Ctrl M→ Ctrl F (especially) and TORC2<sup>DC-/-</sup> → Ctrl F grafts exhibited more severe vacuolar damage, as well as diskeratosis. While the Ctrl M→ Ctrl F grafts showed evidence of vasculitis, the TORC2<sup>DC-/-</sup> M→ Ctrl F showed thrombi and acantholysis. The histological appearance of grafts at POD 7 indicating early pathological changes in TORC2<sup>DC-/-</sup> M → Ctrl F grafts are shown in **Figure 4**.

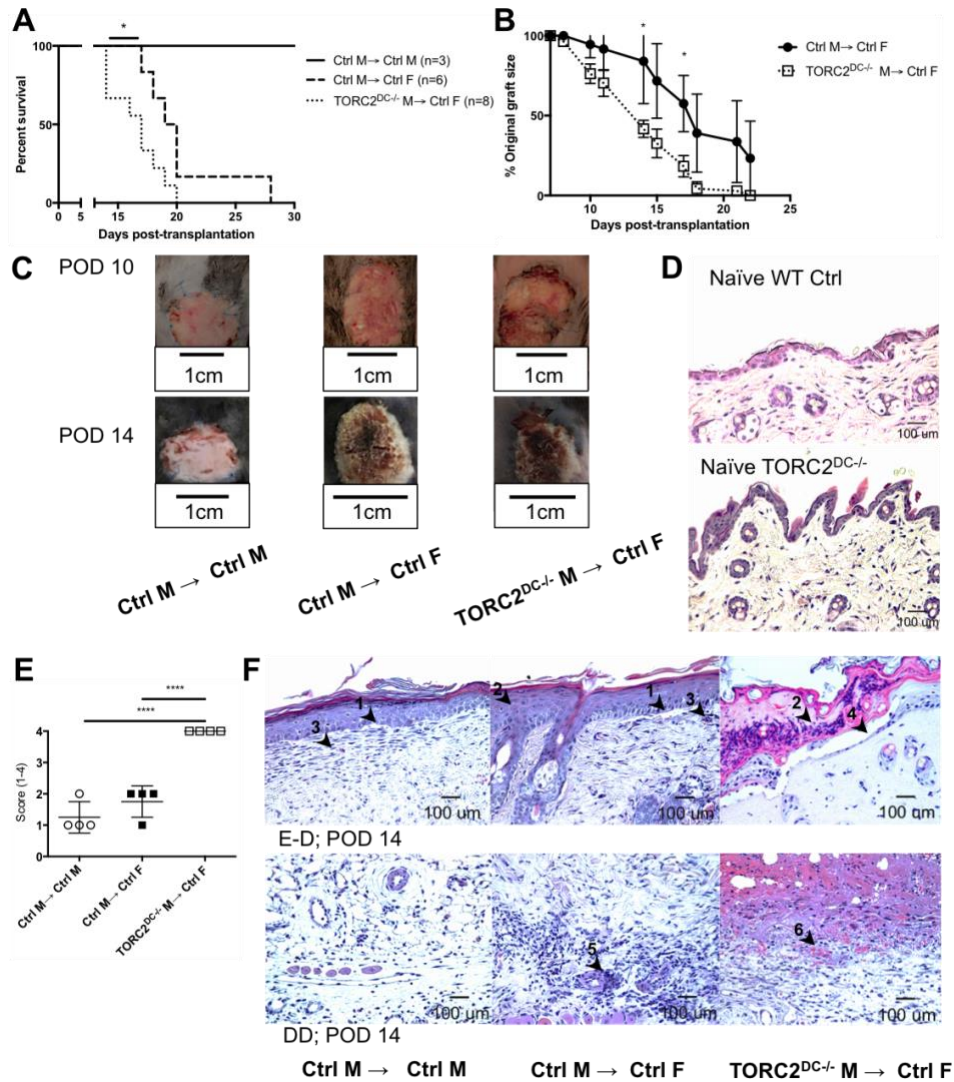


**Figure 3. HY-mismatched skin grafts from TORC2<sup>DC-/-</sup> donors exhibit more severe rejection.**

Male (M) or female (F) wild-type B6 mice were transplanted with full-thickness skin grafts from either B6 WT control M (Ctrl M) or B6 TORC2<sup>DC-/-</sup> M male donors. (A) Graft survival over time, n=3-8 mice per group; Log-rank test, \*, p < 0.05. (B) Skin graft size as a percentage of original graft size over time, n=6-8 mice per group; Student's t-test, \*, p < 0.05. (C) Representative gross morphology of skin grafts at post-operative day (POD) 10 and POD 14. (D) Representative H&E staining of normal naïve (non-transplanted) WT Ctrl and TORC2<sup>DC-/-</sup> trunk skin. (E) Banff rejection scores of skin grafts at POD 14, n=4; one-way ANOVA Tukey's multiple comparisons test, \*, p < 0.05. (F) Representative H&E staining of skin grafts at POD 14 showing the epidermal-dermal junction (E-D) and deep dermal layer (DD). Arrowheads indicate (1) vacuolar damage, (2) pathological dyskeratosis, (3) lichenoid infiltrate/interface dermatitis, (4) pemphigoid acantholysis, (5) vasculitis and (6) thrombosis.

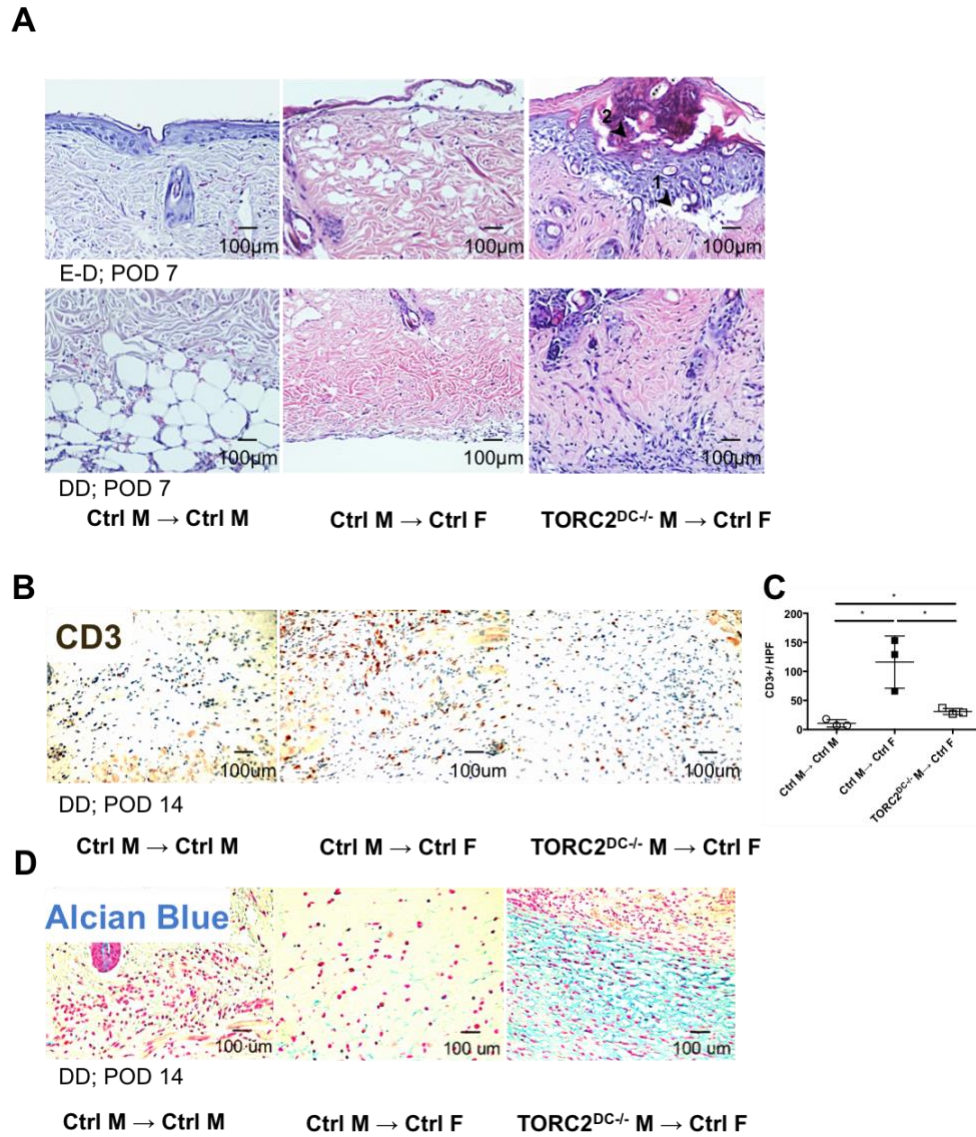


**Figure 4. HY-mismatched skin grafts from TORC2<sup>DC-/-</sup> donors exhibit vacuolar damage and diskeratosis at POD 7, and reduced CD3<sup>+</sup> cell numbers and more severe collagen degradation at POD 14 compared to grafts from WT donors.**

(A) Representative H&E staining of skin grafts at POD 7 showing the epidermal-dermal junction (E-D) and deep dermal layer (DD). Arrowheads in upper right hand panel indicate (1) vacuolar damage and (2) pathological diskeratosis; n=4 mice per group. (B) Representative staining for CD3<sup>+</sup> cells in skin grafts at POD 14; n=3 mice per group. (C) Numbers of CD3<sup>+</sup> cells and mean values in each group. \*, p < 0.05: Student's 't' test. (D) Representative Alcian blue staining of skin grafts at POD 14, showing marked collagen degradation in recipients of TORC2<sup>DC-/-</sup> grafts

### **3.3.3 HY-mismatched skin grafts from TORC2<sup>DC-/-</sup> donors elicit enhanced CD8<sup>+</sup> T cell graft infiltration as compared to WT Ctrl donors**

To characterize the role of host immune cells in graft failure, we first used immunohistochemistry (IHC) to identify CD3<sup>+</sup> cells (**Figure 5A**; quantified in **Figure 5B**) and immunofluorescence staining to identify CD8<sup>+</sup> cells (**Figure 5C**; quantified in **Figure 5D**) in skin graft at POD 7. While there were minimal CD3<sup>+</sup> or CD8<sup>+</sup> cells in the Ctrl M→ Ctrl M grafts, their numbers were increased significantly in the Ctrl M→ Ctrl F grafts. While the mean CD3<sup>+</sup> T cell infiltrate was also increased in the TORC2<sup>DC-/-</sup> M→ Ctrl F grafts compared to the Ctrl M→ Ctrl M grafts, this difference was not significantly different from Ctrl M→ Ctrl F grafts. However, there was a significantly more marked CD8<sup>+</sup> cell infiltrate in the TORC2<sup>DC-/-</sup> M→ Ctrl F compared with Ctrl M→ Ctrl F grafts, consistent with their accelerated rejection. By POD 14, absolute numbers of T cells detected in the TORC2<sup>DC-/-</sup> grafts were lower than those in Ctrl M grafts, coinciding with more extensive tissue injury/collagen degradation in the former (**Figure 4**).

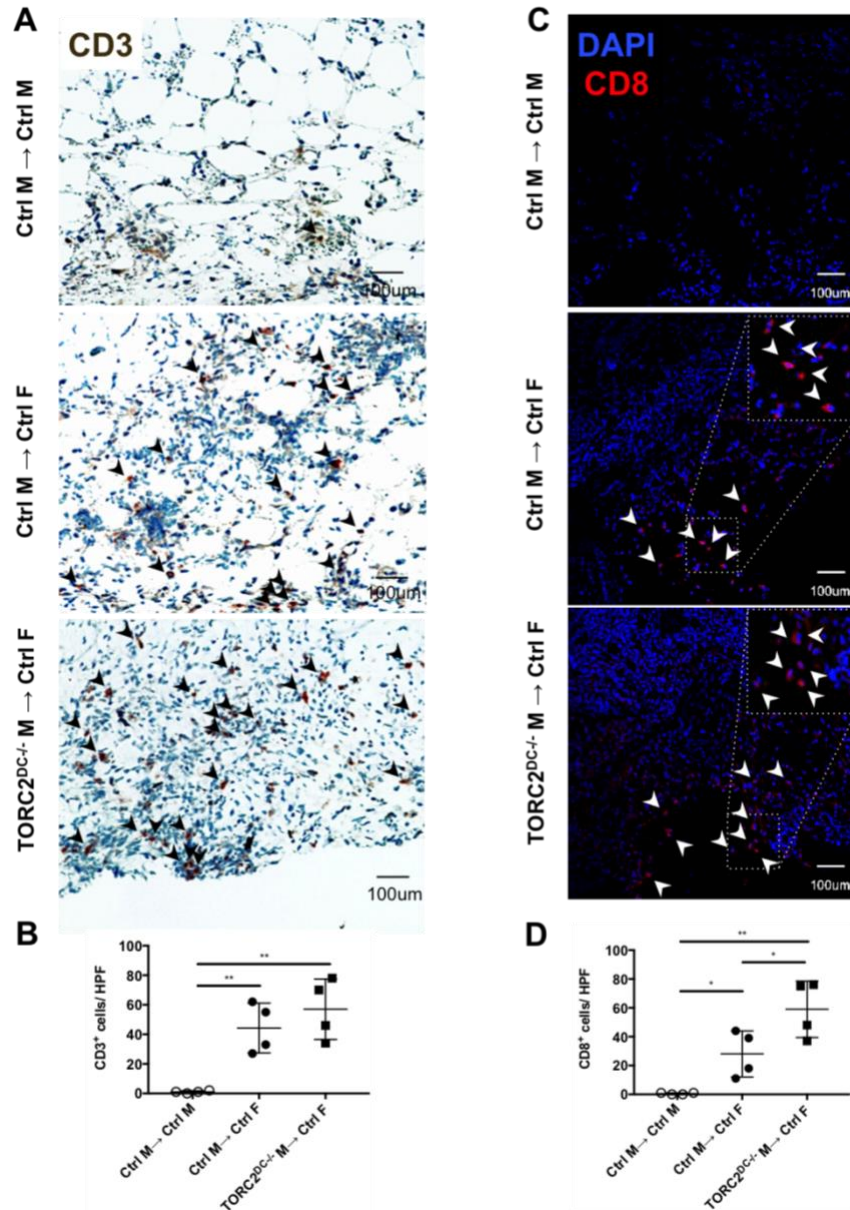


**Figure 5. HY-mismatched skin grafts from TORC2<sup>DC-/-</sup> donors elicit enhanced CD8<sup>+</sup> T cell infiltration compared with grafts from WT Ctrl donors.**

Quantitative analysis of T cell infiltration in skin grafts from WT Ctrl and TORC2<sup>DC-/-</sup> donors was performed on POD 7. (A) Representative immunohistochemical staining for CD3<sup>+</sup> cell (arrowheads);  $n=4$  mice per group. (B) Numbers of CD3<sup>+</sup> cells per high power field (hpf) in skin grafts;  $n=4$  mice per group; one-way ANOVA Tukey's multiple comparisons test, \*,  $p < 0.05$ ; \*\*,  $p < 0.01$ . (C) Representative staining for CD8<sup>+</sup> cells (arrowheads);  $n=4$  mice per group (D) Numbers of CD8<sup>+</sup> cells per hpf in skin grafts;  $n=4$  mice per group; one-way ANOVA Tukey's multiple comparisons test, \*,  $p < 0.05$ ; \*\*,  $p < 0.01$ .

### 3.3.4 HY-mismatched skin grafts from TORC2<sup>DC-/-</sup> donors exhibit enhanced CD8<sup>+</sup>PD-1<sup>+</sup> T cell infiltrate compared with grafts from WT donors

To further investigate the host T cell infiltrate into the graft, we used a collagenase digestion to isolate cells from the graft for analysis via flow cytometry. After gating on live (Zombie<sup>-</sup>) CD45.2<sup>+</sup>CD3<sup>+</sup> cells, we quantified the total numbers of CD4<sup>+</sup> T effector cells (CD4<sup>+</sup>Foxp3<sup>-</sup>), CD8<sup>+</sup> T cells, and T<sub>reg</sub> (CD4<sup>+</sup>Foxp3<sup>+</sup>) (**Figure 6A**). As seen via IHC, there were minimal graft-infiltrating T cells within the Ctrl M→ Ctrl M grafts. Both Ctrl M→ Ctrl F grafts and TORC2<sup>DC-/-</sup> M→ Ctrl F grafts exhibited significant increases in CD4<sup>+</sup> and CD8<sup>+</sup> graft infiltrating T effector cells as well as an augmented ratio of T<sub>eff</sub> : T<sub>reg</sub>; however, the TORC2<sup>DC-/-</sup> M donors showed an enriched CD8<sup>+</sup> T cell infiltrate as compared to Ctrl M→ Ctrl F. We also assessed expression of PD-1 on graft-infiltrating CD8<sup>+</sup> T cells (representative histograms **Figure 6B**, quantified in **Figure 6C**). There were minimal CD8<sup>+</sup>PD-1<sup>+</sup> T cells within the Ctrl M→ Ctrl M grafts, with significant increases in both the Ctrl M→ Ctrl F and TORC2<sup>DC-/-</sup> M→ Ctrl F grafts; however, there was a significant increase in the number of CD8<sup>+</sup>PD-1<sup>+</sup> T cells in the TORC2<sup>DC-/-</sup> M→ Ctrl F grafts as compared to Ctrl M→ Ctrl F grafts. We did not observe any differences in the expression of PD-1 on PD-1<sup>+</sup> cells between any of the groups.

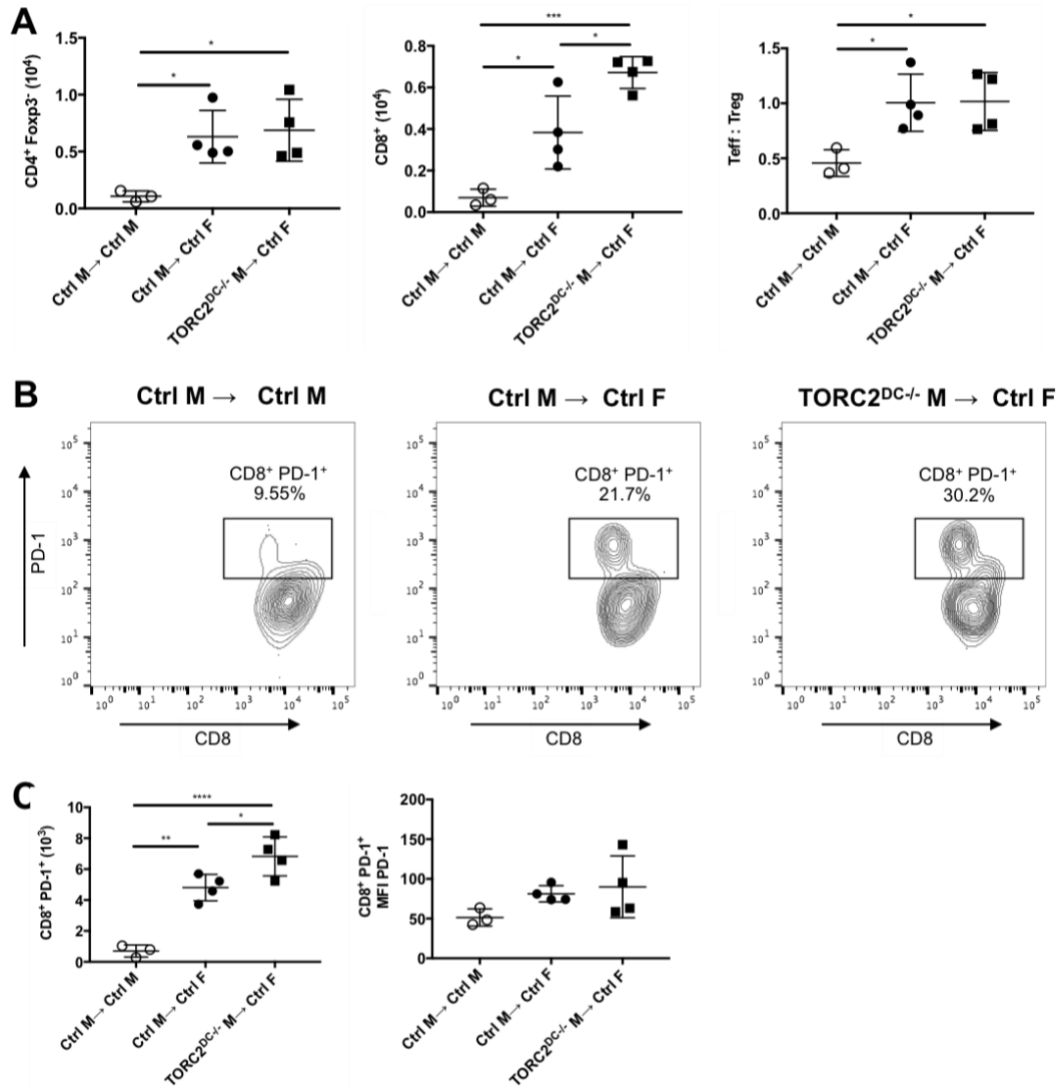


**Figure 6. HY-mismatched skin grafts from TORC2DC<sup>-/-</sup> donors exhibit enhanced CD8<sup>+</sup>PD-1<sup>+</sup> T cell infiltrate compared with grafts from WT donors.**

Cells were isolated from skin grafts on POD7 via a collagenase digestion and analyzed via flow cytometry. T cells were gated on live (Zombie<sup>-</sup>) CD45.2<sup>+</sup>CD3<sup>+</sup> cells. (A) Total numbers of CD4<sup>+</sup>Foxp3<sup>-</sup>, CD8<sup>+</sup>, and CD4<sup>+</sup>Foxp3<sup>+</sup> cells within the graft. (B) Representative histograms of CD8<sup>+</sup>PD-1<sup>+</sup> T cells within the graft. (C) Quantification of CD8<sup>+</sup>PD-1<sup>+</sup> T cells within the graft (left) and MFI of PD-1 on PD-1<sup>+</sup> cells (right). *n*=4 mice per group; one-way ANOVA Tukey's multiple comparisons test, \*, *p* < 0.05; \*\*, *p* < 0.01, \*\*\*, *p* < 0.001, \*\*\*\*, *p* < 0.0001.

### **3.3.5 Skin grafts from TORC2<sup>DC-/-</sup> donors elicit enhanced CD8<sup>+</sup> T effector cell responses in regional LN and augmented IFN $\gamma$ and IL-2 production in response to donor Ag stimulation**

To investigate the function of host T cells in graft recipients, we isolated T cells from the draining axillary LN on POD 7 for quantitative and functional analysis (**Figure 7A**). While there were significantly more CD4<sup>+</sup>CD25<sup>-</sup>Foxp3<sup>-</sup> T effector (T<sub>eff</sub>) cells and an increased ratio of CD4<sup>+</sup>T<sub>eff</sub>: Foxp3<sup>+</sup> (T<sub>reg</sub>) cells in the Ctrl M $\rightarrow$  Ctrl F and TORC2<sup>DC-/-</sup> M $\rightarrow$  Ctrl F graft recipients than in the Ctrl M $\rightarrow$  Ctrl M group, there was no significant difference between the former two groups. However, as observed within the graft itself, there was a significant increase in CD8<sup>+</sup> T cell numbers within the draining LN of the TORC2<sup>DC-/-</sup> M $\rightarrow$  Ctrl F recipients compared with the M $\rightarrow$  Ctrl F recipients (**Figure 7A; center panel**).

Cytokine production by draining LN T cells after 3 days stimulation by DC from Flt3L-mobilized normal male donors was measured by ELISA. As shown in **Figure 7B**, T cells from Ctrl F recipients of TORC2<sup>DC-/-</sup> M grafts produced significantly more IFN $\gamma$  than those from Ctrl F recipients of normal Ctrl M grafts. Moreover, while M $\rightarrow$  Ctrl F T cells produced more IL-2 than the M $\rightarrow$  Ctrl M T cells, TORC2<sup>DC-/-</sup> M $\rightarrow$  Ctrl F T cells produced greater levels of IL-2 than either of those groups. There were no differences, however, in the very low levels of IL-4 production between the groups.

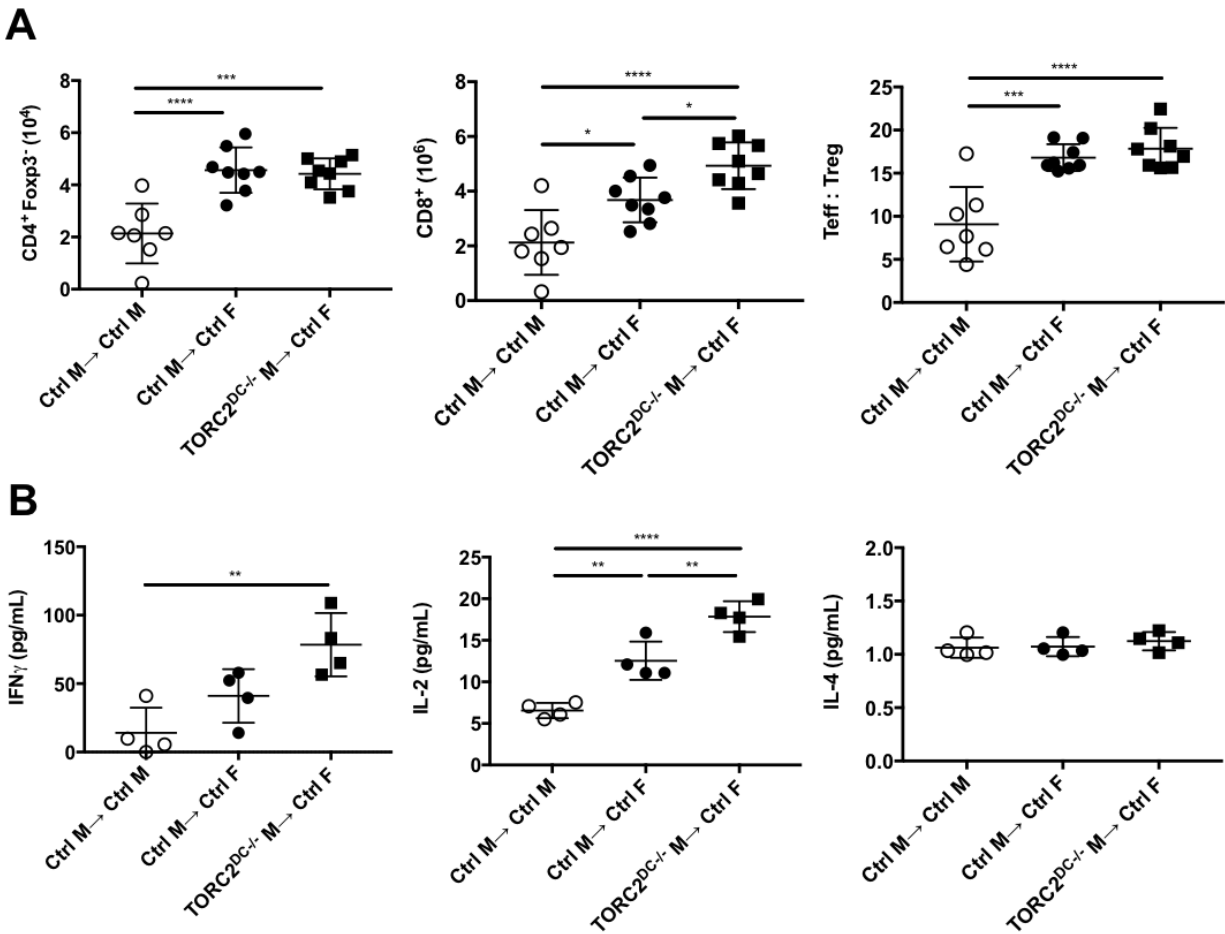


**Figure 7. HY-mismatched skin grafts from TORC2<sup>DC-/-</sup> donors elicit enhanced numbers of CD8<sup>+</sup> T cells in draining LNs and augmented IFN $\gamma$  and IL-2 production in response to donor Ag stimulation.**

T cells were isolated from the axillary LNs of skin graft recipients on POD 7.  $n=8$  mice per group; one-way ANOVA Tukey's multiple comparisons test, \*,  $p < 0.05$ ; \*\*,  $p < 0.01$ , \*\*\*,  $p < 0.001$ , \*\*\*\*,  $p < 0.0001$ . (A) Numbers of CD4<sup>+</sup>CD25<sup>+</sup>Foxp3<sup>+</sup> T effector (T<sub>eff</sub>) cells CD8<sup>+</sup> T cells and the ratio of T<sub>eff</sub>: T<sub>reg</sub> (CD4<sup>+</sup>CD25<sup>+</sup>Foxp3<sup>+</sup>) cells. (B) Isolated T cells were co-cultured with splenic DCs isolated from Flt3L-mobilized male mice for 3 d. Quantification of IFN $\gamma$ , IL-2, and IL-4 present in the supernatant.  $n=4$  mice per group; one-way ANOVA Tukey's multiple comparisons test, \*,  $p < 0.05$ ; \*\*,  $p < 0.01$ , \*\*\*,  $p < 0.001$ , \*\*\*\*,  $p < 0.0001$ .

### 3.3.6 MHC-mismatched skin grafts from TORC2<sup>DC-/-</sup> donors do not exhibit significantly accelerated rejection but do show evidence of rejection earlier than grafts from Ctrl donors

We next wanted to determine if mTORC2 deficiency in donor skin DC would also enhance rejection in a full MHC-mismatch model, in which the frequency of precursor donor-reactive T cells was higher. To this end, we grafted trunk skin from either WT BALB/c, WT control B6 (Ctrl B6), or TORC2<sup>DC-/-</sup> B6 (TORC2<sup>DC-/-</sup> B6) mice onto BALB/c mice. BALB/c → BALB/c grafts were maintained intact up 30 days after which the experiment was terminated, while TORC2<sup>DC-/-</sup> B6 → BALB/c grafts and Ctrl B6 → BALB/c grafts did not have significantly different graft survival (MST of 8.0 and 9.2 days, respectively; **Figure 8A**). Inspection of the grafts at POD 5 and POD 7 showed evidence of advanced necrosis in both the TORC2<sup>DC-/-</sup> B6 → BALB/c and Ctrl B6 → BALB/c grafts (**Figure 8B**). Banff scoring at POD 5 showed more severe rejection in the TORC2<sup>DC-/-</sup> B6 → BALB/c grafts compared with the Ctrl B6 → BALB/c grafts (**Figure 8C**), as evidenced by (1) vacuolar damage, (2) diskeratosis, (3) thrombosis, and (4) vasculitis (**Figure 8D**). While there was some thrombosis in the BALB/c → BALB/c grafts, both the Ctrl B6 → BALB/c and TORC2<sup>DC-/-</sup> B6 → BALB/c grafts exhibited more severe thrombosis (with the most severe observed in the TORC2<sup>DC-/-</sup> B6 → BALB/c grafts). In addition, while only the Ctrl B6 → BALB/c grafts showed evidence of vacuolar damage, diskeratosis and vasculitis were only observed in the TORC2<sup>DC-/-</sup> B6 → BALB/c grafts.

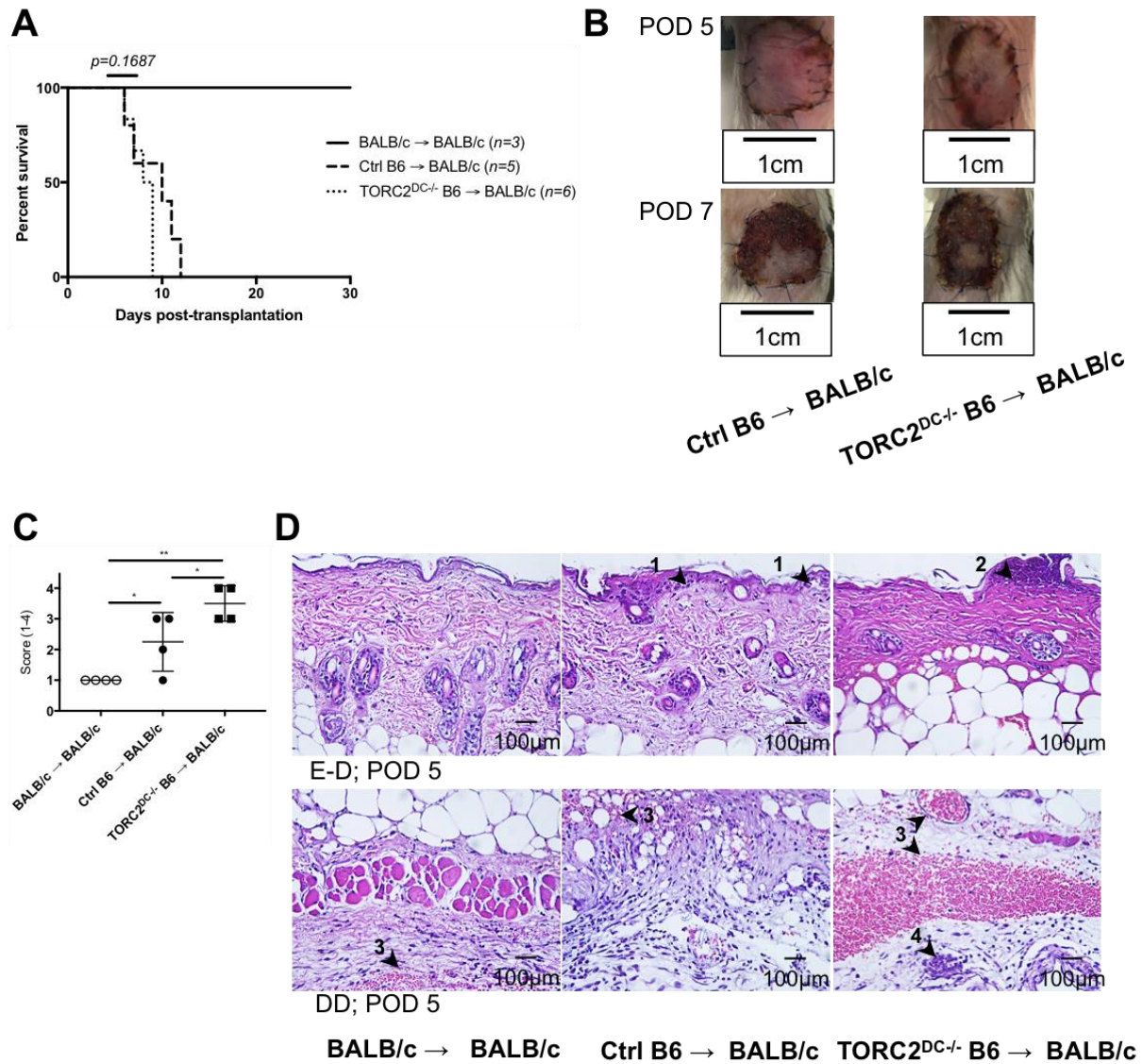


**Figure 8. MHC-mismatched skin grafts from TORC2<sup>DC-/-</sup> donors do not exhibit significantly accelerated rejection but do show evidence of rejection earlier than grafts from Ctrl donors.**

Wild-type BALB/c mice were transplanted with full-thickness skin grafts from either B6 WT control (Ctrl B6) or TORC2<sup>DC-/-</sup> B6 donors. (A) Graft survival over time,  $n=3-6$  mice per group; Log-rank test, \*,  $p < 0.05$ . (B) Representative gross morphology of skin grafts at post-operative day (POD) 5 and POD 7. (C) Banff rejection scores of skin grafts at POD 5,  $n=4$ ; one-way ANOVA Tukey's multiple comparisons test, \*,  $p < 0.05$ . (D) Representative H&E staining of skin grafts at POD 5 showing the epidermal-dermal junction (E-D) and deep dermal layer (DD). Arrowheads indicate (1) vacuolar damage, (2) pathological diskeratosis, (3) thrombosis, and (4) vasculitis.

### **3.3.7 MHC-mismatched skin grafts from TORC2<sup>DC-/-</sup> donors do not elicit enhanced CD8<sup>+</sup> T cell infiltration compared with grafts from WT Ctrl donors**

To characterize the role of host immune cells in graft failure, we first used IHC to identify CD3<sup>+</sup> cells (**Figure 9A**; quantified in **Figure 9B**) and immunofluorescence staining to identify CD8<sup>+</sup> cells (**Figure 9C**; quantified in **Figure 9D**) in skin graft at POD 5. While there were minimal CD3<sup>+</sup> or CD8<sup>+</sup> cells in the BALB/c→BALB/c grafts, their numbers were increased significantly in the Ctrl B6→BALB/c grafts. While the mean CD3<sup>+</sup> T cell infiltrate was also increased in the TORC2<sup>DC-/-</sup> B6→BALB/c grafts compared to the BALB/c→BALB/c grafts, this difference was not significantly different from Ctrl B6→BALB/c grafts. However, there was a significantly more marked CD8<sup>+</sup> cell infiltrate in the TORC2<sup>DC-/-</sup> B6→BALB/c compared with Ctrl B6→BALB/c grafts, consistent with their accelerated rejection.

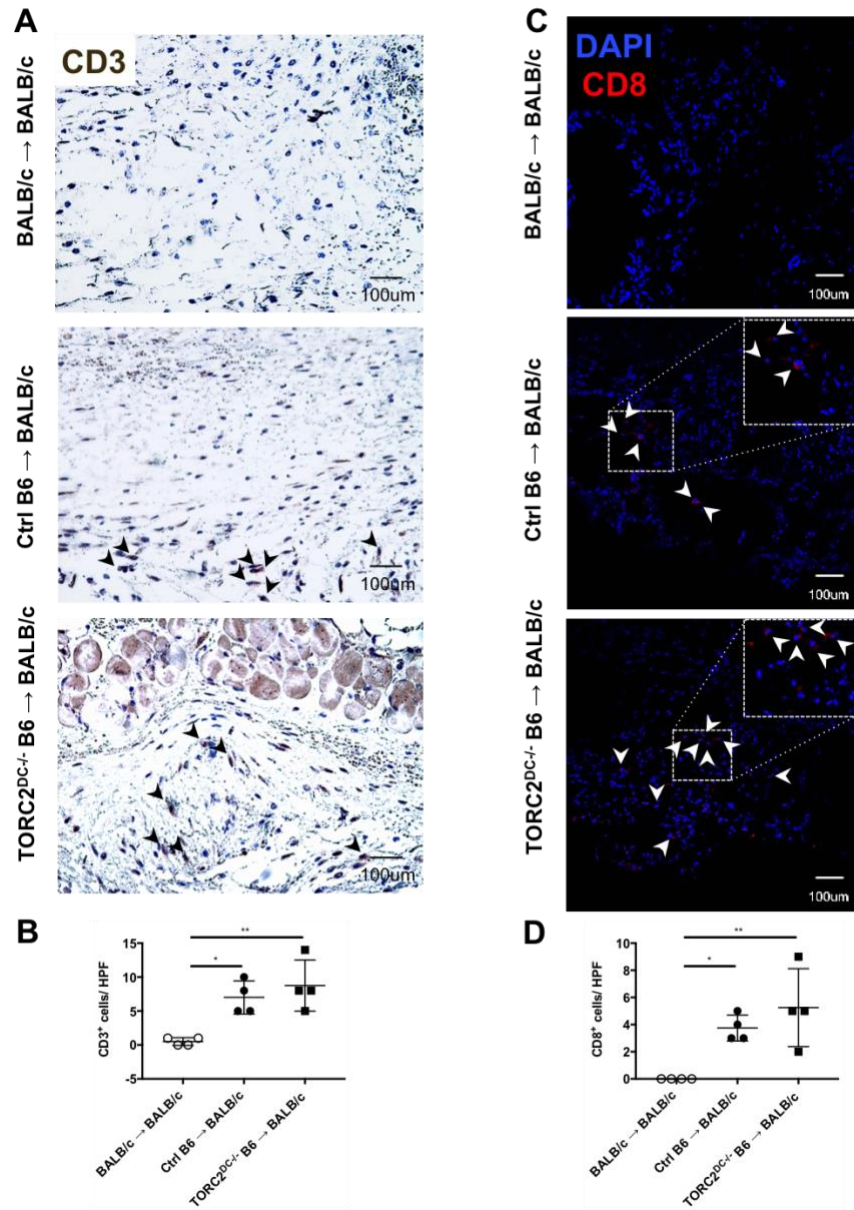


**Figure 9. MHC-mismatched skin grafts from TORC2<sup>DC</sup>-/- donors do not elicit enhanced CD8<sup>+</sup> T cell infiltration compared with grafts from WT Ctrl donors.**

Quantitative analysis of T cell infiltration in skin grafts from WT Ctrl and TORC2<sup>DC</sup>-/- donors was performed on POD 5. (A) Representative immunohistochemical staining for CD3<sup>+</sup> cell (arrowheads);  $n=4$  mice per group. (B) Numbers of CD3<sup>+</sup> cells per high power field (hpf) in skin grafts;  $n=4$  mice per group; one-way ANOVA Tukey's multiple comparisons test, \*,  $p < 0.05$ ; \*\*,  $p < 0.01$ . (C) Representative staining for CD8<sup>+</sup> cells (arrowheads);  $n=4$  mice per group (D) Numbers of CD8<sup>+</sup> cells per hpf in skin grafts;  $n=4$  mice per group; one-way ANOVA Tukey's multiple comparisons test, \*,  $p < 0.05$ ; \*\*,  $p < 0.01$ .

### 3.3.8 MHC-mismatched skin grafts from TORC2<sup>DC-/-</sup> donors elicit enhanced number of CD8<sup>+</sup> and CD8<sup>+</sup>PD-1<sup>+</sup> T cells in draining LN compared with grafts from WT donors

To investigate the function of host T cells in graft recipients, we isolated T cells from the draining axillary LN on POD 5 for quantitative analysis. We observed a significant increase in the number of CD4<sup>+</sup>Foxp3<sup>-</sup> T cells (Teff) in both the Ctrl B6 and TORC2<sup>DC-/-</sup> B6 donor groups as compared to the BALB/c donor group; however this number was not significantly different between the Ctrl and TORC2<sup>DC-/-</sup> group (**Figure 10A; left panel**). Both the Ctrl B6 and TORC2<sup>DC-/-</sup> B6 donor groups also exhibited increased numbers of CD8<sup>+</sup> T cells with the LN, while the TORC2<sup>DC-/-</sup> donor group had significantly more CD8<sup>+</sup> T cells than the Ctrl B6 donor group (**Figure 10A; center panel**). We did not observe any differences between groups pertaining to the ratio of Teff:Treg (**Figure 10A; right panel**). We also assessed the number of PD-1<sup>+</sup> CD8<sup>+</sup> T cells within the LN of graft recipients (representative histograms **Figure 10B**, quantified in **Figure 10C**). While there were minimal CD8<sup>+</sup>PD-1<sup>+</sup> cells in BALB/c and Ctrl B6 donor group, we observed a significant increase in the number of CD8<sup>+</sup>PD-1<sup>+</sup> cells within the LN of the TORC2<sup>DC-/-</sup> B6 donor group. We did not observe any difference in expression of PD-1 on PD-1<sup>+</sup> cells between any of the groups.

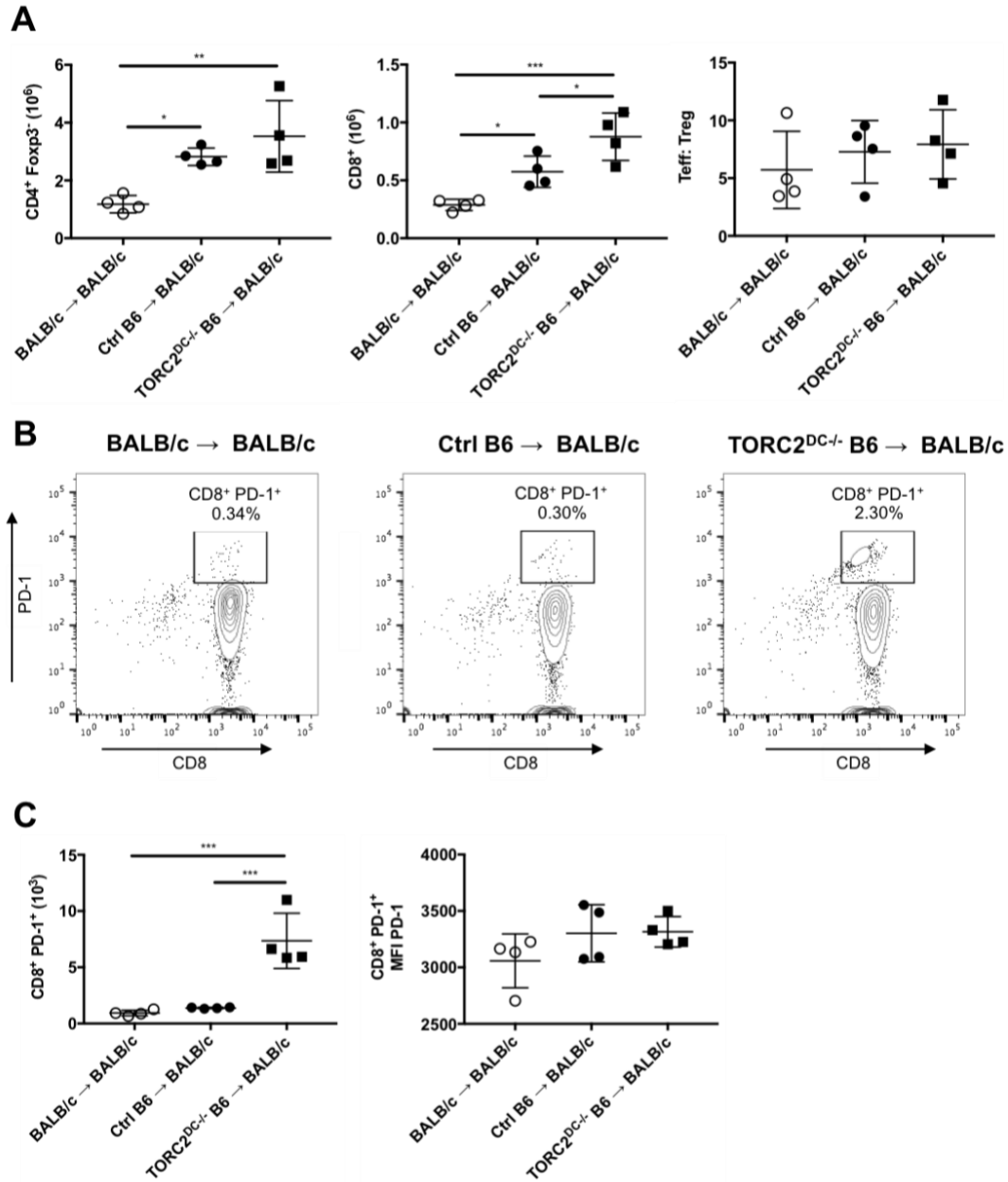


**Figure 10. MHC-mismatched skin grafts from TORC2<sup>DC-/-</sup> donors elicit enhanced number of CD8<sup>+</sup> and CD8<sup>+</sup>PD-1<sup>+</sup> T cells in draining LN compared with grafts from WT donors.**

T cells were isolated from the axillary LNs of skin graft recipients on POD 5. (A) Numbers of CD4<sup>+</sup>CD25<sup>+</sup>Foxp3<sup>+</sup> T effector (T<sub>eff</sub>) cells, CD8<sup>+</sup> T cells, and the ratio of T<sub>eff</sub>: T<sub>reg</sub> (CD4<sup>+</sup>CD25<sup>+</sup>Foxp3<sup>+</sup>) cells. (B) Representative histograms of CD8<sup>+</sup>PD-1<sup>+</sup> T cells within the LN. (C) Quantification of CD8<sup>+</sup>PD-1<sup>+</sup> T cells within the LN (left) and MFI of PD-1 on PD-1<sup>+</sup> cells (right). *n*=4 mice per group; one-way ANOVA Tukey's multiple comparisons test, \*, *p* < 0.05; \*\*, *p* < 0.01, \*\*\*, *p* < 0.001, \*\*\*\*, *p* < 0.0001.

### **3.3.9 MHC-mismatched skin grafts from TORC2<sup>DC-/-</sup> donors elicit enhanced proliferation of CD8<sup>+</sup> T cells in draining LNs and augmented IFN $\gamma$ and Granzyme-B production in response to donor Ag**

To further investigate the function of host T cells in graft recipients, we isolated T cells from the draining axillary LN of graft recipients on POD 5 for functional analysis. T cells were labeled with the cell proliferation dye CFSE, and co-cultured with B6 splenic DC to assess their proliferation and cytokine production in response to donor Ag. While there were no significant differences in the percentage of proliferating (CFSE<sup>lo</sup>) CD4<sup>+</sup>Foxp3<sup>-</sup> T cells between groups (**Figure 11A; top panel**), nor the division index of CD4<sup>+</sup>Foxp3<sup>-</sup> T cells (**Figure 11A; bottom panel**), we did observe significant increases in the percentage of proliferating CD8<sup>+</sup> T cells in both the Ctrl B6 and TORC2<sup>DC-/-</sup> B6 donor groups as compared to the BALB/c donor group (**Figure 11B; top panel**). In addition, the CD8<sup>+</sup> T cell division index was augmented significantly in the TORC2<sup>DC-/-</sup> B6 donor group as compared to both the BALB/c $\rightarrow$ BALB/c and Ctrl B6 $\rightarrow$ BALB/c groups (**Figure 11B, bottom panel**, representative histograms **Figure 11C**). Furthermore, while both the Ctrl B6 and TORC2<sup>DC-/-</sup> B6 donor groups had significantly elevated IFN $\gamma$ , IL-2, and Granzyme-B production as compared to the BALB/c donor group in response to B6 antigen, T cells isolated from the TORC2<sup>DC-/-</sup> donor group also produced significantly more IFN $\gamma$  and Granzyme-B as compared to the Ctrl B6 donor group.

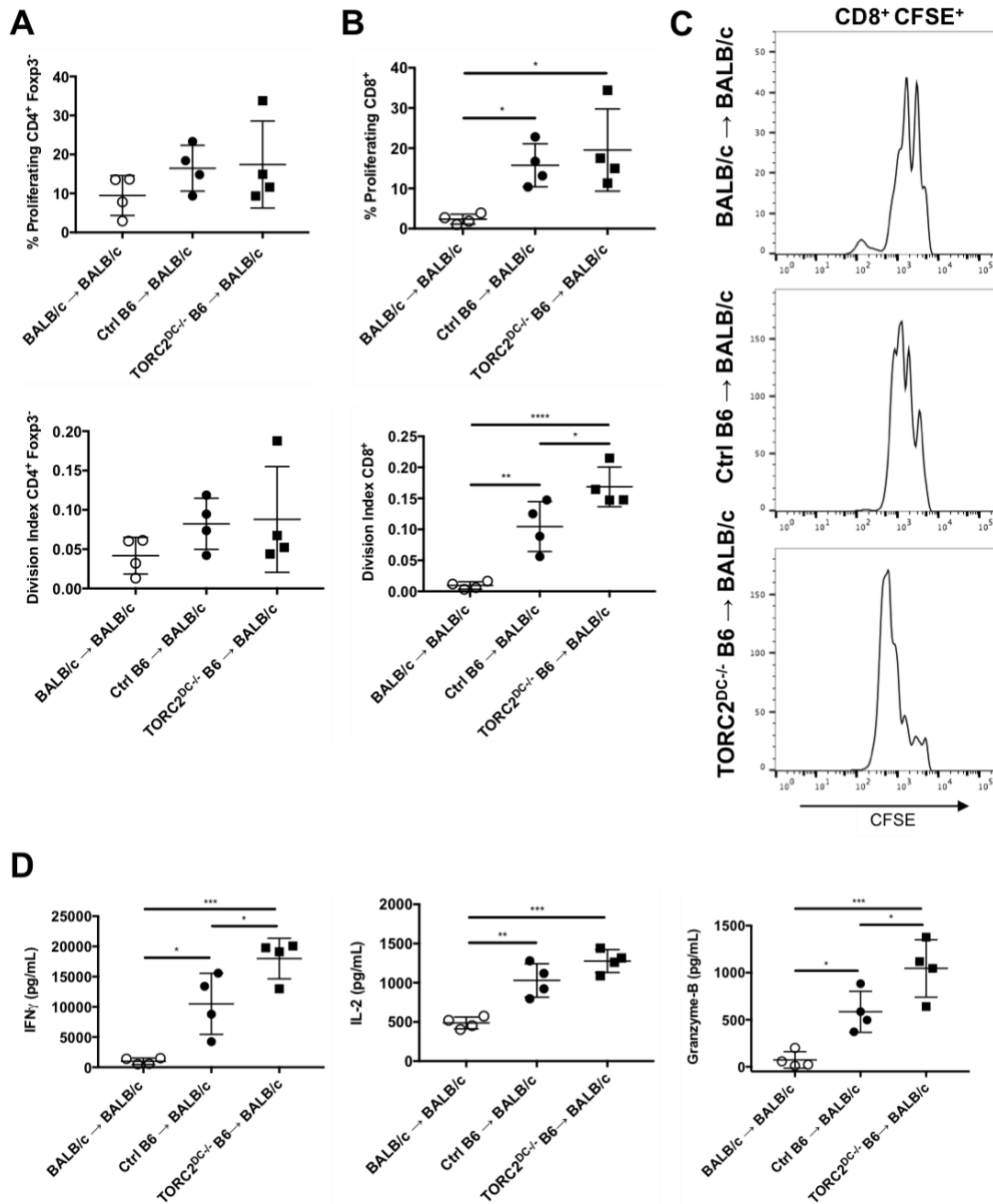


**Figure 11. MHC-mismatched skin grafts from TORC2<sup>DC-/-</sup> donors elicit enhanced proliferation of CD8<sup>+</sup> T cells in draining LNs and augmented IFN $\gamma$  and IL-2 production in response to donor Ag (B6) stimulation.**

T cells were isolated from the axillary LNs of skin graft recipients on POD 5. Isolated T cells were labeled with the cell proliferation dye CFSE, and co-cultured with splenic DCs isolated from B6 mice for 3 d. (A) Proliferation of CD4<sup>+</sup>Foxp3<sup>-</sup> T cells as measured by cellular CFSE content (top, percent dividing; bottom, division index). (B) Proliferation of CD8<sup>+</sup> T cells as measured by cellular CFSE content (top, percent dividing; bottom, division index). (C) Quantification of IFN $\gamma$ , IL-2, and Granzyme-B within the supernatant. *n*=4 mice per group; one-way ANOVA Tukey's multiple comparisons test, \*, *p* < 0.05; \*\*, *p* < 0.01, \*\*\*, *p* < 0.001, \*\*\*\*, *p* < 0.0001.

### 3.3.10 Skin graft rejection is not affected in TORC2<sup>DC-/-</sup> recipients

Having observed that mTORC2 deficiency in donor DC led to accelerated minor H Ag-mismatched skin graft rejection, we next investigated whether, conversely, mTORC2 deficiency only in recipient DC might also affect graft rejection. To address this question, we grafted trunk skin from either B6 WT Ctrl mice (OVA<sup>-</sup>) or OVA<sup>+</sup> mice (OVA<sup>+</sup>) onto syngeneic B6 WT Ctrl or TORC2<sup>DC-/-</sup> mice. While all OVA<sup>-</sup> → Ctrl grafts remained intact after 25 days, the MST for OVA<sup>+</sup> → TORC2<sup>DC-/-</sup> and OVA<sup>+</sup> → Ctrl grafts were 16.5 days and 18.5 days, respectively and did not differ significantly (**Figure 12A**). The OVA<sup>+</sup> grafts were reduced slightly but significantly in size at days 21 and 23 post-transplant in TORC2<sup>DC-/-</sup> compared to Ctrl recipients (**Figure 12B**). Gross morphology of the grafts on POD 14 showed more extensive necrosis of both the OVA<sup>+</sup> → Ctrl and OVA<sup>+</sup> → TORC2<sup>DC-/-</sup> grafts compared to those from OVA<sup>-</sup> donor mice (**Figure 12C**). Banff rejection criteria confirmed similar levels of rejection in the OVA<sup>+</sup> → TORC2<sup>DC-/-</sup> and OVA<sup>+</sup> → Ctrl grafts at POD 14 (**Figure 12D**), as evidenced by (1) vacuolar damage, (2) diskeratosis, (3) interface dermatitis, and (4) vasculitis (**Figure 12E**). While some vacuolar damage was noted in the OVA<sup>-</sup> → Ctrl grafts, both the OVA<sup>+</sup> → Ctrl and OVA<sup>+</sup> → TORC2<sup>DC-/-</sup> grafts exhibited more severe vacuolar damage, as well as diskeratosis and vasculitis.

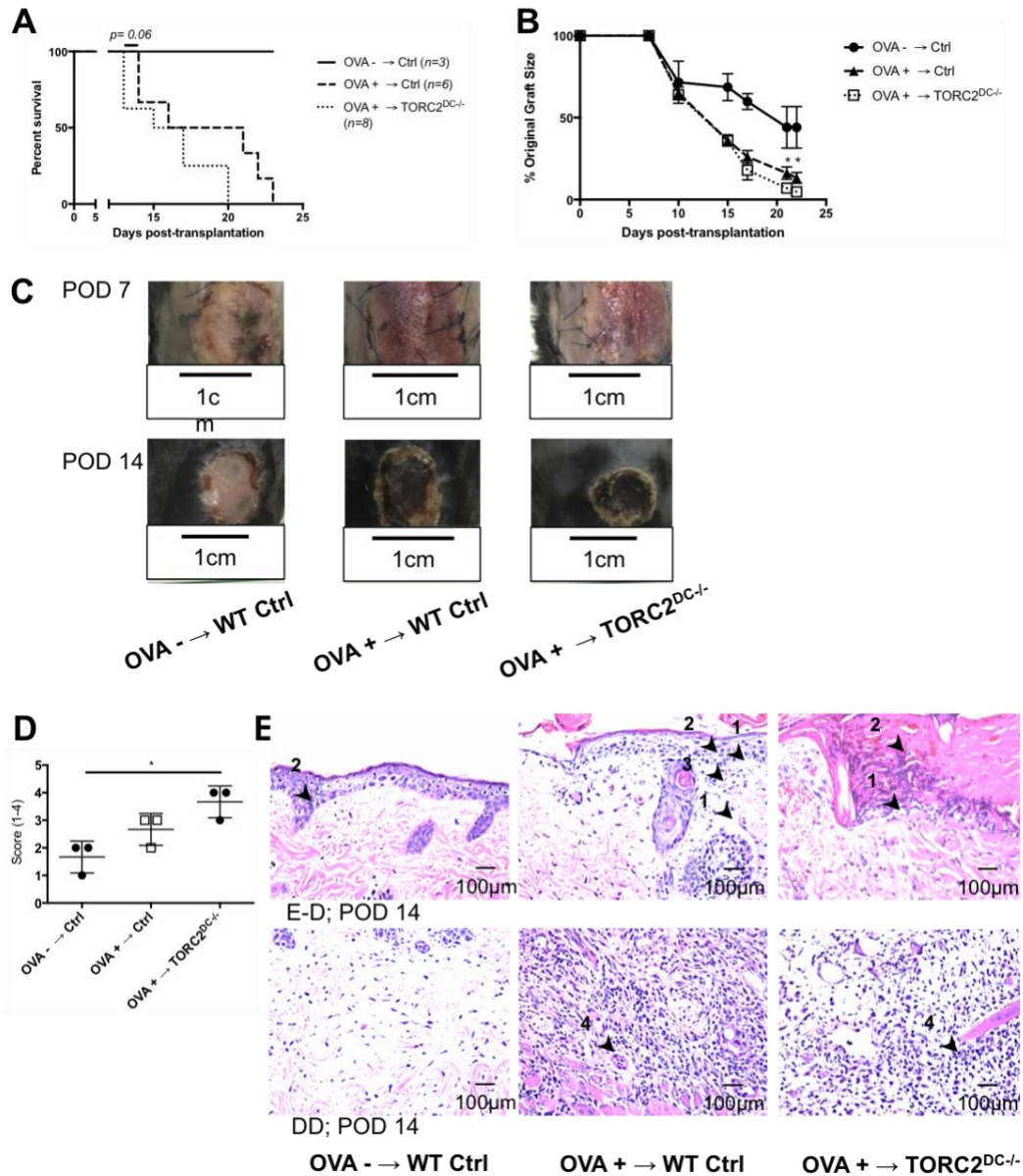
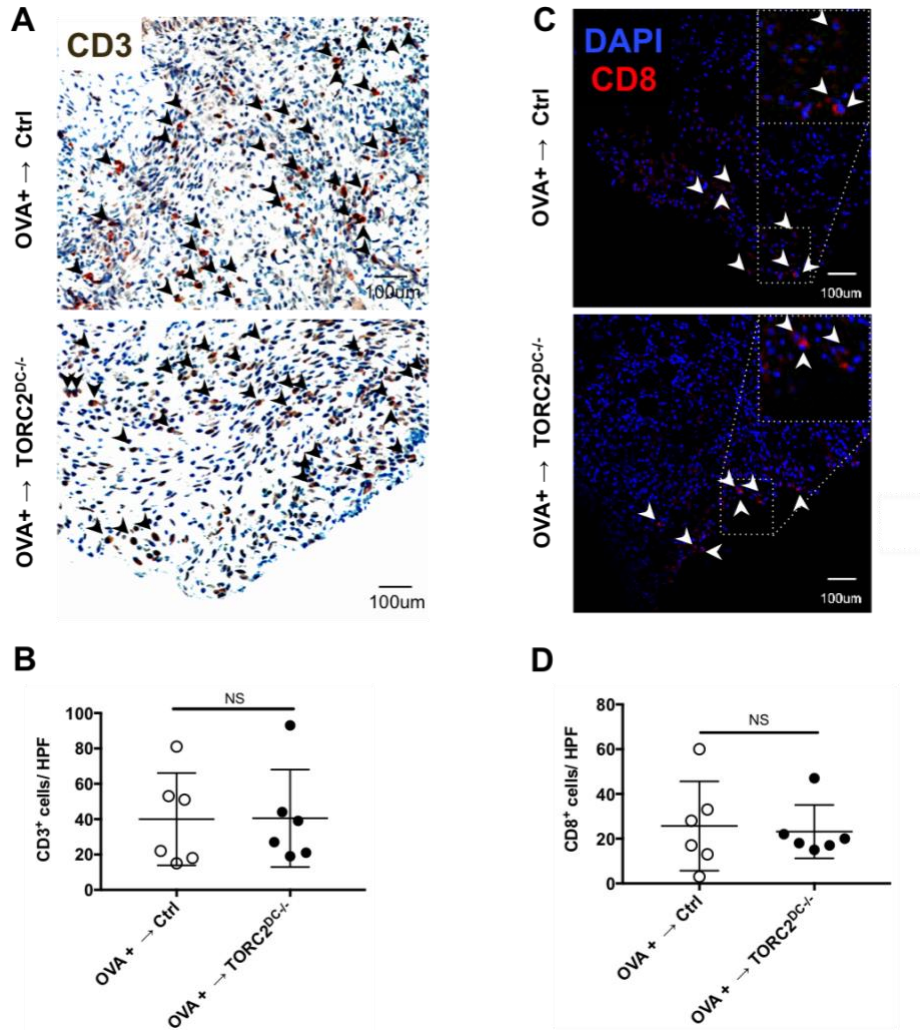


**Figure 12. Skin graft rejection is not affected in TORC2<sup>DC-/-</sup> recipients.**

B6 WT Ctrl or B6 TORC2<sup>DC-/-</sup> mice received full-thickness skin grafts from either B6 OVA<sup>-</sup> or B6 OVA<sup>+</sup> mice. (A) Graft survival over time;  $n=3-8$  mice per group, Log-rank test. (B) Size of skin grafts as a percentage of original size over time;  $n=3-8$  mice per group Student's *t*-test, \*,  $p < 0.05$ . (C) Representative gross morphology of skin grafts at POD 7 and 14. (D) Banff scores of skin grafts at POD 14;  $n=3$  mice per group, Student's *t*-test, \*,  $p < 0.05$ . (E) Representative H&E staining of skin grafts at POD 14 showing the epidermal-dermal junction (E-D; above) and deep dermal layer (DD; below). Arrowheads indicate (1) vacuolar damage, (2) pathological dyskeratosis, (3) lichenoid infiltrate/interface dermatitis and (4) vasculitis.

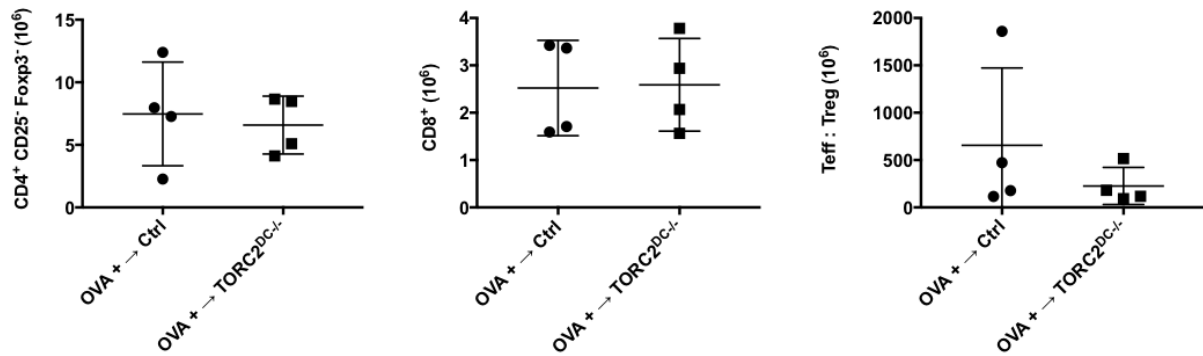
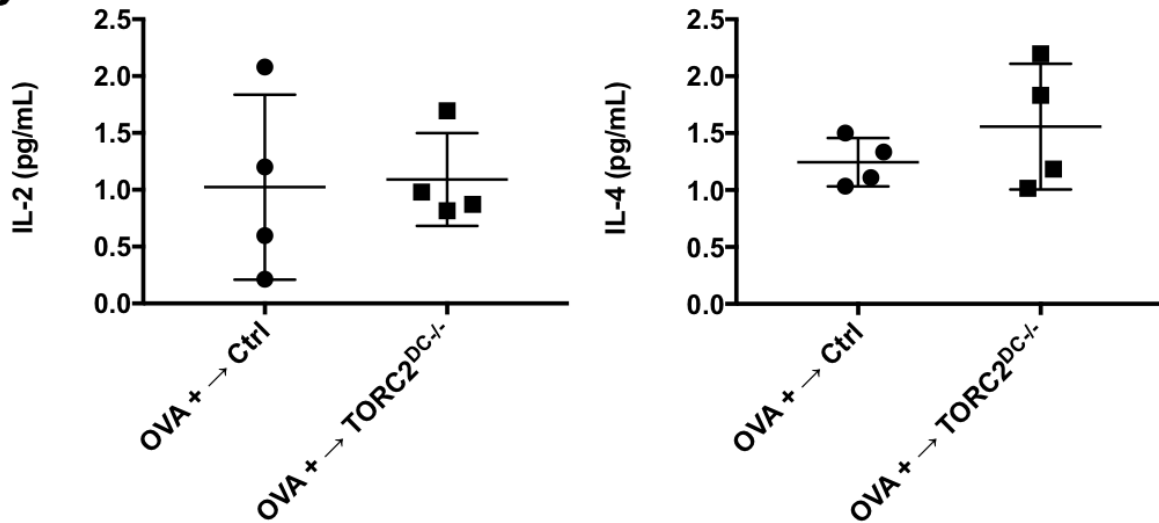
### **3.3.11 OVA<sub>tg</sub> skin grafts in TORC2<sup>DC-/-</sup> recipients do not exhibit enhanced T cell infiltrates**

As with the skin transplants from TORC2<sup>DC-/-</sup> donors in WT recipients, we assessed the T cell response to OVA<sub>tg</sub> grafts in TORC2<sup>DC-/-</sup> recipients. Grafts were stained for CD3<sup>+</sup> (**Figure 13A**; quantified in **Figure 13B**) and CD8<sup>+</sup> cells (**Figure 13C**; quantified in **Figure 13D**) on POD 7 to characterize and quantify the T cell infiltrate. There were no differences in numbers of CD3<sup>+</sup> or CD8<sup>+</sup> cells between the OVA<sup>+</sup> → Ctrl and OVA<sup>+</sup> → TORC2<sup>DC-/-</sup> grafts. There were also no differences in numbers of CD3<sup>+</sup>, CD4<sup>+</sup>, CD8<sup>+</sup>, B220<sup>+</sup> or Ly6G/C<sup>+</sup> cells in secondary lymphoid tissue or in the Teff:Treg ratio or the low cytokine production by T cells between the groups (**Figures 14 and 15**). Thus, in contrast to transplants from TORC2<sup>DC-/-</sup> donors in WT recipients, grafts from WT donors to TORC2<sup>DC-/-</sup> recipients did not exhibit augmented T cell responses or increased tissue injury.



**Figure 13. OVA skin grafts in TORC2<sup>DC-/-</sup> recipients do not elicit augmented T cell infiltration into the graft**

T cell infiltration was analyzed in skin grafts from WT and TORC2<sup>DC-/-</sup> donors on POD 7. (A) Representative staining for CD3<sup>+</sup> cells (arrowheads);  $n=6$  mice per group. (B) Numbers of CD3<sup>+</sup> cells (red) per high power field (hpf);  $n=6$  mice per group; NS = not significant; Student's t-test. (C) Representative staining for CD8<sup>+</sup> cells (arrowheads);  $n=6$  mice per group. (D) Numbers of CD8<sup>+</sup> cells;  $n=6$  mice per group. Student's t-test.

**A****B**

**Figure 14. OVA<sub>13</sub> skin grafts in TORC2<sup>DC-/-</sup> recipients do not enhance T cell numbers in the regional LNs and, in response to donor antigen, these T cells do not produce increased IL-2 or IL-4 compared to WT recipients**

On POD 7, T cells were isolated from the axillary LN of skin graft recipients. (A) Numbers of CD4<sup>+</sup> T effector (T<sub>eff</sub>) cells (CD3<sup>+</sup> CD4<sup>+</sup> Foxp3<sup>-</sup>), CD8<sup>+</sup> cells and the ratio of T<sub>eff</sub>:T<sub>reg</sub> (CD3<sup>+</sup> CD4<sup>+</sup> Foxp3<sup>+</sup>) cells. (B) Isolated T cells were co-cultured with splenic DC from OVA<sub>13</sub> mice for 3 d and IL-2 and IL-4 levels in the culture supernatants determined by ELISA. *n*=4 mice per group. All differences between groups were not significant (Student's 't' test).

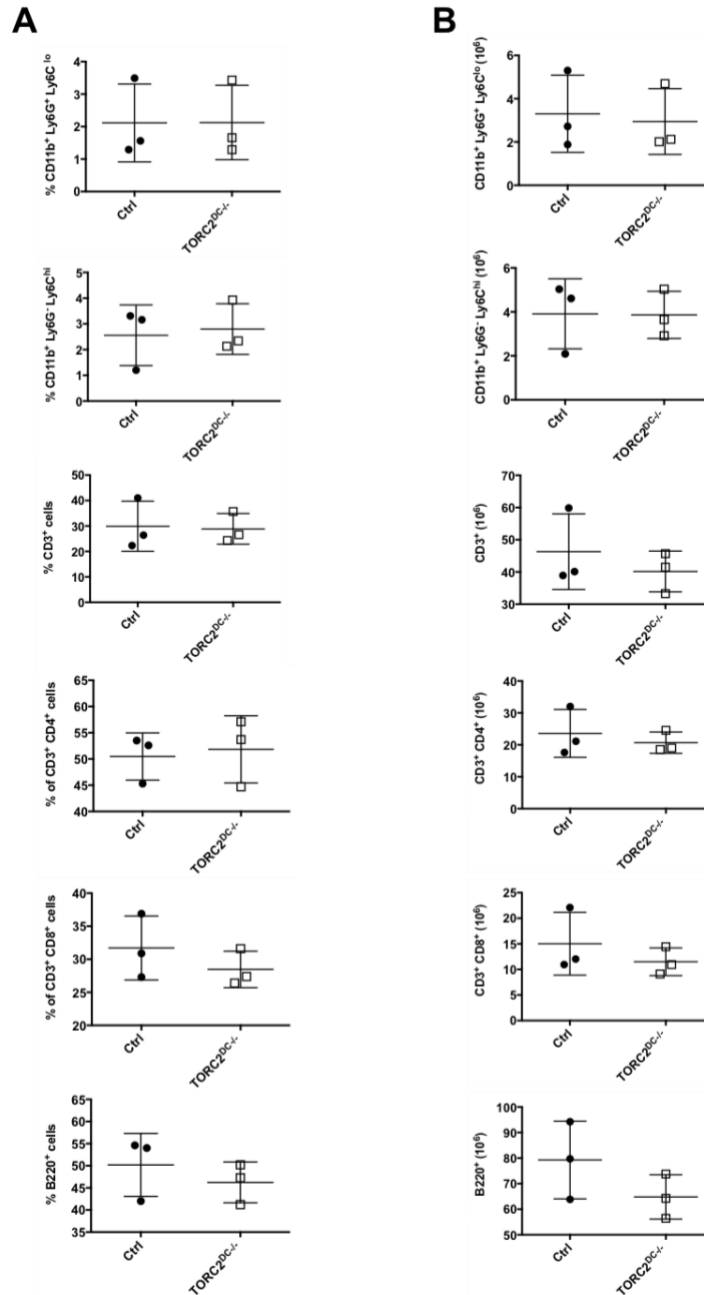


**Figure 15. TORC2<sup>DC-/-</sup> B6 mice show no significant differences in immune cell populations compared with WT B6 Ctrl mice**

Splenocytes were harvested from naïve mice and assessed via flow cytometry. (A) Percentages of polymorphonuclear MDSCs (CD11b<sup>+</sup> Ly6G<sup>+</sup> Ly6C<sup>lo</sup>), monocytic MDSCs (CD11b<sup>+</sup> Ly6G<sup>-</sup> Ly6C<sup>hi</sup>), CD3<sup>+</sup> T cells, CD4<sup>+</sup> T cells, CD8<sup>+</sup> T cells and B cells (B220<sup>+</sup>). (B) Absolute numbers of cells from (A). *n*=3 mice per group. All differences between groups were not significant (Student's 't' test).

### 3.4 Discussion

We have reported previously<sup>88</sup> that ex vivo-generated, conventional BM-derived myeloid DC lacking functional mTORC2 display an enhanced pro-inflammatory phenotype and can augment allogeneic Th1/Th17 polarization and proliferation in vitro, as well as Ag-specific Th1/Th17 responses in vivo. We now show, using a non MHC-mismatched (M→F) transplant model in which rejection occurs in response to male HY Ag<sup>121</sup>, that TORC2<sup>DC-/-</sup> skin grafts undergo accelerated rejection, accompanied by enhanced CD8<sup>+</sup> T cell responses. While it has been reported that conditional disruption of mTORC1 in DC dysregulates epidermal Langerhans cell (LC) homeostasis<sup>122</sup> and that, based on inactivation of mTOR complexes specifically in the epidermis, both mTORC1 and mTORC2 in keratinocytes are integral components of skin morphogenesis<sup>123</sup>, conditional deletion of mTORC2 in DC does not impact skin morphogenesis. Moreover, in the present study, histological comparison of naïve trunk skin between TORC2<sup>DC-/-</sup> and WT B6 male skin did not reveal any morphological differences. Thus, inherent anatomic or skin-resident DC homeostatic abnormalities are unlikely to account for the accelerated failure/rejection of TORC2<sup>DC-/-</sup> grafts that we observed.

Donor DC are required for direct priming of immune responses to Ags expressed by MHC-mismatched grafts. With MHC-matched, minor H Ag-mismatched grafts (such as donor male skin grafts in syngeneic female recipients), the intensity of the T cell response to directly-presented Ags is reduced, while the indirect pathway of Ag recognition is also thought to be important<sup>107</sup>. However, conditional depletion of epidermal LC or conventional dermal DC in

male skin grafts prolongs graft survival but does not prevent their rejection in female recipients<sup>107</sup> and delayed rejection is correlated with delayed expansion of HY Ag-specific CD8<sup>+</sup> T cells. Therefore, the ability of interstitial donor mTORC2<sup>-/-</sup> DC in this study to elicit enriched CD8<sup>+</sup> T cell responses not only highlights the importance of CD8<sup>+</sup> T cells in graft rejection, but also mirrors our previous finding that intratumoral injection of syngeneic BM-derived mTORC2<sup>-/-</sup> DC delays B16 melanoma growth in a CD8<sup>+</sup> T cell-dependent manner<sup>90</sup>. Moreover, the increased incidence of CD8<sup>+</sup>PD-1<sup>+</sup> T cells elicited by interstitial donor mTORC2<sup>-/-</sup> DC suggests these T cells are also more activated, as PD-1 expression has been used to identify tumor-reactive CD8<sup>+</sup> tumor-infiltrating T cells<sup>124,125</sup>. Although overexpression of PD-1 has been associated with T cell exhaustion<sup>126</sup>, we did not observe any significant differences in the intensity of PD-1 expression by graft-infiltrating CD8<sup>+</sup> PD-1<sup>+</sup> T cells.

As we observed within the minor H Ag-mismatched grafts, elevated numbers of CD8<sup>+</sup> T cells were also found in regional LN of TORC2<sup>DC-/-</sup> skin recipients. Moreover, TORC2<sup>DC-/-</sup> graft recipient T cells produced elevated levels of pro-inflammatory IFN $\gamma$  and IL-2 in response to donor Ag stimulation. IFN $\gamma$  is well-known to skew CD4<sup>+</sup> T cell responses to a Th1 phenotype<sup>127</sup> and has also been implicated in direct control of CD8<sup>+</sup> T cell expansion<sup>128</sup>.

In addition to enhanced T cell infiltration, we also observed greater collagen degradation in the minor H Ag-mismatched TORC2<sup>DC-/-</sup> grafts. Collagen degradation is found in rejecting bilayered skin constructs grafted onto patients with chronic wound-healing defects<sup>129</sup> and collagen type I formation is a positive indicator of graft survival in facial plastic and reconstructive surgery<sup>130</sup>. Thus, pronounced collagen degradation in the TORC2<sup>DC-/-</sup> skin grafts provides additional evidence of their enhanced rejection compared to WT grafts.

We also investigated whether DC-specific mTORC2 deficiency in donor grafts would accelerate rejection in a full-MHC mismatch model, in which the donor Ag-specific precursor T cell population is larger than that in a non-MHC mismatch, minor mismatch model. Although there was a trend for TORC2<sup>DC-/-</sup> B6 → BALB/c grafts to fail more rapidly than Ctrl B6 → BALB/c grafts, this was not statistically significant. However, draining LN of the TORC2<sup>DC-/-</sup> graft recipients contained more activated CD8<sup>+</sup> T cells, based on their expression of PD-1. Moreover, when stimulated with donor Ag, CD8<sup>+</sup> T cells from TORC2<sup>DC-/-</sup> graft recipients had a significantly higher division index, indicative of multiple divisions per cell. In addition, LN T cells from TORC2<sup>DC-/-</sup> graft recipients produced more IFN $\gamma$  and GrB than Ctrl graft recipient T cells. As it has been demonstrated that CD8<sup>+</sup> T cells are critical for the production of GrB in rejecting skin grafts<sup>131</sup>, this provides further evidence of the augmented ability of mTORC2<sup>-/-</sup> DC to stimulate CD8<sup>+</sup> T cells in the context of skin transplantation.

Defects in wound healing can cause graft displacement and loss of function<sup>132</sup>, while treatment of transplant recipients with the mTORC1 inhibitor rapamycin impairs wound healing via its lymphopenic properties<sup>133</sup>. However, we do not believe that impaired wound healing contributed to the accelerated rejection of TORC2<sup>DC-/-</sup> grafts as this effect has not been ascribed to mTORC2 inhibition. Additionally, since DC and T cells positively regulate wound healing<sup>134</sup> and since mTORC2<sup>-/-</sup> DC augment graft T cell infiltration, impaired wound healing is considered unlikely.

We also examined, conversely, the fate of WT skin grafts in TORC2<sup>DC-/-</sup> recipients. Donor-derived DC have long been regarded (via the direct pathway of allorecognition) as instigators of acute, MHC-mismatched allograft rejection, but are thought to be eliminated soon after transplant, while host DC have been implicated (via the indirect pathway) in

development/maintenance of chronic rejection. Recent evidence<sup>115</sup> acquired using the tg OVA Ag skin transplant model suggests however that, by acquiring intact donor MHC class I Ag (semi-direct allorecognition) host DC may play an essential role in the instigation/regulation of acute rejection. Utilizing this OVA<sup>tg</sup> skin transplant model in which OVA functions as a minor H Ag<sup>108</sup> to investigate whether mTORC2 deficiency in host DC that indirectly/semi-directly present donor Ag affects skin graft outcome, we did not observe any significant difference in graft rejection. OVA may not be captured efficiently by recipient APC that repopulate the graft<sup>108</sup> with the result that absence of mTORC2 in host DC does not significantly affect graft survival. Pronounced CD8<sup>+</sup> T cell infiltrates were observed in both WT Ctrl and TORC2<sup>DC-/-</sup> recipients of these minor H Ag-mismatched grafts at POD 7. When considered together with the data showing no differences in numbers of CD4<sup>+</sup> Teff, CD8<sup>+</sup> T cells or CD4<sup>+</sup>Treg at POD 7 within regional LN, or differences in cytokine production following host T cell challenge with OVA<sup>+</sup> DC, it appears that selective mTORC2 deficiency in recipient DC does not affect T cell-mediated graft rejection in this model.

Based upon all of the data in Chapter 3, it is clear that mTORC2 deficiency in donor DC accelerates graft rejection and enhances recipient CD8<sup>+</sup> T cell responses to donor Ag. However, while we have previously published on the pro-inflammatory phenotype and function of bone marrow-derived mTORC2-deficient DC, we had never conducted a parallel study of skin-resident DC. Therefore, we next assessed if skin resident DC in TORC2<sup>DC-/-</sup> were more inflammatory than in Ctrl mice.

## **4.0 DC-Specific mTORC2 Deletion Augments Cell-Mediated Delayed Type Hypersensitivity (DTH) Responses**

### **4.1 Introduction**

Contact hypersensitivity, also known as cell-mediated DTH and DTH type IV is a DC-dependent, T cell-mediated response to haptens which occurs in two phases: the sensitization phase in which skin-resident DC capture haptens and migrate to the proximal LN and activate precursor T cells, and the elicitation phase in which re-exposure to the same hapten at a different site on the skin activates leads to rapid recruitment and activation of hapten-specific T cells and subsequent localized inflammatory response at the secondary site. This inflammatory response is mainly mediated by recruitment of cytotoxic CD8<sup>+</sup> T cells to the site of elicitation<sup>135,136</sup>.

One well-established and characterized model of cutaneous DTH-IV utilizes the hapten 2,4-dinitrofluorobenzene (DNFB)<sup>137</sup>. To investigate if skin-resident DC in TORC2<sup>DC-/-</sup> mice were more inflammatory, we utilized DNFB for the sensitization/elicitation of a DTH response, then measured inflammation as an increase in ear thickness (the secondary hapten application site) following elicitation. We also quantified the numbers of CD8<sup>+</sup> T cells and Ly6G/C<sup>+</sup> inflammatory monocytes within the ear following elicitation.

## 4.2 Methods

### 4.2.1 Mice

TORC2<sup>DC-/-</sup> mice (as described in section 3.2.1) were utilized for these experiments, and CD11c-Cre- littermates were used as negative controls. All studies were performed according to an Institutional Animal Care and Use Committee-approved protocol in accordance with NIH guidelines.

### 4.2.2 DTH assay

Cutaneous DTH reactions to DNFB were induced and elicited (in ear pinnae) as described<sup>138</sup> with minor modifications<sup>139</sup>. On day 0, mice were sensitized on the abdomen with 1% DNFB (Sigma Aldrich 42085) mixed in a 1:4 ration of acetone and olive oil. On day 5, mice were elicited with 0.5% DNFB on the ear pinnae. 24, 48, and 72 hours post-elicitation, ear thickness was quantified using an electronic caliper (Mitutoya 700-118-20, Aurora, IL). Thickness of the non-elicited ear was used as the baseline.

### 4.2.3 Immunohistochemistry and Immunofluorescence

DNFB-challenged and control ear pinnae were obtained 72 hours post-challenge, flash-frozen and embedded in OCT compound. Cryostat sections (7 $\mu$ m) were fixed in 4% v/v PFA at room temperature for 1 hour. Sections were H&E stained or stained for CD8 $\alpha$  (eBioscience; clone# 53-

6.7) or Ly6G/C (eBioscience; RB6-8C5) and counterstained with DAPI. Images were recorded using an Olympus Provis fluorescent microscope (H&E, Ly6G/C) or an Olympus Fluoview 1000 confocal microscope (CD8).

#### 4.2.4 Statistical analyses

Results are expressed as means  $\pm$  1SD. Significances of differences between groups were determined via Student's 't'-test, with  $p < 0.05$  considered significant.

### 4.3 Results

#### 4.3.1 TORC2<sup>DC-/-</sup> mice exhibit enhanced cutaneous DTH responses

Utilizing a cell-mediated DTH model in which the skin was sensitized with DNFB, then challenged 5 days later with DNFB, TORC2<sup>DC-/-</sup> mice exhibited significant increases in responses compared with WT Ctrl animals (**Figure 16A**). These enhanced responses were accompanied by increases in epidermal thickness (**Figure 16B**) and significant increases in CD8<sup>+</sup> T cell infiltration (**Figure 16C, D**). Moreover, significant increases in skin-infiltrating Ly6G/C<sup>+</sup> cells (**Figure 16E, F**) were also observed in TORC2<sup>DC-/-</sup> mice.

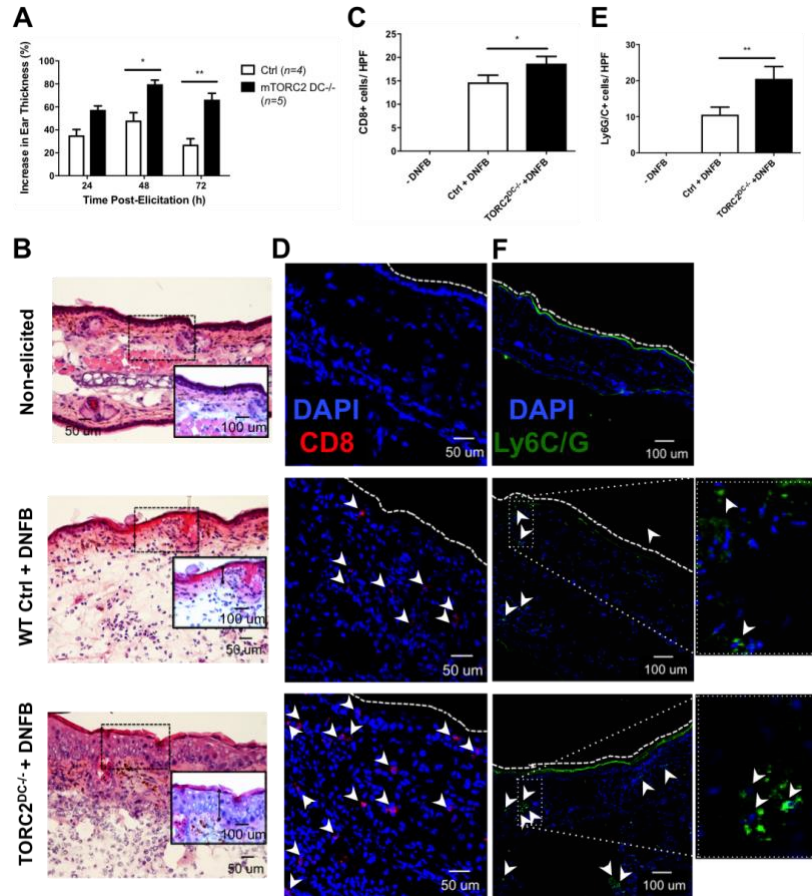


**Figure 16. TORC2<sup>DC-/-</sup> mice exhibit enhanced delayed-type hypersensitivity responses**

Female WT Ctrl or TORC2<sup>DC-/-</sup> mice were sensitized with DNFB on the skin of the abdomen on day 0, then challenged 5 days later with DNFB on the right ear pinna to elicit a DTH response. (A) Percent increase in pinna thickness of the elicited ear compared with the non-elicited ear 24, 48, and 72h post-challenge; Student's t-test \*,  $p < 0.05$ ; \*\*,  $p < 0.01$ . (B) Representative H&E staining of non-elicited and DNFB-challenged ears, as indicated; images are representative of  $n=4-5$  mice. Insets are higher power views of the areas highlighted. Vertical inverted arrows indicate thickness of the epidermal layer. (C) Numbers of CD8<sup>+</sup> cells within the ear pinna 72h post-challenge;  $n=3$  high-powered fields (HPF) per mouse; 4-5 mice per group; Student's t-test, \*,  $p < 0.05$ . (D) Representative immunofluorescence (IF) DAPI (blue) and CD8 (red) staining (arrowheads) of non-elicited and challenged ears. (E) Numbers of Ly6G/C<sup>+</sup> cells within the ear pinna 72h post-challenge;  $n=4-5$  mice per group; Student's t-test, \*\*,  $p < 0.01$ . (F) Representative IF DAPI (blue) and Ly6G/C (green; arrowheads) staining of non-elicited and challenged ears. Images on the far right are higher power views of the areas outlined by dotted lines in (F).

#### 4.4 Discussion

The enhanced cutaneous DTH responses we observed in TORC2<sup>DC-/-</sup> compared to Ctrl mice were characterized by increased CD8<sup>+</sup> T cell and Ly6C/G<sup>+</sup> myeloid cell infiltration, confirming that the absence of functional mTORC2 in skin-resident DC induced augmented cutaneous cell-mediated immunity. The type of responses that we examined (T cell-mediated contact hypersensitivity) are dependent on epidermal immunomodulatory LC that express CD11c<sup>140</sup>, capture the sensitizing hapten and migrate to regional LN for direct presentation to CD8<sup>+</sup> T cells (the predominant effectors of contact hypersensitivity<sup>141-143</sup>) and also on dermal DC<sup>144</sup> that can also play essential roles in inducing immunity<sup>41,145</sup>. Since LC have also been shown to dampen murine contact hypersensitivity responses by tolerizing CD8<sup>+</sup> T cells<sup>146,147</sup>, the augmented responses seen in TORC2<sup>DC-/-</sup> skin may be a consequence of reduction in their immunoregulatory function. However, if the skin-resident DC in TORC2<sup>DC-/-</sup> mice were more readily able to migrate from the hapten site to the proximal LN, this could also explain these results. Therefore, we next set out to investigate if TORC2<sup>DC-/-</sup> skin DC may have an altered migratory ability.

## **5.0 Cutaneous DC Deficient in mTORC2 Do Not Display Defects in Migration or Lymph Node Homing**

### **5.1 Introduction**

Migration of LC from the epidermis to the dLN through afferent lymph following hapten exposure is crucial for the presentation of hapten Ag to T cells within the LN and there subsequent activation and inflammatory response. While not demonstrated in DC, other cell types in which TORC2 was inhibited or functionally deleted have displayed defects in their migratory capacity. In breast cancer cell lines, targeted knockdown of mTORC2 has been demonstrated to inhibit their migration<sup>148</sup>. In neutrophils, mTORC2 has been demonstrated to impact actin dynamics, and thereby promote chemotaxis through cell-rear contraction<sup>149</sup>. We therefore had to ascertain if deletion of mTORC2 in skin-resident DC would impact their migration to dLN, as this would impact their T cell stimulatory function.

To assess the migratory capacity of skin-resident DC, we utilized FITC as a hapten applied to the ear pinnae of TORC2<sup>DC-/-</sup> and Ctrl mice, then analyzed the prevalence of FITC<sup>+</sup> cDCs within the draining superficial and deep cervical LN via flow cytometry. In addition, we also analyzed the expression of CCR7, a critical chemokine receptor in DC LN homing. Finally, we assessed the expression of the co-stimulatory molecule CD86 and the co-inhibitory molecule PD-L1 by the migrating FITC<sup>+</sup> cDC within the dLN. This would give insights not only into the migratory capacity of skin-resident DC, but also the phenotype of the migrating DC.

## 5.2 Methods

### 5.2.1 Mice

TORC2<sup>DC-/-</sup> mice (as described in section 3.2.1) were utilized for these experiments, and CD11c-Cre- littermates were used as negative controls. All studies were performed according to an Institutional Animal Care and Use Committee-approved protocol in accordance with NIH guidelines.

### 5.2.2 *In vivo* migration assay

One percent v/v FITC (Sigma Aldrich; cat # F3651) in 1:1 acetone: dibutyl phthalate was applied to the dorsal surface of the ear pinna and 24 hours later, cells were isolated from the superficial and deep cervical LN.

### 5.2.3 Flow cytometry

Cells were stained with mAbs against CD11c (clone #N418), I-A<sup>b</sup> (AF6-120.1), CCR7 (4B12), CD86 (GL-1) and B7-H1 (10F 9G2) (all BioLegend), then fixed with 2% v/v PFA. Flow data were acquired using a Fortessa flow cytometer (BD Biosciences, San Jose, CA) and analyzed using FlowJo (Tree Star, Ashland, OR).

## 5.2.4 Statistical analyses

Results are expressed as means  $\pm$  1SD. Significances of differences between groups were determined via Student's 't'-test, with  $p < 0.05$  considered significant.

## 5.3 Results

### 5.3.1 TORC2<sup>DC-/-</sup> mice do not exhibit alterations in skin DC migration, but display a more pro-stimulatory DC phenotype than WT Ctrl mice

To investigate whether the augmented cutaneous cell-mediated inflammatory responses observed in TORC2<sup>DC-/-</sup> mice could be ascribed to altered DC phenotype and/or DC migratory capacity, we painted the ear pinnae of TORC2<sup>DC-/-</sup> or WT Ctrl mice with FITC. After 24h, cells in the draining superficial and deep cervical LN were isolated and migratory DC identified as FITC<sup>+</sup>. There were no significant differences between WT Ctrl and TORC2<sup>DC-/-</sup> mice in terms of total number of CD11c<sup>+</sup> DC (**Figure 17A**), FITC<sup>+</sup>CD11c<sup>+</sup>I-A<sup>b</sup> hi DC (**Figure 17B**), FITC expression by DC (**Figure 17C**) or CCR7 expression on FITC<sup>+</sup> DC (**Figure 17D**). Taken together, these data indicate that mTORC2<sup>-/-</sup> DC did not differ in their migratory capacity compared with Ctrl DC. On the other hand, while co-stimulatory CD86 expression did not differ on migrating FITC<sup>+</sup> DC between WT Ctrl and TORC2<sup>DC-/-</sup> mice (**Figure 17E**), co-inhibitory B7-H1 (PD-L1) expression was reduced significantly on the migrating mTORC2<sup>DC-/-</sup> compared to WT Ctrl DC (**Figure 17F**), suggesting enhanced T cell stimulatory potential of the LN-homing mTORC2-deficient skin DC.

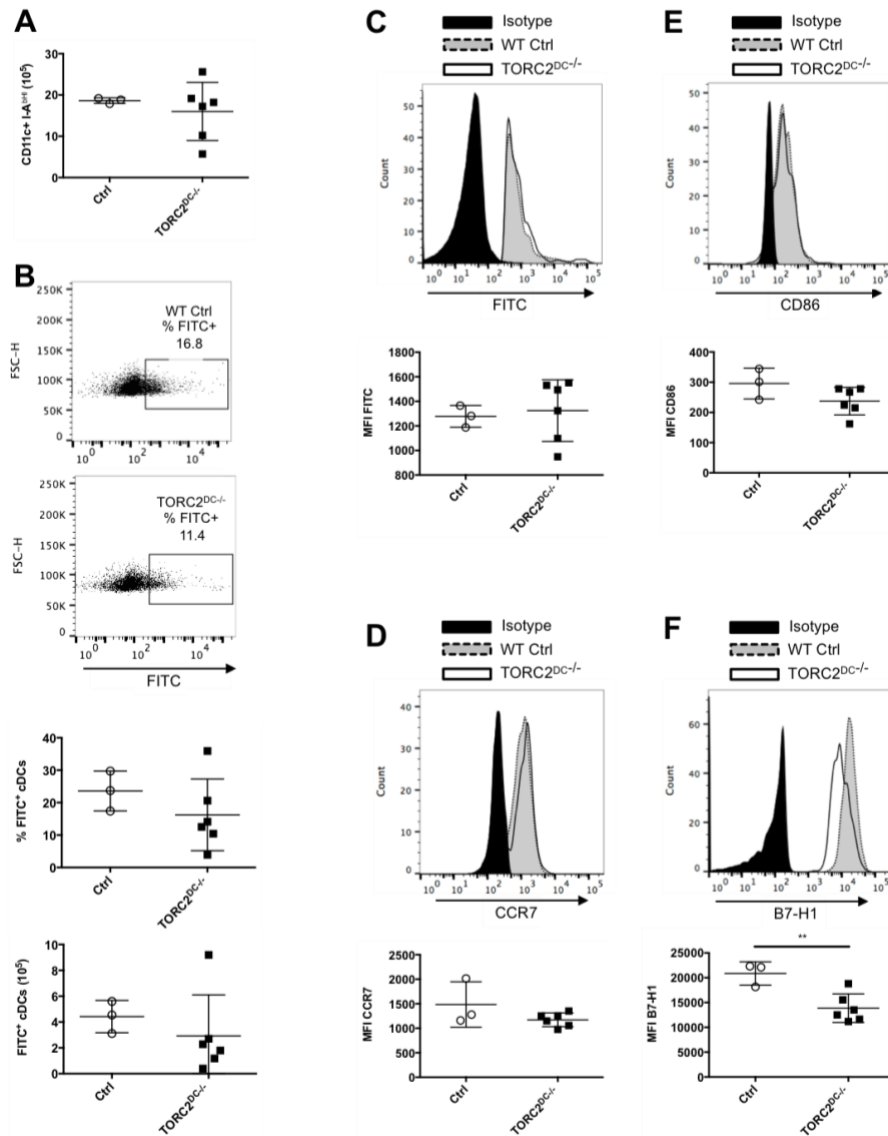


**Figure 17. TORC2<sup>DC-/-</sup> mice do not exhibit enhanced skin DC migration to regional LN, but display reduced B7-H1 (PD-L1) expression on DC compared with WT control mice**

WT control (Ctrl) or TORC2<sup>DC-/-</sup> B6 mice were painted with FITC on the back of the ear pinna and cells were isolated from the cervical LNs after 24 h. (A) Numbers of (CD11c<sup>+</sup>IA<sup>b hi</sup>) DC in the LN. (B) Incidence and absolute

numbers of FITC<sup>+</sup> cDCs (CD11c<sup>+</sup> I-A<sup>b</sup> hi). (C) Top, representative flow profiles and below, mean intensity (MFI) of FITC staining on FITC<sup>+</sup> DC. (D) Top, representative flow profiles and below, mean fluorescence intensity (MFI) of CCR7 staining on FITC<sup>+</sup> DC. (E) Top, representative flow profiles and below intensity (MFI) of CD86 staining on FITC<sup>+</sup> DC. (F) Top, representative flow cytometry and below, intensity (MFI) of B7-H1 staining on FITC<sup>+</sup> DC in LN. *n*=3-6 mice per group; Student's t-test, \*, *p* < 0.05; \*\*, *p*<0.01.

## 5.4 Discussion

Previous studies have implicated a role for mTORC2 in regulation of cell migration. Thus, breast cancer cells lacking mTORC2 function exhibit reduced migratory function<sup>148</sup>. Whether mTORC2 affects skin DC migration following hapten sensitization has not previously been examined. We therefore considered whether the enhanced cutaneous cell-mediated immune reactions that we observed in TORC2<sup>DC-/-</sup> mice might reflect altered migration of skin-resident TORC2<sup>DC-/-</sup> to secondary lymphoid tissue. However, we did not observe any significant differences in skin DC migration to regional LN between Ctrl and TORC2<sup>DC-/-</sup> mice, or in acquisition/expression of the sensitizing agent by migrating, hapten-expressing (FITC<sup>+</sup>) DC between Ctrl DC and TORC2<sup>DC-/-</sup> DC. There was also no significant difference in the expression by these DC of CCR7, a chemokine receptor that guides their migration to cognate ligands in secondary lymphoid tissue<sup>150</sup>. Taken together, these data suggest that the accelerated rejection of minor H Ag-mismatched TORC2<sup>DC-/-</sup> skin grafts and the enhanced cutaneous DTH responses in TORC2<sup>DC-/-</sup> mice are not due to significant alterations in DC migration to regional lymphoid tissue. Interestingly, however, migratory mTORC2-deficient DC displayed decreased cell surface B7-H1 (PD-L1) expression relative to unmodified costimulatory CD86 expression, indicative of

a more T cell stimulatory phenotype and providing further evidence that skin-resident DC that specifically lack mTORC2 are more immunostimulatory than Ctrl skin-resident DC.

## 6.0 mTORC2 Retrains mTORC1-REGULATED Metabolic Function in DC

### 6.1 Introduction

Recent studies have also linked mTOR function with metabolic programming in immune cells<sup>92,93,151-159</sup>. While naïve T cells have low bioenergetic demands, activated T cells must be able to grow and proliferate, as well as produce cytokines and effector molecules<sup>160</sup>. To rapidly increase their biosynthetic capacity, activated T cells undergo a switch in glucose metabolism from oxidative phosphorylation to aerobic glycolysis<sup>160,161</sup>. This metabolic reprogramming from quiescence allows T cells to use glucose as a carbon source in the form of lactate for many biosynthetic processes, including lipogenesis, nucleic acid synthesis, and amino acid synthesis<sup>162</sup>. As aerobic glycolysis only generates about 5% of the amount of ATP oxidative phosphorylation does, activated T cells upregulate expression of glucose transporters such as GLUT1 in order to sustain elevated glycolytic flux necessary to meet the ATP demands of the cell<sup>162,163</sup>.

It has been demonstrated that DN4 thymocytes are reliant on the mTORC1/PI3K signaling axis to upregulate GLUT1 and meet the metabolic demands of development in the thymus<sup>164,165</sup>. There is also evidence to suggest that the mTORC1/PI3K signaling axis may play a minor role in the metabolic reprogramming of activated naïve T cells in the periphery<sup>160</sup>. In addition, while CD8<sup>+</sup> cytotoxic T cells CTLs, Th1, and Th17 CD4<sup>+</sup> T cells are supported by the aerobic glycolytic processes described above, there is evidence that CD8<sup>+</sup> memory T cell and T<sub>Reg</sub> development relies on fatty acid oxidation via mitochondrial oxidative phosphorylation<sup>166</sup>. The differential bioenergetics of memory T cells/T<sub>Regs</sub> and CTLs/Th cells has already been identified as an

immunosuppressive target in solid organ transplantation<sup>167</sup>. Taken together, there is a clear relationship between the function of mTOR and cellular metabolism, and this plays an important role in maintaining T cell phenotype and function after expansion in the context of transplantation. This begs the question of what role mTOR and bioenergetics play in modulating DC phenotype and function in the transplant setting.

Research by Edward and Erika Pearce has highlighted the metabolic phenotype of DCs upon activation via LPS stimulation of TLR4. Like T cells, quiescent DCs have relatively low metabolic needs, yet upon activation these demands greatly increase due to bioenergetic pressure to produce cytokines and upregulate co-stimulatory molecules (unlike T cells, DCs do not proliferate upon activation)<sup>21,22</sup>. Also like T cells, activated DCs undergo a metabolic reprogramming to aerobic glycolysis to meet these new biosynthetic demands<sup>21,22</sup>. Commitment to glycolysis by BMDCs is dependent on the mTORC1/PI3K signaling axis driving expression of iNOS and the transcription factor hypoxia inducible factor 1 Hif-1 $\alpha$ . Hif-1 $\alpha$  induces increased glucose transporter expression, and NO from iNOS poisons the mitochondrial respiratory chain thereby biasing the cell towards glycolysis<sup>168</sup>.

More recently, the Pearce group also identified an mTORC1/PI3K-independent mechanism by which DCs initially convert to aerobic glycolysis following activation<sup>93</sup>. This process is driven by mTORC1/PI3K-independent TBK1/IKK $\epsilon$  phosphorylation and activation of Akt. While the role of mTORC1 was investigated in both initial switch and maintenance of aerobic glycolysis in DCs, to date no studies have been conducted assessing the role of mTORC2 in these processes. As mTORC2 phosphorylates Akt at the hydrophobic S473 and enhances Akt activity, and there is possible interplay between mTORC1 and mTORC2 function<sup>169</sup>, elucidating

the function of mTORC2 in driving metabolic reprogramming in DCs can provide information on how mTORC1 and mTORC2 shape DC phenotype and function.

To investigate the discrete role mTORC2 may play in regulating DC metabolism, we generated BMDC from TORC2<sup>DC-/-</sup> and Ctrl mice. We then measured the glycolytic activity and spare respiratory capacity of these cells via an extracellular flux assay. We also measured the glycolysis and OXPHOS-dependent ATP production of the DC. In addition, we utilized a gene expression panel and qPCR to identify the possible underlying signaling mechanisms by which mTORC2 could regulate DC metabolism.

## **6.2 Methods**

### **6.2.1 Mice**

TORC2<sup>DC-/-</sup> mice (as described in section 3.2.1) were utilized for these experiments, and CD11c-Cre- littermates were used as negative controls. All studies were performed according to an Institutional Animal Care and Use Committee-approved protocol in accordance with NIH guidelines.

### **6.2.2 Bone marrow-derived DC generation**

Femoral BM cells were harvested and cultured as described<sup>170</sup> using mouse recombinant (r)GM-CSF (1000 U/mL; R&D Systems, Minneapolis, MN; CAA26822). On day 6 of culture, DC were

purified using anti-CD11c immunomagnetic beads (Miltenyi Biotec, Bergisch, Germany). Where indicated, the TLR4 ligand LPS (100 ng/mL; *Salmonella minnesota* R595; Alexis Biochemicals, San Diego, CA; ALX-581-008) was used to stimulate the DC for 16-18 h.

### **6.2.3 Extracellular flux assay**

A Seahorse XFe96 Bioanalyzer (Agilent, Santa Clara, CA) was utilized to measure metabolic flux in real-time. DC were plated on Cell-Tak-coated Seahorse culture plates (100,000 cells/well) in assay media consisting of minimal, unbuffered DMEM supplemented with 1% v/v bovine serum albumin (BSA) and 25 mM glucose, 1mM pyruvate, and 2 mM glutamine. Basal extracellular acidification and oxygen consumption rates were taken for 30 min. Cells were stimulated with oligomycin (2  $\mu$ M), the potent mitochondrial oxidative phosphorylation uncoupler carbonyl cyanide 4 p-(trifluoromethoxy) phenylhydrazone (FCCP) that disrupts ATP synthesis (1  $\mu$ M), 2-deoxyglucose (10mM) and rotenone/antimycin A (0.5  $\mu$ M) to obtain maximal respiratory and control values. Where indicated, DC were cultured with rapamycin (10ng/mL; LC Laboratories, Woburn, MA) for 18h after CD11c<sup>+</sup> immunomagnetic bead selection on culture day 6. Where indicated, DC were stimulated with LPS (100 ng/mL) injected either into the extracellular flux system or added to cultures for 18h as indicated above.

#### **6.2.4 ATP production assay**

ATP concentrations were determined using a luciferase-based ATP determination kit (ThermoFisher, Waltham, MA) as per the manufacturer's instructions. Where indicated, DC were stimulated with LPS (100 ng/mL) for 1h.

#### **6.2.5 Mitochondrial staining and flow cytometry**

Mitochondrial mass and membrane potential were assessed using MitoTracker® Green FM (0.1µM, Cell Signaling Technology, Danvers, MA) and tetramethylrhodamine ethyl ester (TMRE; 0.05µM, ThermoFisher, Waltham, MA), respectively according to the manufacturer's instructions.

For assessment of cell viability, cells were stained with ZombieAqua dye (BioLegend, San Diego, CA) according to the manufacturer's instructions. Data were acquired with a Fortessa flow cytometer (BD Biosciences, San Jose, CA) and analyzed using FlowJo (TreeStar, Ashland, OR).

#### **6.2.6 Golgi staining and confocal microscopy**

Cell suspensions were fixed for 1 hr in 2% paraformaldehyde then cytopspin (ThermoFisher CytoSpin 4) onto charged slides (Superfrost/Plus, ThermoFisher, Pittsburgh, PA). Slides were stained with primary antibody directed against Trans Golgi Network 38 (rabbit anti-TGN38, Novus, Littleton, CO) rhodamine Phalloidin (F-actin, ThermoFisher) and 0.1% Hoechst's dye (nuclei, ThermoFisher). Confocal images were obtained by the Center for Biological Imaging,

University of Pittsburgh, on an Nikon A1 Microscope using 100x objective and zoomed using 1.24 Nyquist, Maximum intensity projections were constructed and analyzed using NIS Elements software.

### **6.2.7 Transmission electron microscopy (TEM)**

Cell suspensions were fixed in 2.5% glutaraldehyde then immediately pelleted in a 1.5 ml microfuge tube at 300 x G. Pellets were then post-fixed in 1% OsO<sub>4</sub>, 1% K<sub>3</sub>Fe(CN)<sub>6</sub> and dehydrated through a graded series of 30-100% ethanol, 100% propylene oxide, then infiltrated in 1:1 mixture of propylene oxide:Polybed 812 epoxy resin (Polysciences, Warrington, PA) for 1 hr. After several changes of 100% resin over 24 hrs, pellet was embedded in a final change of resin, cured at 37°C overnight, followed by additional hardening at 65°C for two more days. Ultrathin (70 nm) sections were collected on 200 mesh copper grids, stained with 2% uranyl acetate in 50% methanol for 10 minutes, followed by 1% lead citrate for 7 min. Sections were imaged using a JEOL JEM 1400 transmission electron microscope (Peabody, MA) at 80 kV fitted with a side mount AMT 2k digital camera (Advanced Microscopy Techniques, Danvers, MA).

### **6.2.8 NanoString gene profiling**

Total RNA was extracted from bead-purified CD11c<sup>+</sup> DC generated from bone marrow of Ctrl or TORC2<sup>DC-/-</sup> mice using an RNeasy Mini Kit (Qiagen, Hilden, Germany) as per the manufacturer's instructions. NanoString analysis was performed using a Mouse Immunology Panel (NanoString Technologies, Seattle, WA) as has been previously described<sup>171</sup>.

### **6.2.9 Quantitative PCR**

Total RNA was extracted from bead-purified CD11c<sup>+</sup> DC generated from bone marrow of Ctrl or TORC2<sup>DC-/-</sup> mice using an RNeasy Mini Kit (Qiagen, Hilden, Germany) as per the manufacturer's instructions. cDNA was amplified using Platinum Quantitative PCR SuperMix-UDG (Invitrogen) in 10  $\mu$ l volumes in quadruplicate with gene-specific primers and probed on the ABI Prism 7900HT Sequence Detection System (Applied Biosystems, Foster City, CA) according to the manufacturer's instructions. Thermal cycling conditions were 50°C for 2 min then 95°C for 2 min, followed by 40 cycles of 95°C for 15 sec and 60°C for 1 min. Data were analyzed using the  $\Delta\Delta$ Ct method with expression normalized to the housekeeping gene, glyceraldehyde-3-phosphate dehydrogenase (GAPDH).

### **6.2.10 Statistical analyses**

Results are expressed as mean  $\pm$  1SD. Significances of differences between groups were determined using Student's 't'-test or one-way ANOVA Tukey's multiple comparisons test (GraphPad Prism) as indicated, with  $p < 0.05$  considered significant.

## 6.3 Results

### 6.3.1 TORC2<sup>DC-/-</sup> have augmented glycolytic activity, glycolysis-dependent ATP production and viability compared to Ctrl DC

To investigate the impact of TORC2 deletion on DC metabolic function, we assessed glycolysis via extracellular flux as measured by basal extracellular acidification rate (ECAR). Glycolysis was elevated significantly in both Ctrl DC and TORC2<sup>-/-</sup> DC following LPS stimulation (representative ECAR **Figure 18A**; quantified in **Figure 18B**). Interestingly, glycolytic function was also increased significantly in non-stimulated (ns) TORC2<sup>-/-</sup> DC compared to Ctrl DC, but not in LPS-stimulated TORC2<sup>-/-</sup> DC compared to Ctrl DC. While there was no difference in ATP production between Ctrl DC and TORC2<sup>-/-</sup> DC following inhibition of OXPHOS with oligomycin, TORC2<sup>-/-</sup> DC displayed significantly decreased ATP production when glycolysis was inhibited with 2-deoxyglucose (2-DG) (**Figure 18C**; ns left panel; + LPS 1h right panel). TORC2<sup>-/-</sup> DC stimulated with LPS also had significantly higher viability than Ctrl DC stimulated with LPS (representative histogram **Figure 18D**; quantified in **Figure 18E**); however, the immediate glycolytic response to LPS stimulation was not significantly different between Ctrl DC and TORC2<sup>-/-</sup> DC (representative ECAR **Figure 19A**; quantified in **Figure 19B**).

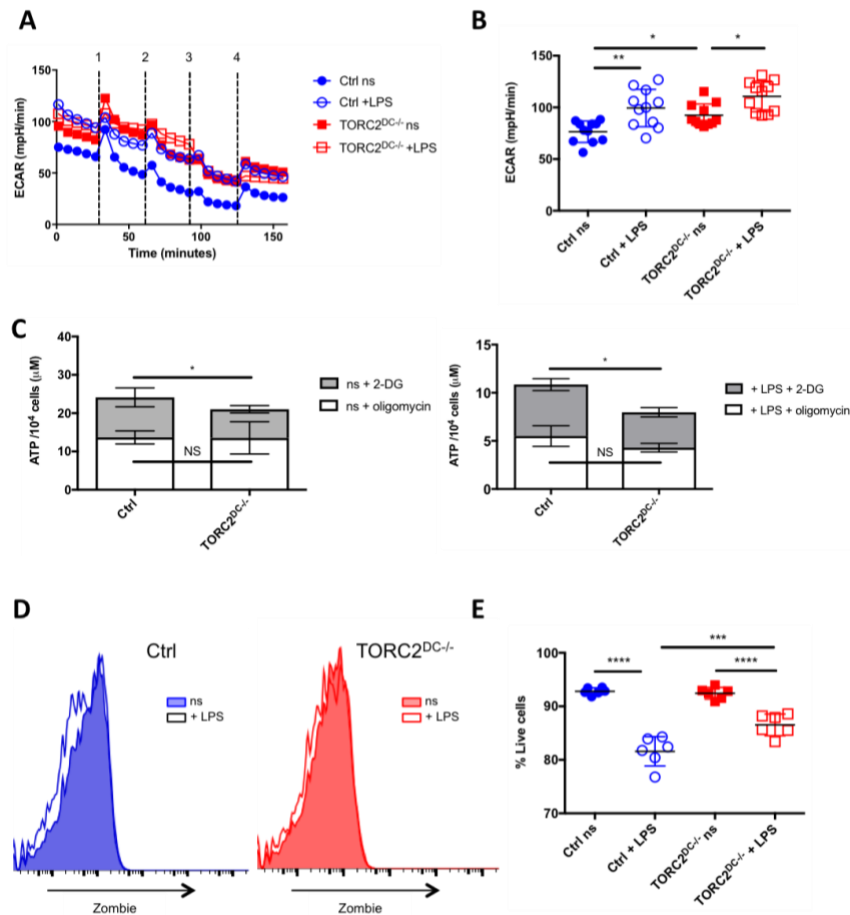


**Figure 18. TORC2<sup>DC-/-</sup> have augmented glycolytic activity, glycolysis-dependent ATP production, and viability as compared to Ctrl DC**

Bone marrow-derived DC were generated from WT Ctrl or TORC2<sup>DC-/-</sup> mice and analyzed using a Seahorse XFe96 Bioanalyzer for metabolic flux in real-time over 150 min with oligomycin (1), FCCP (2), 2-DG (3) and rotenone/antimycin (4) injected at indicated times to obtain control values. DC were stimulated with LPS for 18h as indicated. (A) Representative extracellular acidification rate (ECAR). (B) Quantification of basal glycolysis prior to addition of oligomycin (1);  $n=10-11$  mice; one-way ANOVA Tukey's multiple comparisons test,  $*p<0.05$ ,  $**p<0.01$ . (C) ATP production in non-stimulated DC (left panel) and DC stimulated with LPS for 1 h (right panel) as measured using an ATP determination kit as per manufacturer instructions;  $n=6$  mice; Student's t-test,  $*p < 0.05$ . (D) Representative histogram of Zombie viability dye staining. (E) Quantification of viability as percentage of live (Zombie<sup>-</sup>) cells;  $n=6$  mice; one-way ANOVA Tukey's multiple comparisons test,  $*p<0.05$ ,  $**p<0.01$ ,  $***p<0.001$ ,  $****p<0.0001$ .

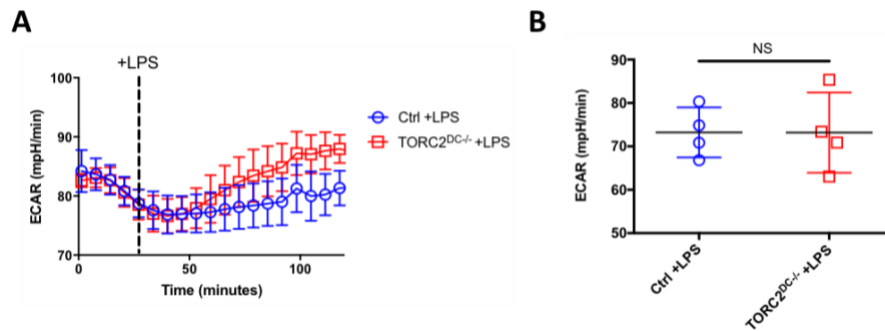


**Figure 19. Quiescent non-stimulated TORC2<sup>DC-/-</sup> display augmented viability following LPS stimulation, but no difference in initial glycolytic function following stimulation as compared to Ctrl DC**

Bone marrow-derived DC were generated from Ctrl or TORC2<sup>DC-/-</sup> mice and stimulated with LPS for 18h as indicated. Cell viability was assessed as the percentage of Zombie<sup>-</sup> cells. (A) Representative histogram, quantified in (B);  $n=6$  mice; one-way ANOVA Tukey's multiple comparisons test, NS = not significant. DC were generated from Ctrl or TORC2<sup>DC-/-</sup> mice and analyzed using a Seahorse XFe96 Bioanalyzer for metabolic flux in real-time over 130 min with LPS injected where indicated; the glycolytic response was measured as the average ECAR post-LPS injection over a 100 min period. (B) Representative ECAR, quantified in (D);  $n=4$  mice; Student's t-test  $*p < 0.05$ .

### 6.3.2 TORC2<sup>DC-/-</sup> have increased spare respiratory capacity (SRC), mitochondrial biomass and mitochondria that fail to depolarize following LPS stimulation

SRC, calculated as the difference in oxygen consumption rate (OCR) measured via extracellular flux after addition of 2-DG (3) and prior to addition of FCCP (1) (visualized as the shaded areas in Fig. 2A), was significantly elevated in non-stimulated TORC2<sup>-/-</sup> DC compared to Ctrl DC (representative OCR **Figure 20A**; quantified in **Figure 20B**). We next assessed how TORC2 deletion in DC would influence mitochondrial phenotype. Mitochondrial mass, as determined by fluorescent mitochondrial labeling, decreased significantly in both Ctrl and TORC2<sup>-/-</sup> DC following LPS stimulation; in addition, non-stimulated TORC2<sup>-/-</sup> DC had significantly greater

mitochondrial mass as compared to non-stimulated Ctrl DC (representative histograms **Figure 20C**; quantified in **Figure 20D**). Surprisingly, TORC2<sup>-/-</sup> DC mitochondria failed to depolarize following LPS stimulation (as opposed to Ctrl DC that did), as assessed via uptake of cationic TMRE fluorescent dye (representative histograms **Figure 20E**; quantified in **Figure 20F**).

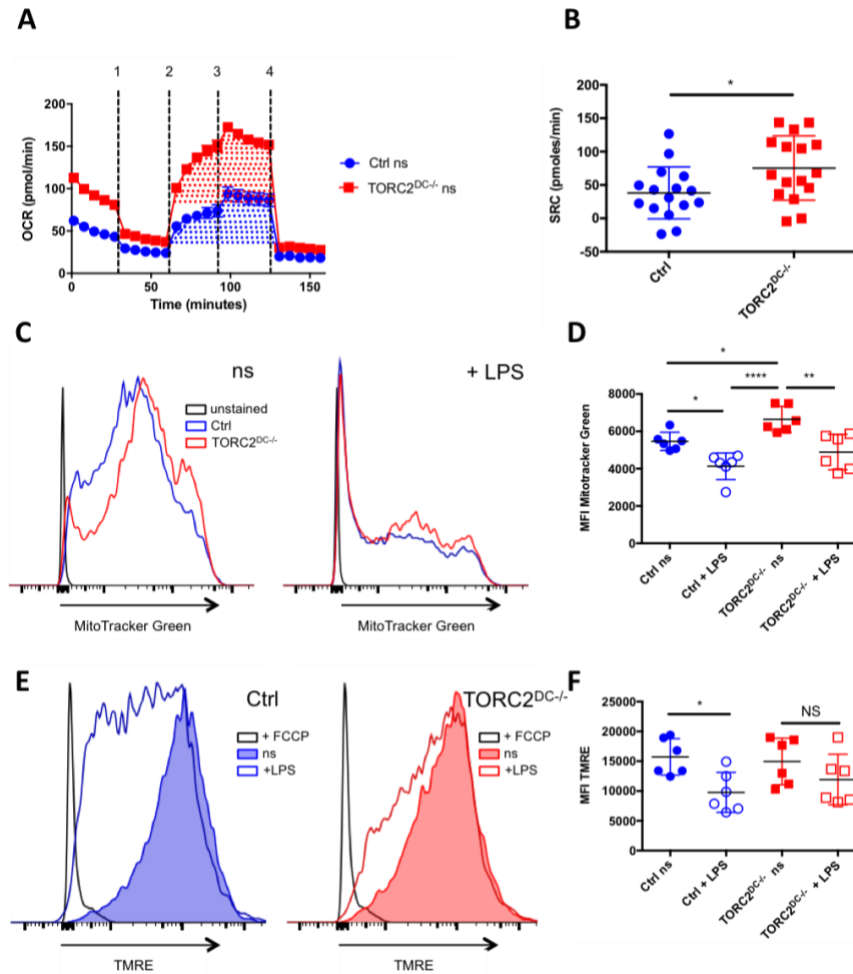


**Figure 20. TORC2<sup>DC-/-</sup> have increased SRC, mitochondrial biomass, and mitochondria which fail to depolarize following LPS stimulation**

BMDC were generated from Ctrl or TORC2<sup>DC-/-</sup> mice, then stimulated with LPS for 18h as indicated. Bone marrow-derived DC were analyzed using a Seahorse XFe96 Bioanalyzer for metabolic flux in real-time over 150 min with oligomycin (1), FCCP (2), 2-DG (3) and rotenone/antimycin (4) injected at indicated times to obtain control values. (A) Representative oxygen consumption rate (OCR) of non-stimulated Ctrl DC and TORC2<sup>DC-/-</sup>. (B) Quantification of spare respiratory capacity calculated as the difference in oxygen consumption rate (OCR) after addition of 2-DG (3) and OCR after the addition of oligomycin (1);  $n=16$  mice; Student's t-test,  $*p<0.05$ . (C) Representative flow cytometry histograms of Ctrl DC and TORC2<sup>DC-/-</sup> stained with MitoTracker Green. (D) Quantification of mean fluorescence intensity (MFI) of MitoTracker Green;  $n=6$  mice. (E) Representative flow cytometry histograms of Ctrl DC and TORC2<sup>DC-/-</sup> stained with TMRE. (F) Quantification of MFI of TMRE;  $n=6$  mice. (D) and (E): one-way ANOVA Tukey's multiple comparisons test.  $*p < 0.05$ ,  $**p < 0.01$ ,  $***p < 0.001$ ,  $****p < 0.0001$ .

### **6.3.3 TORC2<sup>DC-/-</sup> display more compact Golgi stacks with less perinuclear localization as compared to Ctrl DC**

To determine if mTORC2 deficiency in DC impacted the localization, structure, and quantity of Golgi apparatus, we first immunostained DC with anti-TGN38 and assessed the location of the Golgi relative to the nuclei of the cell. In the Ctrl DC, Golgi was perinuclear, whereas in TORC2<sup>DC-/-</sup> the Golgi appeared more dispersed throughout the cell (**Figure 21A, top panel**). We next used TEM to assess the structure of the Golgi in DC. In Ctrl DC, the Golgi cisternae appear more dilated, and more Golgi is observed perinuclearly; in contrast, the Golgi in TORC2<sup>DC-/-</sup> appears more compact, and less Golgi is visible perinuclearly (**Figure 21A, bottom panel**). Finally, we quantified the MFI of TGN38 staining from 3-D stacks of confocal images taken of DC to assess the total Golgi content of the DC, and observed no differences in total Golgi content in Ctrl DC as compared to TORC2<sup>DC-/-</sup> (**Figure 21B**).

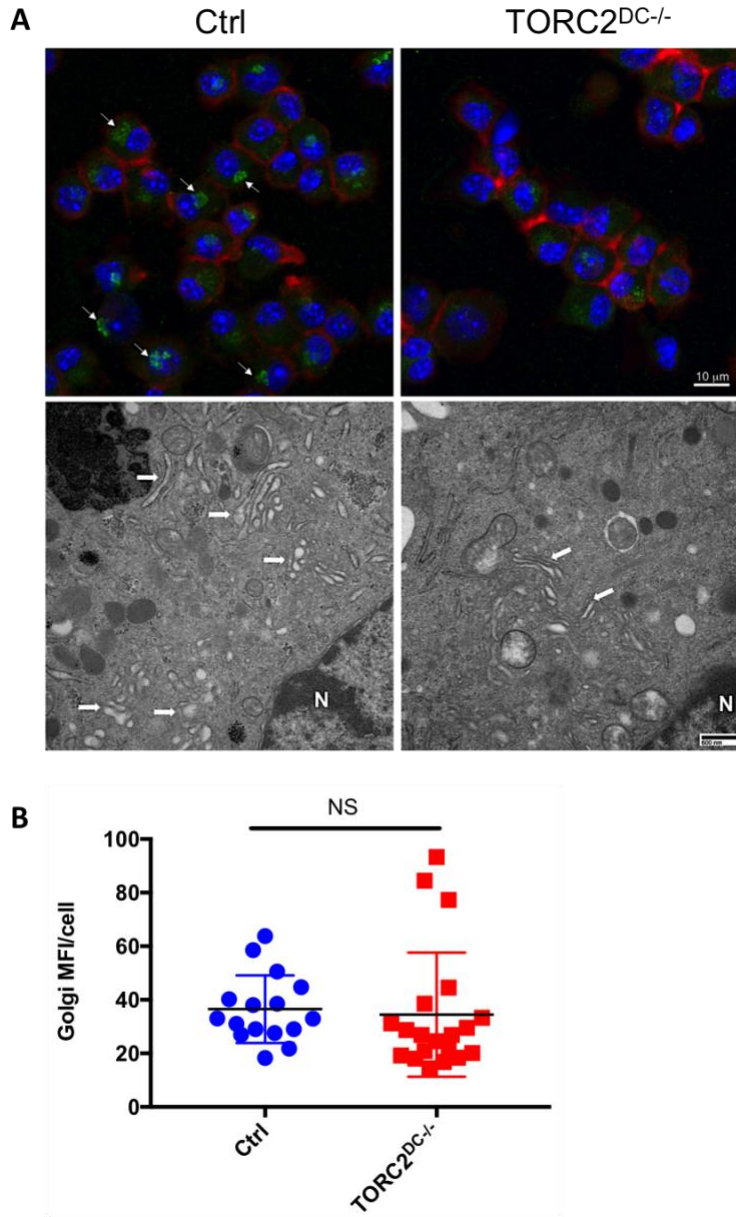


**Figure 21. TORC2<sup>DC-/-</sup> display more compact Golgi stacks with less perinuclear localization as compared to Ctrl DC**

BMDC were generated from control (Ctrl) or TORC2<sup>DC-/-</sup> mice, and prepared for TEM and confocal microscopy.

(A) Representative maximum intensity projection of DC immunostained for Golgi (green), F-actin (red), and nuclei (blue), with arrows marking perinuclear Golgi (top panel); representative TEM of DC with arrows marking Golgi, and N marking the cell nucleus (bottom panel). (B) Quantification of total MFI of Golgi stain per cell; each point represents values from one high powered field (HPF);  $n=5$  mice and 4-5 HPFs per mouse; Student's t-test,  $*p < 0.05$ .

#### **6.3.4 Inhibition of mTORC1 activity in TORC2<sup>DC-/-</sup> leads to loss of their enhanced spare respiratory capacity and glycolysis**

To elucidate whether mTORC2 in DC had mTORC1-independent or mTORC1-dependent metabolic regulation, we incubated both Ctrl DC and TORC2<sup>-/-</sup> DC with RAPA (10ng/mL) for 18h, then analyzed their SRC and glycolysis via extracellular flux as in Figure 1. Inhibition of mTORC1 in TORC2<sup>-/-</sup> DC abolished the increase in SRC (representative OCR **Figure 22A**; quantified in **Figure 22B**) and glycolysis (representative ECAR **Figure 22C**; quantified in **Figure 22D**) in non-stimulated cells as compared with Ctrl DC. Notably, administration of RAPA to non-stimulated Ctrl DC did not decrease their glycolytic activity. Inhibition of mTORC1 in both LPS-stimulated Ctrl DC and TORC2<sup>-/-</sup> DC significantly reduced their glycolytic activity (representative ECAR **Figure 22E**; quantified in **Figure 22F**).

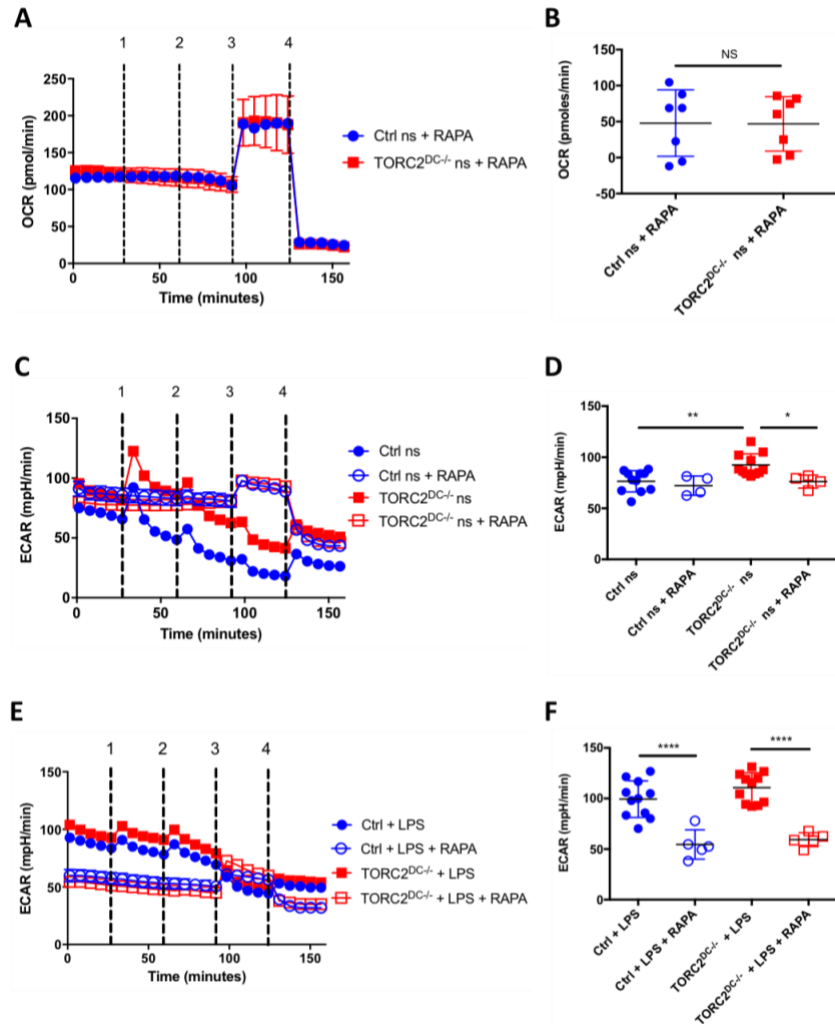


**Figure 22. Inhibition of mTORC1 in TORC2<sup>DC-/-</sup> leads to loss of their enhanced spare respiratory capacity and glycolysis**

BMDC were generated from Ctrl or TORC2<sup>DC-/-</sup> mice, then cultured with low-dose RAPA (10ng/mL) for 18h. DC were analyzed using a Seahorse XFe96 Bioanalyzer for metabolic flux in real-time over 150 min with oligomycin (1), FCCP (2), 2-DG (3) and rotenone/antimycin (4) injected at indicated times to obtain control values. (A) Representative OCR. (B) Quantification of SRC, calculated as the difference in OCR after addition of 2-DG (3) and prior to addition of FCCP (1);  $n=6$  mice; Student's t-test,  $*p < 0.05$ . (C) Representative ECAR of non-stimulated DC. (D) Quantification of basal glycolysis in non-stimulated DC prior to addition of oligomycin (1);  $n=6-11$  mice. (E) Representative ECAR of LPS-stimulated DC. (F) Quantification of basal glycolysis in LPS-stimulated DC prior to addition of oligomycin (1);  $n=6-11$  mice. (D) and (F): one-way ANOVA Tukey's multiple comparisons test,  $*p < 0.05$ ,  $**p < 0.01$ ,  $***p < 0.001$ ,  $****p < 0.0001$ .

### 6.3.5 TORC2<sup>DC-/-</sup> exhibit a distinct gene expression profile from Ctrl DC

To determine the mechanism by which TORC2<sup>DC-/-</sup> had enhanced mTORC1 metabolic activity, we performed a gene expression analysis to identify changes in expression of genes involved in mTORC1 signaling in TORC2<sup>DC-/-</sup>. We identified a total of 22 genes on a 378 gene panel with differential expression between Ctrl DC and TORC2<sup>DC-/-</sup>, as represented by the heat map in **Figure 23A**, of which 5 genes we identified as possible upstream mediators of mTORC1 activity (**Figure 23B**). We then performed qPCR to determine the relative expression of the downstream targets of mTORC1 Ppar $\gamma$ , Srebf1, and Yy1 in Ctrl DC and TORC2<sup>DC-/-</sup>. Both Ppar $\gamma$  and Srebf1 are significantly more highly expressed in TORC2<sup>DC-/-</sup> as compared to Ctrl DC (**Figure 23C**).

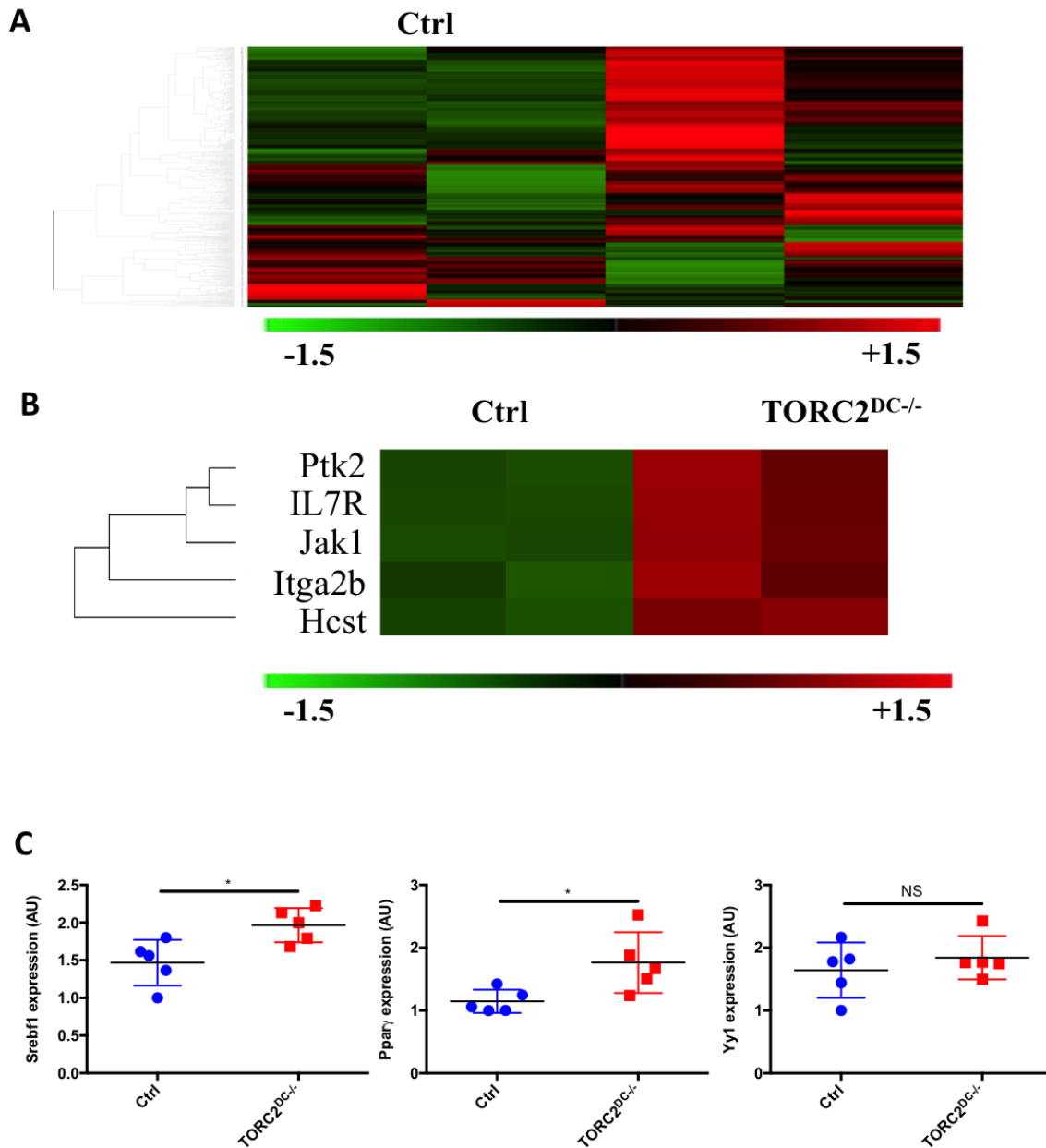


**Figure 23. TORC2<sup>DC-/-</sup> exhibit a distinct gene expression profile from Ctrl DC**

(A) Expression of 378 genes comprised from the NanoString Mouse Immunology Panel, shown as a heat map. Red indicates an increased gene expression and green indicates decreased gene expression as compared to Ctrl DC; n=2 mice in each group. (B) Selection highlighting five genes of interest from the panel in (A) which were significantly changed between Ctrl DC and TORC2<sup>DC-/-</sup>. (C) mRNA expression of Srebf1, Ppar $\gamma$ , and Yy1 in Ctrl DC and TORC2<sup>DC-/-</sup>, normalized to the housekeeping gene GAPDH, with Ctrl DC used as the referent control; n=5 mice per group, Student's t-test, \* $p < 0.05$ .

## 6.4 Discussion

Earlier studies have demonstrated that while quiescent, immature DC have relatively low metabolic needs, these needs increase upon cell activation and maturation due to bioenergetic pressure to produce pro-inflammatory cytokines and upregulate co-stimulatory molecules<sup>92</sup>. The metabolic process that permits DC to meet these enhanced new metabolic demands occurs by a “switch” from oxidative phosphorylation to aerobic glycolysis. It has previously been reported that this initial “switch” towards increased glycolytic metabolism is not dependent on the mTOR signaling axis<sup>93</sup>; indeed, we did not observe any differences in glycolytic activity immediately following LPS stimulation between TORC2<sup>DC-/-</sup> and Ctrl DC. However, mTORC1 (but not mTORC2) has been described as essential for DC glycolytic commitment<sup>168</sup>. We observed that immature (non-stimulated) DC lacking functional mTORC2 had significantly increased glycolytic function as compared to immature Ctrl DC, but that this increase was not observed in the DC following stimulation with LPS. This finding, together with our previous observations showing enhanced expression of the co-stimulatory molecule CD86 together with decreased expression of the co-inhibitory molecule PD-L1<sup>88</sup> on immature TORC2<sup>DC-/-</sup>, suggests that immature TORC2<sup>DC-/-</sup> may have an intermediate maturity phenotype. This is further supported by the increased dependence that we observed of non-stimulated TORC2<sup>DC-/-</sup> on glycolysis for ATP production.

There is evidence that, in addition to its importance for nascent protein production, glycolytic commitment by mature BMDC is critical for their survival<sup>168</sup>. Indeed, in conjunction with an increase in glycolytic activity, TORC2<sup>DC-/-</sup> also appeared to have limited protection from cell death following TLR4 agonism. The enhanced pro-inflammatory nature of TORC2<sup>DC-/-</sup> may also be attributed in part to this more robust viability. It has been reported that LPS can induce

programmed cell death in DC<sup>172</sup>, and that T cells can also trigger apoptosis in DC through Fas and perforin as a mechanism to self-limit T cell activation<sup>173,174</sup>. Therefore, the enhanced viability of TORC2<sup>DC-/-</sup> may allow them to produce cytokines and interact with T cells for an extended period of time.

In addition to their augmented glycolytic activity, TORC2<sup>DC-/-</sup> also have increased SRC, in conjunction with increased mitochondrial biomass and mitochondria that fail to depolarize following LPS stimulation. Mitochondrial SRC has been described as the extra capacity of mitochondria to produce energy under circumstances of increased cell stress and is correlated positively with prolonged cell survival and function<sup>94</sup>. Given the enhanced viability of TORC2<sup>DC-/-</sup>, an increase in SRC corroborates our findings. As CD8<sup>+</sup> memory T cells have been described as having enhanced SRC due to increased mitochondrial biomass<sup>94</sup>, that TORC2<sup>DC-/-</sup> also showed an increase in mitochondrial content compared with Ctrl DC also fits with our other findings. Strikingly, the mitochondrial membrane of TORC2<sup>DC-/-</sup> failed to depolarize following stimulation with LPS, which was surprising as LPS has been shown to collapse mitochondrial membrane potential ( $\Delta\Psi_m$ ) in macrophages<sup>175</sup>. However, it has been reported that, in macrophages, that disproportionately utilize ATP generated via glycolysis as protection against cell death (as we observed in the TORC2<sup>DC-/-</sup>), high  $\Delta\Psi_m$  is maintained via reverse functioning of F(o)F(1)-ATP synthase and adenine nucleotide translocase<sup>175</sup>.

As enhanced glycolytic activity has been described as a means by which activated DC augment lipogenesis for the increased production and transport of cytokines and co-stimulatory proteins<sup>93</sup>, we assessed whether TORC2<sup>DC-/-</sup> had variations in the localization, dilation, and amount of Golgi apparatus. The Golgi body, in conjunction with endoplasmic reticulum (ER), is an organelle critical for the processing and transport of proteins. Surprisingly, given the

enhanced glycolytic activity of TORC2<sup>DC-/-</sup>, we did not observe any increase in the overall Golgi content of the DC. However, we did observe that the Golgi of TORC2<sup>DC-/-</sup> were less dilated than in Ctrl DC, as well as less perinuclearly localized. Recent studies have favored a cisternal progenitor model of protein transport, whereby proteins are transported along tightly-compacted Golgi subcompartments. These subcompartments undergo fission and fusion events which allow stable protein transport to the membrane<sup>176</sup>. Thus, the tightly compacted Golgi cisternae and diffuse TGN localization may reflect enhanced protein transport by TORC2<sup>DC-/-</sup>.

Given the mitochondrial dysregulation observed in TORC2<sup>DC-/-</sup>, we next investigated the mechanism underlying this change. Cells maintain mitochondrial homeostasis by controlling both the number and quality of mitochondria via mitophagy<sup>177</sup>. Interestingly, mTORC1 is known to be an important regulator of the nuclear transcription of mitochondrial genes necessary for mitochondrial biogenesis through peroxisome-proliferator-activated receptor coactivator-1 $\alpha$  (PGC-1 $\alpha$ ) and yin-yang 1 (YY1)<sup>158</sup>. In addition, mTORC1 has been described to regulate mitochondrial activity via phosphorylation of mitochondrial membrane protein Bcl-X<sub>L</sub><sup>178</sup>. mTORC1 has also been described to positively regulate glucose uptake<sup>179</sup> and mitophagy<sup>180</sup>. As there is possible interplay between mTORC1 and mTORC2 through their interactions with Akt and TSC1/2, we assessed whether the mitochondrial dysregulation in TORC2<sup>-/-</sup> DC could be attributed to augmented mTORC1 activity. Indeed, inhibition of mTORC1 with rapamycin abolished the enhanced glycolytic function and SRC of TORC2<sup>DC-/-</sup>.

While we and others have reported that the enhanced pro-inflammatory phenotype/function of DC lacking functional mTORC2 may be partially attributed to altered Forkhead box O1 (FoxO1)<sup>87</sup> and GSK3 $\beta$ <sup>88</sup> phosphorylation/nuclear translocation, and due to the inability of these DC to phosphorylate Akt on S473<sup>88</sup> the degree to which these phosphorylations

are dampened in TORC2<sup>DC-/-</sup> are not consistent between these reports. In addition, alterations in these signaling mechanisms would not underlie the metabolic and mitochondrial dysregulation that we have observed in TORC2<sup>DC-/-</sup>. We therefore completed a gene expression analysis panel that covered 378 genes, and identified 5 genes of interest that were significantly differentially expressed between Ctrl DC and TORC2<sup>DC-/-</sup>. One set of these genes highlights a signaling pathway in which the integrin subunit Integrin alpha IIb (Itga2b), Protein tyrosine kinase (Ptk2, also known as focal adhesion kinase, FAK), and Hematopoietic cell signal transducer (Hcst, also known as PIK3 associated protein, PIK3AP) are upregulated in TORC2<sup>DC-/-</sup>. Integrin clustering has been demonstrated to mediate intracellular signaling via the catalytic kinase Ptk2 (FAK)<sup>181</sup>, which ultimately leads to activation of the PI3K/Akt/mTORC1 signaling pathway<sup>182</sup>. Another possible mechanism for upregulation of mTORC1 activity in TORC2<sup>DC-/-</sup> uncovered by the gene expression analysis panel is the upregulation of the IL-7 cytokine receptor and Janus kinase 1 (JAK1) in TORC2<sup>DC-/-</sup>, as IL-7R/JAK1 signaling can activate the PI3K signaling pathway<sup>183</sup>.

Downstream of mTORC1 signaling, we identified upregulation of two genes in TORC2<sup>DC-/-</sup> which are known to regulate metabolic function: Ppar $\gamma$  and Srebf1. Activation of both of these transcription factors downstream of mTORC1 leads to the expression of lipogenic genes<sup>184</sup>. It has been demonstrated that glycolysis in DC drives lipogenesis and subsequent Golgi/ER expansion upon DC activation<sup>93</sup>, and more recently that Ppar $\gamma$  signaling can also promote glycolysis in hematopoietic stem cells<sup>185</sup>. Interestingly, in yeast it has been described that loss of TORC2 function results in enhanced lipogenesis<sup>186</sup>. Taken together, our data suggest mTORC2 plays a role in transcriptional control of mTORC1-regulated metabolic processes (**Figure 24**).

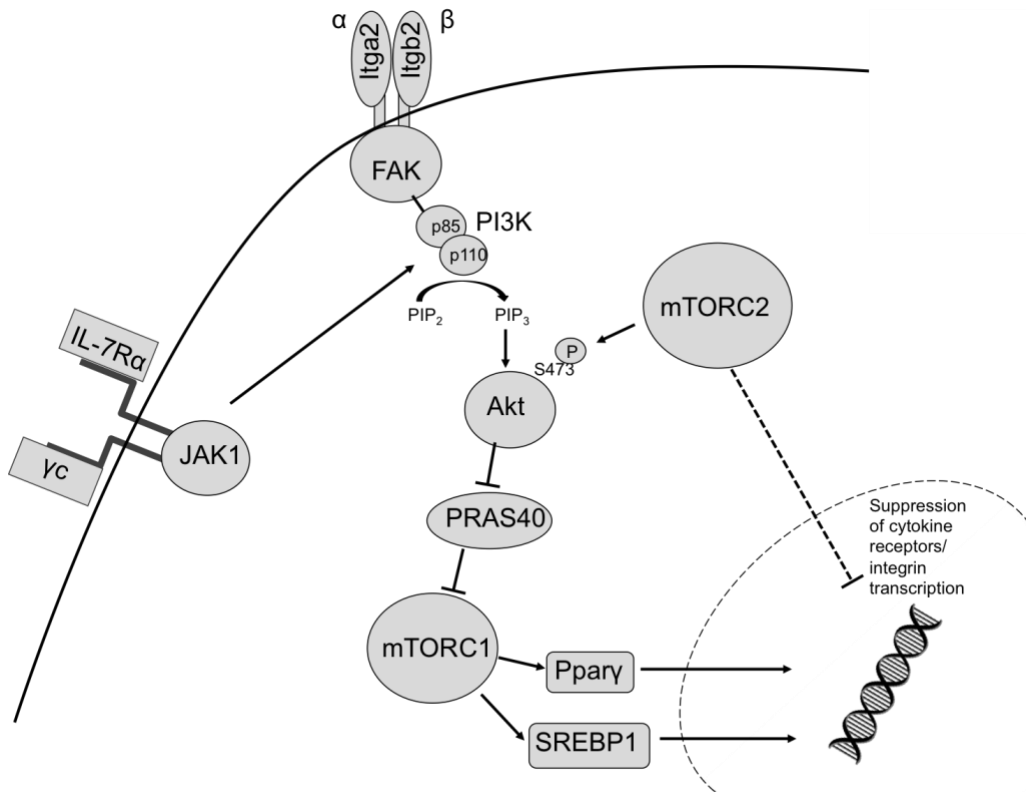


**Figure 24. Proposed signaling mechanism of mTORC1 regulation by mTORC2**

These findings describe a novel role for mTORC2 in the regulation of DC metabolism. DC lacking functional mTORC2 are more glycolytically active and have an increased dependence on glycolysis for ATP production. TORC2<sup>DC-/-</sup> also have abnormalities in mitochondrial regulation, characterized by enhanced mitochondrial biomass and mitochondria that fail to depolarize following DC activation. The metabolic phenotype of TORC2<sup>DC-/-</sup> is lost upon inhibition of mTORC1; in addition, we have identified several genes upstream of mTORC1 and the transcription factors Ppar $\gamma$  and Srebf1 downstream of mTORC1 that are upregulated in TORC2<sup>DC-/-</sup>. These data strongly suggest mTORC2 functions to restrain mTORC1-driven anabolic metabolism in DC.

## 7.0 Final Discussion and Biomedical Relevance

### 7.1 mTORC2 Restrains DC Function and mTORC1 Regulated

#### Metabolic Control

The goal of these studies was to determine the function of mTORC2 in DC in regards to T cell stimulatory function in the context of transplantation, and if the enhanced inflammatory phenotype/function of TORC2<sup>DC-/-</sup> could be ascribed to an altered metabolic program in these cells. Although the role of mTORC1 in regulating DC immunometabolism and T cell stimulatory function in transplantation has been studied extensively using the potent mTORC1 inhibitor RAPA, there is a paucity of parallel studies examining the discrete role of mTORC2 in DC as there is not yet available an mTORC2-specific pharmacological inhibitor. A recent study by our group utilized an innovative mouse model in which Rictor, a scaffolding protein critical for mTORC2 assembly, is deleted specifically in CD11c<sup>+</sup> DC demonstrated that TORC2<sup>DC-/-</sup> have an enhanced pro-inflammatory phenotype and allostimulatory function *in vitro*<sup>88</sup>. Therefore, these studies expanded upon our previous report and served to provide a more complete picture of how mTOR functions to link DC metabolism and immune function.

We first demonstrate that when DC in heterotopic heart transplant donor tissue lack mTORC2, the beating function of these grafts is decreased and the cellular infiltrate increased as opposed to WT Ctrl heart donors. When TORC2<sup>DC-/-</sup> are used as skin graft donors in both minor Ag mismatch and full MHC mismatch mouse models, graft rejection is more severe and accompanied by enhanced CD8<sup>+</sup> T cell responses and inflammatory cytokine production. These data complement a previous study in which TORC2<sup>DC-/-</sup> injection into B16 melanoma-bearing

mice delayed tumor progression in a CD8<sup>+</sup> T cell-dependent fashion<sup>90</sup>. Surprisingly, mTORC2 deletion in the DC of skin graft recipients did not impact graft survival or T cell infiltration into the graft, as recent evidence acquired using the tg OVA Ag skin transplant model suggests that host DC may play an essential role in regulating acute rejection by acquiring intact donor MHC class I Ag (semi-direct allorecognition)<sup>115</sup>. However, as graft-resident DC are quickly eliminated by host natural killer cells, it is possible that OVA may not be captured efficiently by recipient APC that repopulate the graft<sup>108</sup> and consequently absence of mTORC2 in host DC does not significantly affect graft survival.

It should be noted that defects in wound healing have been described to cause graft displacement and loss of function<sup>132</sup>, and treatment of transplant recipients with the mTORC1 inhibitor Sirolimus impairs wound healing via its lymphopenic properties<sup>133</sup>. However, we do not believe impaired wound healing contributed to the accelerated rejection of TORC2<sup>DC-/-</sup> grafts, as impaired wound healing has not been ascribed to mTORC2 inhibition. Additionally, DC and T cells have been reported to positively regulate wound healing<sup>134</sup>; as TORC2<sup>DC-/-</sup> augment T cell graft infiltrate, impaired wound healing is not likely. Similarly, we did not observe differential LN homing of skin-resident TORC2<sup>DC-/-</sup>, but did observe a more inflammatory phenotype in migrating DC along with enhanced CD8<sup>+</sup> T cell responses in a cell-mediated DTH assay in TORC2<sup>DC-/-</sup> mice. This strongly suggests the accelerated rejection observed in TORC2<sup>DC-/-</sup> donor grafts is a result of the augmented ability of these DC to activate CD8<sup>+</sup> T cells; therefore, in DC mTORC2 functions to suppress T cell stimulatory function.

Next, we sought to identify the mechanism by which mTORC2 suppressed DC function. It is now appreciated that metabolic regulation is integral in controlling DC function, and mTORC1 is a key regulator of immunometabolism. Namely, upon activation DC will increase

their dependence on aerobic glycolysis in order to enhance anabolic processes, and maintenance of this glycolytic phenotype is crucial for DC survival and dependent on mTORC1<sup>82</sup>. However, a role for mTORC2 in DC metabolic regulation had not been defined. We therefore wanted to determine if the inflammatory phenotype and enhanced stimulatory function of TORC2<sup>DC-/-</sup> could be a result of an altered metabolic program in these cells.

We observed that TORC2<sup>DC-/-</sup> displayed an enhanced glycolytic phenotype as compared to Ctrl DC, which correlated with an increased dependence on glycolysis for ATP production. In addition, following stimulation with LPS TORC2<sup>DC-/-</sup> were more resistant to cell death than Ctrl DC; this strengthened the glycolytic findings as glycolytic bias has been demonstrated to confer increased viability in DC<sup>82</sup>. TORC2<sup>DC-/-</sup> also displayed enhanced SRC as compared to Ctrl DC, which has also been correlated to increased cell survival as well as function in CD8<sup>+</sup> T memory cells<sup>94</sup>. TORC2<sup>DC-/-</sup> appeared to have mitochondrial dysregulation, as they had increased mitochondrial biomass, as well as mitochondria that failed to significantly depolarize in response to LPS stimulation. Finally, TORC2<sup>DC-/-</sup> displayed differences in Golgi body structure and localization as compared to Ctrl DC, which follows previous studies in which glycolytic bias in DC was shown to enhance anabolic processes<sup>93</sup>. As there is evidence that mTORC2 and mTORC1 may have some overlap of signaling through their interactions with Akt and TSC1/2, and mTORC1 exerts control over mitochondrial number and function via a number of processes, including regulating the transcription of mitochondrial genes<sup>158</sup> and mitophagy<sup>180</sup>, we wanted to test if deletion of mTORC2 increased mTORC1 activity. Indeed, TORC2<sup>DC-/-</sup> exposed to RAPA lost their enhanced glycolytic and SRC phenotype.

An RNA sequencing analysis of TORC2<sup>DC-/-</sup> revealed two possible pathways by which mTORC2 could serve to restrain mTORC1 function, as in TORC2<sup>DC-/-</sup> displayed increased

expression of components integral for integrin clustering, as well as increased expression of IL-7R and JAK1. Both integrin signaling and cytokine receptor signaling have been demonstrated to enhance mTORC1 activity<sup>182,183</sup>. As we also observed increased expression of Pparg and Srebf1, two transcription factors downstream of mTORC1 which have been described to regulate mitochondria, as well as lipogenesis and glycolytic function (Pparg)<sup>184,185</sup>, we postulate that in DC mTORC2 has a role as a metabolic regulator by suppressing activating signals upstream of mTORC1. In conclusion, mTORC2 negatively regulates DC inflammatory phenotype and T cell stimulatory function by suppressing mTORC1-dependent anabolic metabolism, which should be taken into consideration regarding the use of dual mTORC1/2 ATP-competitive inhibitors.

## **7.2 mTORC2 Targeting in Transplantation and Cancer**

### **Immunotherapy**

Our lab has previously published that the dual mTORC1/2 inhibitor AZD8055 is a potent suppressor of T cell proliferation that prolongs survival of MHC-mismatched heterotopic heart allografts, as well as increases T<sub>reg</sub> infiltration into the graft and decreases IFN $\gamma$  production by host T cells<sup>187</sup>. However, a follow-up study by our group comparing the efficacy of AZD and RAPA in prolonging heart allograft survival showed RAPA to be the superior immunosuppressant, in terms of graft survival time, prolonged T<sub>reg</sub> graft infiltration, and prolonged suppression of donor-specific immunoglobulin G (IgG)1 and IgG2c antibodies<sup>188</sup>. While this study concluded these results may in part reflect differential pharmacokinetics between AZD and RAPA, given the studies presented here that inhibition of mTORC2 enhances

DC T cell stimulatory function, dual mTOR inhibitors may not be promising as immunosuppressants in transplant recipients. as loss of mTORC2 function as a result of chronic exposure to RAPA in transplant recipients has been implicated in the development of insulin insensitivity and the development of diabetes mellitus

Conversely, there are currently 29 active studies and 24 completed studies in which various cancers are being tested as indications for the use of dual mTORC1/2 inhibitors. While these second-generation mTOR inhibitors may more completely shut down the PI3K/mTOR pathway, which has been shown to be dysregulated in many types of tumors including renal cell carcinoma, breast cancer, and hepatocellular carcinoma<sup>189</sup>, they may also impact patient immune cell function. Tumors are notorious immune evaders, and a number of immunotherapies have been developed in order to circumvent this and permit the patient's immune system to attack these foreign bodies, the most well-characterized of which are checkpoint blockade monoclonal antibodies such as Pembrolizumab (Keytruda; anti-programmed cell death protein 1 [PD-1])<sup>190</sup>. A recent study has demonstrated AZD2014 to enhance the efficacy of anti-PD-1 and anti-CTLA4 in mouse models of colon carcinoma cell line subcutaneous injections<sup>191</sup>. Therefore, it is possible dual mTORC1/2 inhibitors could serve as an adjuvant to cancer immunotherapies to enhance anti-tumor immunity. However, as loss of mTORC2 function as a result of chronic exposure to RAPA in transplant recipients has been implicated in the development of insulin resistance and the development of diabetes mellitus-like symptoms<sup>192</sup>, long-term studies to identify dosing regimens may be crucial for the clinical application of checkpoint blockade/dual mTOR inhibitor combination therapies.

### 7.3 Future Directions

Although the studies presented here, as well as previous studies conducted by our lab, indicate inhibition of mTORC2 may not be promising in terms of immunosuppression in the context of transplantation (or other contexts in which immune suppression is desirable, such as autoimmunity), it does follow that enhancing mTORC2 activity in DC may have pro-immunosuppressive results. In addition, it has also been suggested that enhanced activation of mTORC2 may be protective against ischemia reperfusion injury by regulating apoptosis and autophagy, as well as macrophage infiltration<sup>193</sup>. While identification of upstream activators of mTORC2 activity has been elusive, recent studies have demonstrated a mechanism of mTORC2 activation which is temporally and spatially regulated by phosphatidylinositol(3,4,5) trisphosphate (PtdIns(3,4,5)P<sub>3</sub>)<sup>85,194</sup>. The pleckstrin homology (PH) domain of Sin1, a protein unique to mTORC2, interacts with and inhibits the kinase domain of mTOR in mTORC2. PtdIns(3,4,5)P<sub>3</sub> can associate with the Sin1 PH domain and release it from the mTOR kinase domain, thereby activating mTORC2. Of particular interest, mutations within the Sin1 PH domain have been identified in cancer patients with pathologically augmented mTORC2 activity<sup>194</sup>. Therefore, agents which disrupt Sin1 PH or increase PtdIns(3,4,5)P<sub>3</sub> could enhance mTORC2 activity and have potential as immunosuppressants. However, it should be noted that regulation of both mTOR complexes is critical for the differentiation and function of T cells, and overexpression of mTORC2 may destabilize T<sub>reg</sub><sup>195</sup>.

Another recent study has highlighted the importance of subcellular localization of mTORC2 in regards to its activity. Namely, mTORC2 was shown to localize to the cell membrane, mitochondria, and early/late endosomal vesicles, and this localization impacted the activation landscape of mTORC2. While mTORC2 localized to endosomal vesicles was

activated in a growth factor, PI3K, and PtdIns(3,4,5)P<sub>3</sub>-dependent fashion, mTORC2 localized to the cell membrane was activated independently of these components<sup>196</sup>. This suggests that in some subcellular contexts, mTORC2 activity may enhance mTORC1 activity, while in other subcellular locations mTORC2 may suppress mTORC1 (as observed in our studies), and agents impacting Sin1 or PtdIns(3,4,5)P<sub>3</sub> to enhance mTORC2 activation may actually also enhance mTORC1 and be ineffective immunosuppressants. Therefore, further studies of how subcellular localization impacts the upstream activators of mTORC2 and the downstream targets of mTORC2 will be crucial in identifying appropriate pro-immunosuppressive drugable targets upstream of mTORC2.

## Appendix

- $\Delta\Psi_m$ —Mitochondrial membrane potential
- 2-DG—2-deoxyglucose
- 4E-BP1—eIF4E –binding protein 1
- A—Aorta
- Ab—Antibody
- Ab—Antibody
- Ag—Antigen
- Akt—Protein kinase B
- AMPK—AMP-activated protein kinase
- APC—Antigen presenting cell
- ATG—Anti-thymocyte globulin
- ATP—Adenosine triphosphate
- ATP—Adenosine trisphospate
- BAC—Bacterial artificial chromosome

- BATF3—Basic leucine zipper ATF-like 3 transcription factor
- BMDC—Bone marrow-derived DC
- CA—Carotid artery
- CCR—C-C chemokine receptor
- CD—Cluster of differentiation
- cDC—Classical dendritic cell
- CNI—Calcineurin inhibitor
- CTL—Cytotoxic T lymphocyte
- CTLA-4—Cytotoxic T-lymphocyte associated protein 4
- Ctrl—Wild-type control
- CXCL—C-X-C motif chemokine ligand
- DAMP—Damage-associated molecular pattern
- DC—Dendritic cell
- Deptor—DEP domain-containing mTOR-interacting protein
- dLN—Draining lymph node
- DNFB—2,4-dinitrofluorobenzene
- DON—6-diazo-5-oxo-l-norleucine
- DTH—Delayed-type hypersensitivity
- ECAR—Extracellular acidification rate
- eIF4E—Eukaryotic initiation factor 4E
- EJV—External jugular vein
- ER—Endoplasmic reticulum
- ETC—Electron transport chain

- F—Female
- FAK—Focal adhesion kinase
- FAO—Fatty acid oxidation
- FAS—Fatty acid synthesis
- FcγR1—Fc-gamma receptor 1
- FKBP12—12 kDa FK506 binding protein
- Foxo1—Forkhead box O1
- Foxp3—Forkhead box P3
- GAP—GTPase activating protein
- GAPDH—glyceraldehyde-3-phosphate dehydrogenase
- GATA3—GATA binding protein 3
- GM-CSF—Granulocyte-macrophage-colony stimulating factor
- GSK3—Glycogen synthase kinase 3
- GTP—Guanosine triphosphate
- GVHD—Graft-versus-host disease
- Hcst—Hematopoietic cell signal transducer
- HEK—Human embryonic kidney
- HEV—High endothelial venules
- HHT—Heterotopic heart transplant
- HIF-1 $\alpha$ —Hypoxia-inducible factor 1
- HK-II—Hexokinase II
- HLA—Human leukocyte antigen
- HMGB1—high mobility box group 1

- HNS—Heparinized normal saline
- HSP—Heat shock protein
- Id2—Inhibitor of DNA binding 2
- IDO—indoleamine 2,3-dioxygenase
- IFN—Interferon
- IgG—Immunoglobulin G
- IKK $\epsilon$ —Inhibitor of nuclear factor kappa-B kinase subunit epsilon
- iNOS—Inducible nitric oxide synthetase
- IRF8—Interferon regulatory factor 8
- IRS-1—Insulin receptor substrate
- Itga2b—Integrin alpha IIb
- IVC—Inferior vena cava
- LAG3—Lymphocyte-activated gene 3
- LC—Langerhans cells
- Leu—Leucine
- LPS—Lipopolysaccharide
- M—Male
- MAPK—Mitogen-activated protein kinase
- MHC—Major histocompatibility complex
- MHCI—Major histocompatibility complex class I
- MHCII—Major histocompatibility complex class II
- MLR—Mixed leukocyte reaction
- mLST8—mammalian lethal with SEC13 protein 8

- MMP—Matrix metalloprotease
- moDC—Monocyte-derived dendritic cell
- mRNA—Messenger ribonucleic acid
- mSIN1—mammalian stress-activated MAP kinase-interacting protein 1
- MST—Mean survival time
- mTOR—mechanistic target of rapamycin
- mTORC—mTOR complex
- NF- $\kappa$ B—nuclear factor kappa-light-chain-enhancer of activated B cells
- NFIL3—Nuclear factor interleukin 3 regulated
- NO—Nitric oxide
- NOD—Nucleotide-binding oligomerization domain
- NOTCH2—Neurogenic locus notch homolog protein 2
- OXPHOS—Oxidative phosphorylation
- PA—Pulmonary artery
- PAMP—Pathogen-associated molecular pattern
- PCR—Polymerase chain reaction
- PD-1—Programmed cell death protein 1
- pDC—Plasmacytoid dendritic cell
- PGC-1 $\alpha$ —peroxisome-proliferator-activated receptor coactivator-1 $\alpha$
- PI3K—Phosphoinositide 3 kinase
- PIK3AP—PI3K associated protein
- POD—Post-operative day
- PPAR $\gamma$ —Peroxisome proliferator-activated receptor- $\gamma$

- PRAS40—proline-rich Akt substrate of 40kDa
- Protor—Protein observed with Rictor
- PRR—Pattern recognition receptor
- PtdIns(3,4,5)P<sub>3</sub>—phosphatidylinositol(3,4,5) trisphosphate
- Ptk—Protein tyrosine kinase
- RAGE—Receptor for advanced glycation end products
- RAPA—Rapamycin
- Raptor—regulatory-associated protein of mTOR
- RBP-J—Recombining binding protein suppressor of hairless
- Rheb—Ras homolog enriched in brain
- Rictor—Rapamycin-insensitive companion of mTOR
- RIG-1—Retinoid acid-inducible gene 1
- ROR $\gamma$ t – Retinoic acid receptor-related orphan receptor  $\gamma$ -t
- S6K—p70 ribosomal S6 kinase 1
- Ser—Serine
- SGK1—Serum/glucocorticoid regulated kinase 1
- siRNA—Small interfering RNA
- SRC—Spare respiratory capacity
- SRC—Spare respiratory Capacity
- SREBP1/SREBF1—Sterol regulatory element binding protein 1
- SVC—Superior vena cava
- TANK—TRAF family member-associated NF-kappa-B activator
- TAP—Transporter associated with antigen processing

- TBK1—TANK-binding kinase 1
- TCA—Tricarboxylic acid
- TCR—T cell receptor
- TCR—T cell receptor
- TEM—Transmission electron microscopy
- Tfh—T follicular helper cells
- TGF $\beta$ —Transforming growth factor  $\beta$
- Th—T helper
- Th—T helper cell
- TLR—Toll-like receptor
- TNF $\alpha$ —Tissue necrosis factor  $\alpha$
- T<sub>reg</sub>—Regulatory T cell
- TSC—Tuberous sclerosis complex
- WT—Wild-type
- YY1—Yin-yang 1

## Bibliography

- 1 Liu, L. M. & MacPherson, G. G. Antigen acquisition by dendritic cells: intestinal dendritic cells acquire antigen administered orally and can prime naive T cells in vivo. *The Journal of experimental medicine* **177**, 1299-1307 (1993).
- 2 Janeway's immunobiology. *Choice: Current Reviews for Academic Libraries* **45**, 1793-1794 (2008).
- 3 Tang, D., Kang, R., Coyne, C. B., Zeh, H. J. & Lotze, M. T. PAMPs and DAMPs: signals that spur autophagy and immunity. *Immunological reviews* **249**, 158-175, doi:10.1111/j.1600-065X.2012.01146.x (2012).
- 4 Huotari, J. & Helenius, A. Endosome maturation. *The EMBO journal* **30**, 3481-3500, doi:10.1038/emboj.2011.286 (2011).
- 5 Watts, C. The exogenous pathway for antigen presentation on major histocompatibility complex class II and CD1 molecules. *Nature immunology* **5**, 685-692, doi:10.1038/ni1088 (2004).
- 6 Tan, M. C. *et al.* Mannose receptor-mediated uptake of antigens strongly enhances HLA class II-restricted antigen presentation by cultured dendritic cells. *European journal of immunology* **27**, 2426-2435, doi:10.1002/eji.1830270942 (1997).
- 7 Blum, J. S., Wearsch, P. A. & Cresswell, P. Pathways of antigen processing. *Annual review of immunology* **31**, 443-473, doi:10.1146/annurev-immunol-032712-095910 (2013).
- 8 Albert, M. L. *et al.* Immature dendritic cells phagocytose apoptotic cells via alpha5beta1 and CD36, and cross-present antigens to cytotoxic T lymphocytes. *The Journal of experimental medicine* **188**, 1359-1368 (1998).
- 9 Sauter, B. *et al.* Consequences of cell death: exposure to necrotic tumor cells, but not primary tissue cells or apoptotic cells, induces the maturation of immunostimulatory dendritic cells. *The Journal of experimental medicine* **191**, 423-434 (2000).

- 10 Harshyne, L. A., Watkins, S. C., Gambotto, A. & Barratt-Boyes, S. M. Dendritic cells acquire antigens from live cells for cross-presentation to CTL. *Journal of immunology* **166**, 3717-3723 (2001).
- 11 Burgdorf, S. & Kurts, C. Endocytosis mechanisms and the cell biology of antigen presentation. *Current opinion in immunology* **20**, 89-95, doi:10.1016/j.coi.2007.12.002 (2008).
- 12 Steinman, R. M. & Cohn, Z. A. Identification of a novel cell type in peripheral lymphoid organs of mice. I. Morphology, quantitation, tissue distribution. *The Journal of experimental medicine* **137**, 1142-1162 (1973).
- 13 Crowley, M., Inaba, K., Witmer-Pack, M. & Steinman, R. M. The cell surface of mouse dendritic cells: FACS analyses of dendritic cells from different tissues including thymus. *Cellular immunology* **118**, 108-125 (1989).
- 14 Vremec, D. *et al.* The surface phenotype of dendritic cells purified from mouse thymus and spleen: investigation of the CD8 expression by a subpopulation of dendritic cells. *The Journal of experimental medicine* **176**, 47-58 (1992).
- 15 Bursch, L. S. *et al.* Identification of a novel population of Langerin+ dendritic cells. *The Journal of experimental medicine* **204**, 3147-3156, doi:10.1084/jem.20071966 (2007).
- 16 del Rio, M. L., Rodriguez-Barbosa, J. I., Kremmer, E. & Forster, R. CD103- and CD103+ bronchial lymph node dendritic cells are specialized in presenting and cross-presenting innocuous antigen to CD4+ and CD8+ T cells. *Journal of immunology* **178**, 6861-6866 (2007).
- 17 Aliberti, J. *et al.* Essential role for ICSBP in the in vivo development of murine CD8alpha + dendritic cells. *Blood* **101**, 305-310, doi:10.1182/blood-2002-04-1088 (2003).
- 18 Ginhoux, F. *et al.* The origin and development of nonlymphoid tissue CD103+ DCs. *The Journal of experimental medicine* **206**, 3115-3130, doi:10.1084/jem.20091756 (2009).
- 19 Hacker, C. *et al.* Transcriptional profiling identifies Id2 function in dendritic cell development. *Nature immunology* **4**, 380-386, doi:10.1038/ni903 (2003).
- 20 Hildner, K. *et al.* Batf3 deficiency reveals a critical role for CD8alpha+ dendritic cells in cytotoxic T cell immunity. *Science* **322**, 1097-1100, doi:10.1126/science.1164206 (2008).
- 21 Kashiwada, M., Pham, N. L., Pewe, L. L., Harty, J. T. & Rothman, P. B. NFIL3/E4BP4 is a key transcription factor for CD8alpha(+) dendritic cell development. *Blood* **117**, 6193-6197, doi:10.1182/blood-2010-07-295873 (2011).

- 22 den Haan, J. M., Lehar, S. M. & Bevan, M. J. CD8(+) but not CD8(-) dendritic cells cross-prime cytotoxic T cells in vivo. *The Journal of experimental medicine* **192**, 1685-1696 (2000).
- 23 Bedoui, S. *et al.* Cross-presentation of viral and self antigens by skin-derived CD103+ dendritic cells. *Nature immunology* **10**, 488-495, doi:10.1038/ni.1724 (2009).
- 24 Reis e Sousa, C. *et al.* In vivo microbial stimulation induces rapid CD40 ligand-independent production of interleukin 12 by dendritic cells and their redistribution to T cell areas. *The Journal of experimental medicine* **186**, 1819-1829 (1997).
- 25 Wu, L. *et al.* RelB is essential for the development of myeloid-related CD8alpha-dendritic cells but not of lymphoid-related CD8alpha+ dendritic cells. *Immunity* **9**, 839-847 (1998).
- 26 Lewis, K. L. *et al.* Notch2 receptor signaling controls functional differentiation of dendritic cells in the spleen and intestine. *Immunity* **35**, 780-791, doi:10.1016/j.immuni.2011.08.013 (2011).
- 27 Caton, M. L., Smith-Raska, M. R. & Reizis, B. Notch-RBP-J signaling controls the homeostasis of CD8- dendritic cells in the spleen. *The Journal of experimental medicine* **204**, 1653-1664, doi:10.1084/jem.20062648 (2007).
- 28 Ichikawa, E. *et al.* Defective development of splenic and epidermal CD4+ dendritic cells in mice deficient for IFN regulatory factor-2. *Proceedings of the National Academy of Sciences of the United States of America* **101**, 3909-3914, doi:10.1073/pnas.0400610101 (2004).
- 29 Suzuki, S. *et al.* Critical roles of interferon regulatory factor 4 in CD11bhighCD8alpha-dendritic cell development. *Proceedings of the National Academy of Sciences of the United States of America* **101**, 8981-8986, doi:10.1073/pnas.0402139101 (2004).
- 30 Dudziak, D. *et al.* Differential antigen processing by dendritic cell subsets in vivo. *Science* **315**, 107-111, doi:10.1126/science.1136080 (2007).
- 31 Cisse, B. *et al.* Transcription factor E2-2 is an essential and specific regulator of plasmacytoid dendritic cell development. *Cell* **135**, 37-48, doi:10.1016/j.cell.2008.09.016 (2008).
- 32 Ghosh, H. S., Cisse, B., Bunin, A., Lewis, K. L. & Reizis, B. Continuous expression of the transcription factor e2-2 maintains the cell fate of mature plasmacytoid dendritic cells. *Immunity* **33**, 905-916, doi:10.1016/j.immuni.2010.11.023 (2010).

- 33 Nakano, H., Yanagita, M. & Gunn, M. D. CD11c(+)B220(+)Gr-1(+) cells in mouse lymph nodes and spleen display characteristics of plasmacytoid dendritic cells. *The Journal of experimental medicine* **194**, 1171-1178 (2001).
- 34 Siegal, F. P. *et al.* The nature of the principal type 1 interferon-producing cells in human blood. *Science* **284**, 1835-1837 (1999).
- 35 Serbina, N. V., Salazar-Mather, T. P., Biron, C. A., Kuziel, W. A. & Pamer, E. G. TNF/iNOS-producing dendritic cells mediate innate immune defense against bacterial infection. *Immunity* **19**, 59-70 (2003).
- 36 Sallusto, F. & Lanzavecchia, A. Efficient presentation of soluble antigen by cultured human dendritic cells is maintained by granulocyte/macrophage colony-stimulating factor plus interleukin 4 and downregulated by tumor necrosis factor alpha. *The Journal of experimental medicine* **179**, 1109-1118 (1994).
- 37 Romani, N. *et al.* Presentation of exogenous protein antigens by dendritic cells to T cell clones. Intact protein is presented best by immature, epidermal Langerhans cells. *The Journal of experimental medicine* **169**, 1169-1178 (1989).
- 38 Romani, N., Brunner, P. M. & Stingl, G. Changing views of the role of Langerhans cells. *The Journal of investigative dermatology* **132**, 872-881, doi:10.1038/jid.2011.437 (2012).
- 39 Hoeffel, G. *et al.* Adult Langerhans cells derive predominantly from embryonic fetal liver monocytes with a minor contribution of yolk sac-derived macrophages. *The Journal of experimental medicine* **209**, 1167-1181, doi:10.1084/jem.20120340 (2012).
- 40 Miller, J. C. *et al.* Deciphering the transcriptional network of the dendritic cell lineage. *Nature immunology* **13**, 888-899, doi:10.1038/ni.2370 (2012).
- 41 Henri, S. *et al.* CD207+ CD103+ dermal dendritic cells cross-present keratinocyte-derived antigens irrespective of the presence of Langerhans cells. *The Journal of experimental medicine* **207**, 189-206, doi:10.1084/jem.20091964 (2010).
- 42 Tamoutounour, S. *et al.* Origins and functional specialization of macrophages and of conventional and monocyte-derived dendritic cells in mouse skin. *Immunity* **39**, 925-938, doi:10.1016/j.immuni.2013.10.004 (2013).
- 43 Steinman, R. M. Decisions about dendritic cells: past, present, and future. *Annual review of immunology* **30**, 1-22, doi:10.1146/annurev-immunol-100311-102839 (2012).
- 44 Forster, R., Braun, A. & Worbs, T. Lymph node homing of T cells and dendritic cells via afferent lymphatics. *Trends in immunology* **33**, 271-280, doi:10.1016/j.it.2012.02.007 (2012).

- 45 Tang, A., Amagai, M., Granger, L. G., Stanley, J. R. & Udey, M. C. Adhesion of epidermal Langerhans cells to keratinocytes mediated by E-cadherin. *Nature* **361**, 82-85, doi:10.1038/361082a0 (1993).
- 46 Jiang, A. *et al.* Disruption of E-cadherin-mediated adhesion induces a functionally distinct pathway of dendritic cell maturation. *Immunity* **27**, 610-624, doi:10.1016/j.immuni.2007.08.015 (2007).
- 47 Ratzinger, G. *et al.* Matrix metalloproteinases 9 and 2 are necessary for the migration of Langerhans cells and dermal dendritic cells from human and murine skin. *Journal of immunology* **168**, 4361-4371 (2002).
- 48 Ouwehand, K. *et al.* CXCL12 is essential for migration of activated Langerhans cells from epidermis to dermis. *European journal of immunology* **38**, 3050-3059, doi:10.1002/eji.200838384 (2008).
- 49 Coquet, J. M., Rausch, L. & Borst, J. The importance of co-stimulation in the orchestration of T helper cell differentiation. *Immunology and cell biology* **93**, 780-788, doi:10.1038/icb.2015.45 (2015).
- 50 Miro, F. *et al.* T cell-dependent activation of dendritic cells requires IL-12 and IFN-gamma signaling in T cells. *Journal of immunology* **177**, 3625-3634 (2006).
- 51 Murphy, K. M. *et al.* Signaling and transcription in T helper development. *Annual review of immunology* **18**, 451-494, doi:10.1146/annurev.immunol.18.1.451 (2000).
- 52 Zhu, J. & Paul, W. E. CD4 T cells: fates, functions, and faults. *Blood* **112**, 1557-1569, doi:10.1182/blood-2008-05-078154 (2008).
- 53 Lafaille, J. J. The role of helper T cell subsets in autoimmune diseases. *Cytokine & growth factor reviews* **9**, 139-151 (1998).
- 54 Lighvani, A. A. *et al.* T-bet is rapidly induced by interferon-gamma in lymphoid and myeloid cells. *Proceedings of the National Academy of Sciences of the United States of America* **98**, 15137-15142, doi:10.1073/pnas.261570598 (2001).
- 55 MacDonald, A. S. & Maizels, R. M. Alarming dendritic cells for Th2 induction. *The Journal of experimental medicine* **205**, 13-17, doi:10.1084/jem.20072665 (2008).
- 56 Webb, G. J., Hirschfield, G. M. & Lane, P. J. OX40, OX40L and Autoimmunity: a Comprehensive Review. *Clinical reviews in allergy & immunology* **50**, 312-332, doi:10.1007/s12016-015-8498-3 (2016).

- 57 Everts, B. *et al.* Migratory CD103+ dendritic cells suppress helminth-driven type 2 immunity through constitutive expression of IL-12. *The Journal of experimental medicine* **213**, 35-51, doi:10.1084/jem.20150235 (2016).
- 58 Walker, J. A. & McKenzie, A. N. J. TH2 cell development and function. *Nature reviews. Immunology* **18**, 121-133, doi:10.1038/nri.2017.118 (2018).
- 59 Yagi, R., Zhu, J. & Paul, W. E. An updated view on transcription factor GATA3-mediated regulation of Th1 and Th2 cell differentiation. *International immunology* **23**, 415-420, doi:10.1093/intimm/dxr029 (2011).
- 60 Wynn, T. A. Fibrotic disease and the T(H)1/T(H)2 paradigm. *Nature reviews. Immunology* **4**, 583-594, doi:10.1038/nri1412 (2004).
- 61 Kaiko, G. E., Horvat, J. C., Beagley, K. W. & Hansbro, P. M. Immunological decision-making: how does the immune system decide to mount a helper T-cell response? *Immunology* **123**, 326-338, doi:10.1111/j.1365-2567.2007.02719.x (2008).
- 62 Weaver, C. T., Harrington, L. E., Mangan, P. R., Gavrieli, M. & Murphy, K. M. Th17: an effector CD4 T cell lineage with regulatory T cell ties. *Immunity* **24**, 677-688, doi:10.1016/j.immuni.2006.06.002 (2006).
- 63 Kushwah, R. & Hu, J. Role of dendritic cells in the induction of regulatory T cells. *Cell & bioscience* **1**, 20, doi:10.1186/2045-3701-1-20 (2011).
- 64 Vignali, D. A., Collison, L. W. & Workman, C. J. How regulatory T cells work. *Nature reviews. Immunology* **8**, 523-532, doi:10.1038/nri2343 (2008).
- 65 Morris, P. J. Transplantation--a medical miracle of the 20th century. *The New England journal of medicine* **351**, 2678-2680, doi:10.1056/NEJMp048256 (2004).
- 66 Watson, C. J. & Dark, J. H. Organ transplantation: historical perspective and current practice. *British journal of anaesthesia* **108 Suppl 1**, i29-42, doi:10.1093/bja/aer384 (2012).
- 67 Azzi, J. R., Sayegh, M. H. & Mallat, S. G. Calcineurin inhibitors: 40 years later, can't live without. *Journal of immunology* **191**, 5785-5791, doi:10.4049/jimmunol.1390055 (2013).
- 68 Waldner, M., Fantus, D., Solari, M. & Thomson, A. W. New perspectives on mTOR inhibitors (rapamycin, rapalogs and TORKinibs) in transplantation. *British journal of clinical pharmacology* **82**, 1158-1170, doi:10.1111/bcp.12893 (2016).

- 69 Staatz, C. E. & Tett, S. E. Clinical pharmacokinetics and pharmacodynamics of mycophenolate in solid organ transplant recipients. *Clinical pharmacokinetics* **46**, 13-58, doi:10.2165/00003088-200746010-00002 (2007).
- 70 Nashan, B. Antibody induction therapy in renal transplant patients receiving calcineurin-inhibitor immunosuppressive regimens: a comparative review. *BioDrugs : clinical immunotherapeutics, biopharmaceuticals and gene therapy* **19**, 39-46 (2005).
- 71 Vincenti, F. *et al.* Belatacept and Long-Term Outcomes in Kidney Transplantation. *The New England journal of medicine* **374**, 333-343, doi:10.1056/NEJMoa1506027 (2016).
- 72 Chen, Y. B., Kawai, T. & Spitzer, T. R. Combined Bone Marrow and Kidney Transplantation for the Induction of Specific Tolerance. *Advances in hematology* **2016**, 6471901, doi:10.1155/2016/6471901 (2016).
- 73 Garakani, R. & Saidi, R. F. Recent Progress in Cell Therapy in Solid Organ Transplantation. *International journal of organ transplantation medicine* **8**, 125-131 (2017).
- 74 Geissler, E. K. The ONE Study compares cell therapy products in organ transplantation: introduction to a review series on suppressive monocyte-derived cells. *Transplantation research* **1**, 11, doi:10.1186/2047-1440-1-11 (2012).
- 75 Tanriover, B. *et al.* Acute Rejection Rates and Graft Outcomes According to Induction Regimen among Recipients of Kidneys from Deceased Donors Treated with Tacrolimus and Mycophenolate. *Clinical journal of the American Society of Nephrology : CJASN* **11**, 1650-1661, doi:10.2215/CJN.13171215 (2016).
- 76 Tushla, L. E. *When a transplant fails*, <[https://www.kidney.org/transplantation/transaction/TC/summer09/TCsm09\\_Transplant Fails](https://www.kidney.org/transplantation/transaction/TC/summer09/TCsm09_Transplant_Fails)> (2015).
- 77 Sharing, U. N. f. O. (2018).
- 78 Guertin, D. A. & Sabatini, D. M. The pharmacology of mTOR inhibition. *Science signaling* **2**, pe24, doi:10.1126/scisignal.267pe24 (2009).
- 79 Laplante, M. & Sabatini, D. M. mTOR signaling at a glance. *Journal of cell science* **122**, 3589-3594, doi:10.1242/jcs.051011 (2009).
- 80 Laplante, M. & Sabatini, D. M. mTOR signaling in growth control and disease. *Cell* **149**, 274-293, doi:10.1016/j.cell.2012.03.017 (2012).

- 81 Powell, J. D., Pollizzi, K. N., Heikamp, E. B. & Horton, M. R. Regulation of immune responses by mTOR. *Annual review of immunology* **30**, 39-68, doi:10.1146/annurev-immunol-020711-075024 (2012).
- 82 Everts, B. *et al.* Commitment to glycolysis sustains survival of NO-producing inflammatory dendritic cells. *Blood* **120**, 1422-1431, doi:10.1182/blood-2012-03-419747 (2012).
- 83 Sarbassov, D. D. *et al.* Rictor, a novel binding partner of mTOR, defines a rapamycin-insensitive and raptor-independent pathway that regulates the cytoskeleton. *Current biology : CB* **14**, 1296-1302, doi:10.1016/j.cub.2004.06.054 (2004).
- 84 Bhaskar, P. T. & Hay, N. The two TORCs and Akt. *Developmental cell* **12**, 487-502, doi:10.1016/j.devcel.2007.03.020 (2007).
- 85 Gan, X., Wang, J., Su, B. & Wu, D. Evidence for direct activation of mTORC2 kinase activity by phosphatidylinositol 3,4,5-trisphosphate. *The Journal of biological chemistry* **286**, 10998-11002, doi:10.1074/jbc.M110.195016 (2011).
- 86 Gaubitz, C., Prouteau, M., Kusmider, B. & Loewith, R. TORC2 Structure and Function. *Trends in biochemical sciences* **41**, 532-545, doi:10.1016/j.tibs.2016.04.001 (2016).
- 87 Brown, J., Wang, H., Suttles, J., Graves, D. T. & Martin, M. Mammalian target of rapamycin complex 2 (mTORC2) negatively regulates Toll-like receptor 4-mediated inflammatory response via FoxO1. *The Journal of biological chemistry* **286**, 44295-44305, doi:10.1074/jbc.M111.258053 (2011).
- 88 Raich-Regue, D. *et al.* mTORC2 Deficiency in Myeloid Dendritic Cells Enhances Their Allogeneic Th1 and Th17 Stimulatory Ability after TLR4 Ligation In Vitro and In Vivo. *Journal of immunology*, doi:10.4049/jimmunol.1402551 (2015).
- 89 Rosborough, B. R. *et al.* Murine dendritic cell rapamycin-resistant and rictor-independent mTOR controls IL-10, B7-H1, and regulatory T-cell induction. *Blood* **121**, 3619-3630, doi:10.1182/blood-2012-08-448290 (2013).
- 90 Raich-Regue, D. *et al.* Intratumoral delivery of mTORC2-deficient dendritic cells inhibits B16 melanoma growth by promoting CD8(+) effector T cell responses. *Oncimmunology* **5**, e1146841, doi:10.1080/2162402X.2016.1146841 (2016).
- 91 Warburg, O. On the origin of cancer cells. *Science* **123**, 309-314 (1956).
- 92 Krawczyk, C. M. *et al.* Toll-like receptor-induced changes in glycolytic metabolism regulate dendritic cell activation. *Blood* **115**, 4742-4749, doi:10.1182/blood-2009-10-249540 (2010).

- 93 Everts, B. *et al.* TLR-driven early glycolytic reprogramming via the kinases TBK1-IKK $\epsilon$  supports the anabolic demands of dendritic cell activation. *Nature immunology* **15**, 323-332, doi:10.1038/ni.2833 (2014).
- 94 van der Windt, G. J. *et al.* Mitochondrial respiratory capacity is a critical regulator of CD8<sup>+</sup> T cell memory development. *Immunity* **36**, 68-78, doi:10.1016/j.immuni.2011.12.007 (2012).
- 95 Maroof, A., English, N. R., Bedford, P. A., Gabrilovich, D. I. & Knight, S. C. Developing dendritic cells become 'lacy' cells packed with fat and glycogen. *Immunology* **115**, 473-483, doi:10.1111/j.1365-2567.2005.02181.x (2005).
- 96 Bettencourt, I. A. & Powell, J. D. Targeting Metabolism as a Novel Therapeutic Approach to Autoimmunity, Inflammation, and Transplantation. *Journal of immunology* **198**, 999-1005, doi:10.4049/jimmunol.1601318 (2017).
- 97 Byersdorfer, C. A. *et al.* Effector T cells require fatty acid metabolism during murine graft-versus-host disease. *Blood* **122**, 3230-3237, doi:10.1182/blood-2013-04-495515 (2013).
- 98 Lee, C. F. *et al.* Preventing Allograft Rejection by Targeting Immune Metabolism. *Cell reports* **13**, 760-770, doi:10.1016/j.celrep.2015.09.036 (2015).
- 99 Lee, K. *et al.* Mammalian target of rapamycin protein complex 2 regulates differentiation of Th1 and Th2 cell subsets via distinct signaling pathways. *Immunity* **32**, 743-753, doi:10.1016/j.immuni.2010.06.002 (2010).
- 100 Laboratory, T. J. <<https://www.jax.org/strain/008068>> (
- 101 Suśruta, Bhaṭṭācārya, E. E., Aśvatthanārāyaṇa, E. & University of Mysore. Prasārāṅga. *Suśruta saṃhitā*.
- 102 Snell, G. D. Methods for the study of histocompatibility genes. *Journal of genetics* **49**, 87-108 (1948).
- 103 Medawar, P. B. The behaviour and fate of skin autografts and skin homografts in rabbits: A report to the War Wounds Committee of the Medical Research Council. *Journal of anatomy* **78**, 176-199 (1944).
- 104 Medawar, P. B. A second study of the behaviour and fate of skin homografts in rabbits; a report to the War Wounds Committee of the Medical Research Council. *Journal of anatomy* **79**, 157-176 (1945).

- 105 Benichou, G. *et al.* Immune recognition and rejection of allogeneic skin grafts. *Immunotherapy* **3**, 757-770, doi:10.2217/imt.11.2 (2011).
- 106 Bergstresser, P. R., Toews, G. B., Gilliam, J. N. & Streilein, J. W. Unusual numbers and distribution of Langerhans cells in skin with unique immunologic properties. *The Journal of investigative dermatology* **74**, 312-314 (1980).
- 107 Fernandes, E. *et al.* The role of direct presentation by donor dendritic cells in rejection of minor histocompatibility antigen-mismatched skin and hematopoietic cell grafts. *Transplantation* **91**, 154-160, doi:10.1097/TP.0b013e318201ac27 (2011).
- 108 Ehst, B. D., Ingulli, E. & Jenkins, M. K. Development of a novel transgenic mouse for the study of interactions between CD4 and CD8 T cells during graft rejection. *American journal of transplantation : official journal of the American Society of Transplantation and the American Society of Transplant Surgeons* **3**, 1355-1362 (2003).
- 109 Ratschiller, T. *et al.* Heterotopic Cervical Heart Transplantation in Mice. *Journal of visualized experiments : JoVE*, e52907, doi:10.3791/52907 (2015).
- 110 Delgoffe, G. M. *et al.* The kinase mTOR regulates the differentiation of helper T cells through the selective activation of signaling by mTORC1 and mTORC2. *Nature immunology* **12**, 295-303, doi:10.1038/ni.2005 (2011).
- 111 Pollizzi, K. N. *et al.* mTORC1 and mTORC2 selectively regulate CD8(+) T cell differentiation. *The Journal of clinical investigation* **125**, 2090-2108, doi:10.1172/JCI77746 (2015).
- 112 Zhang, L. *et al.* Mammalian Target of Rapamycin Complex 2 Controls CD8 T Cell Memory Differentiation in a Foxo1-Dependent Manner. *Cell reports* **14**, 1206-1217, doi:10.1016/j.celrep.2015.12.095 (2016).
- 113 Jiang, H., Westerterp, M., Wang, C., Zhu, Y. & Ai, D. Macrophage mTORC1 disruption reduces inflammation and insulin resistance in obese mice. *Diabetologia* **57**, 2393-2404, doi:10.1007/s00125-014-3350-5 (2014).
- 114 Ohtani, M. *et al.* Cutting edge: mTORC1 in intestinal CD11c+ CD11b+ dendritic cells regulates intestinal homeostasis by promoting IL-10 production. *Journal of immunology* **188**, 4736-4740, doi:10.4049/jimmunol.1200069 (2012).
- 115 Smyth, L. A., Lechler, R. I. & Lombardi, G. Continuous Acquisition of MHC:Peptide Complexes by Recipient Cells Contributes to the Generation of Anti-Graft CD8(+) T Cell Immunity. *American journal of transplantation : official journal of the American Society of Transplantation and the American Society of Transplant Surgeons* **17**, 60-68, doi:10.1111/ajt.13996 (2017).

- 116 Billingham, R. E., Brent, L. & Medawar, P. B. Actively acquired tolerance of foreign cells. *Nature* **172**, 603-606 (1953).
- 117 Atif, S. M. *et al.* Cutting Edge: Roles for Batf3-Dependent APCs in the Rejection of Minor Histocompatibility Antigen-Mismatched Grafts. *Journal of immunology* **195**, 46-50, doi:10.4049/jimmunol.1500669 (2015).
- 118 Fischer, S. *et al.* Acute rejection in vascularized composite allotransplantation. *Current opinion in organ transplantation* **19**, 531-544, doi:10.1097/MOT.0000000000000140 (2014).
- 119 Kanitakis, J. *et al.* Capillary Thrombosis in the Skin: A Pathologic Hallmark of Severe/Chronic Rejection of Human Vascularized Composite Tissue Allografts? *Transplantation* **100**, 954-957, doi:10.1097/TP.0000000000000882 (2016).
- 120 Maraskovsky, E. *et al.* Dramatic increase in the numbers of functionally mature dendritic cells in Flt3 ligand-treated mice: multiple dendritic cell subpopulations identified. *The Journal of experimental medicine* **184**, 1953-1962 (1996).
- 121 Eichwald, E. J. & Silmsler, C. R. Skin. *Transplantation bulletin* **2**, 148-149 (1955).
- 122 Kellersch, B. & Brocker, T. Langerhans cell homeostasis in mice is dependent on mTORC1 but not mTORC2 function. *Blood* **121**, 298-307, doi:10.1182/blood-2012-06-439786 (2013).
- 123 Ding, X. *et al.* mTORC1 and mTORC2 regulate skin morphogenesis and epidermal barrier formation. *Nature communications* **7**, 13226, doi:10.1038/ncomms13226 (2016).
- 124 Inozume, T. *et al.* Selection of CD8+PD-1+ lymphocytes in fresh human melanomas enriches for tumor-reactive T cells. *Journal of immunotherapy* **33**, 956-964, doi:10.1097/CJI.0b013e3181fad2b0 (2010).
- 125 Gros, A. *et al.* PD-1 identifies the patient-specific CD8(+) tumor-reactive repertoire infiltrating human tumors. *The Journal of clinical investigation* **124**, 2246-2259, doi:10.1172/JCI73639 (2014).
- 126 Wherry, E. J. T cell exhaustion. *Nature immunology* **12**, 492-499 (2011).
- 127 Wakil, A. E., Wang, Z. E., Ryan, J. C., Fowell, D. J. & Locksley, R. M. Interferon gamma derived from CD4(+) T cells is sufficient to mediate T helper cell type 1 development. *The Journal of experimental medicine* **188**, 1651-1656 (1998).

- 128 Tewari, K., Nakayama, Y. & Suresh, M. Role of direct effects of IFN-gamma on T cells in the regulation of CD8 T cell homeostasis. *Journal of immunology* **179**, 2115-2125 (2007).
- 129 Badiavas, E. V., Paquette, D., Carson, P. & Falanga, V. Human chronic wounds treated with bioengineered skin: histologic evidence of host-graft interactions. *Journal of the American Academy of Dermatology* **46**, 524-530 (2002).
- 130 Reksodiputro, M., Widodo, D., Bashiruddin, J., Siregar, N. & Malik, S. PRFM enhance wound healing process in skin graft. *Facial plastic surgery : FPS* **30**, 670-675, doi:10.1055/s-0034-1396527 (2014).
- 131 Youssef, A. R., Otley, C., Mathieson, P. W. & Smith, R. M. Role of CD4+ and CD8+ T cells in murine skin and heart allograft rejection across different antigenic disparities. *Transplant immunology* **13**, 297-304, doi:10.1016/j.trim.2004.10.005 (2004).
- 132 Mehrabi, A. *et al.* Wound complications following kidney and liver transplantation. *Clinical transplantation* **20 Suppl 17**, 97-110, doi:10.1111/j.1399-0012.2006.00608.x (2006).
- 133 Schaffer, M. *et al.* Sirolimus impairs wound healing. *Langenbeck's archives of surgery* **392**, 297-303, doi:10.1007/s00423-007-0174-5 (2007).
- 134 Vinish, M. *et al.* Dendritic cells modulate burn wound healing by enhancing early proliferation. *Wound repair and regeneration : official publication of the Wound Healing Society [and] the European Tissue Repair Society* **24**, 6-13, doi:10.1111/wrr.12388 (2016).
- 135 Akiba, H. *et al.* Skin inflammation during contact hypersensitivity is mediated by early recruitment of CD8+ T cytotoxic 1 cells inducing keratinocyte apoptosis. *Journal of immunology* **168**, 3079-3087 (2002).
- 136 Xu, H., Banerjee, A., Dilulio, N. A. & Fairchild, R. L. Development of effector CD8+ T cells in contact hypersensitivity occurs independently of CD4+ T cells. *Journal of immunology* **158**, 4721-4728 (1997).
- 137 Phanuphak, P., Moorhead, J. W. & Claman, H. N. Tolerance and contact sensitivity to DNFB in mice. I. In vivo detection by ear swelling and correlation with in vitro cell stimulation. *Journal of immunology* **112**, 115-123 (1974).
- 138 Kaplan, D. H., Jenison, M. C., Saeland, S., Shlomchik, W. D. & Shlomchik, M. J. Epidermal langerhans cell-deficient mice develop enhanced contact hypersensitivity. *Immunity* **23**, 611-620, doi:10.1016/j.immuni.2005.10.008 (2005).

- 139 Mathers, A. R. *et al.* Electrophilic nitro-fatty acids suppress allergic contact dermatitis in mice. *Allergy* **72**, 656-664, doi:10.1111/all.13067 (2017).
- 140 Merad, M., Ginhoux, F. & Collin, M. Origin, homeostasis and function of Langerhans cells and other langerin-expressing dendritic cells. *Nature reviews. Immunology* **8**, 935-947, doi:10.1038/nri2455 (2008).
- 141 Bour, H. *et al.* Major histocompatibility complex class I-restricted CD8+ T cells and class II-restricted CD4+ T cells, respectively, mediate and regulate contact sensitivity to dinitrofluorobenzene. *European journal of immunology* **25**, 3006-3010, doi:10.1002/eji.1830251103 (1995).
- 142 Martin, S. *et al.* Peptide immunization indicates that CD8+ T cells are the dominant effector cells in trinitrophenyl-specific contact hypersensitivity. *The Journal of investigative dermatology* **115**, 260-266, doi:10.1046/j.1523-1747.2000.00038.x (2000).
- 143 Vocanson, M. *et al.* CD8+ T cells are effector cells of contact dermatitis to common skin allergens in mice. *The Journal of investigative dermatology* **126**, 815-820, doi:10.1038/sj.jid.5700174 (2006).
- 144 Honda, T. *et al.* Compensatory role of Langerhans cells and langerin-positive dermal dendritic cells in the sensitization phase of murine contact hypersensitivity. *The Journal of allergy and clinical immunology* **125**, 1154-1156 e1152, doi:10.1016/j.jaci.2009.12.005 (2010).
- 145 Fukunaga, A., Khaskhely, N. M., Sreevidya, C. S., Byrne, S. N. & Ullrich, S. E. Dermal dendritic cells, and not Langerhans cells, play an essential role in inducing an immune response. *Journal of immunology* **180**, 3057-3064 (2008).
- 146 Igyarto, B. Z. *et al.* Langerhans cells suppress contact hypersensitivity responses via cognate CD4 interaction and langerhans cell-derived IL-10. *Journal of immunology* **183**, 5085-5093, doi:10.4049/jimmunol.0901884 (2009).
- 147 Gomez de Agüero, M. *et al.* Langerhans cells protect from allergic contact dermatitis in mice by tolerizing CD8(+) T cells and activating Foxp3(+) regulatory T cells. *The Journal of clinical investigation* **122**, 1700-1711, doi:10.1172/JCI59725 (2012).
- 148 Li, H. *et al.* Targeting of mTORC2 prevents cell migration and promotes apoptosis in breast cancer. *Breast cancer research and treatment* **134**, 1057-1066, doi:10.1007/s10549-012-2036-2 (2012).
- 149 Liu, L., Das, S., Losert, W. & Parent, C. A. mTORC2 regulates neutrophil chemotaxis in a cAMP- and RhoA-dependent fashion. *Developmental cell* **19**, 845-857, doi:10.1016/j.devcel.2010.11.004 (2010).

- 150 Riol-Blanco, L. *et al.* The chemokine receptor CCR7 activates in dendritic cells two signaling modules that independently regulate chemotaxis and migratory speed. *Journal of immunology* **174**, 4070-4080 (2005).
- 151 Pearce, E. L. Metabolism in T cell activation and differentiation. *Current opinion in immunology* **22**, 314-320, doi:10.1016/j.coi.2010.01.018 (2010).
- 152 Michalek, R. D. & Rathmell, J. C. The metabolic life and times of a T-cell. *Immunological reviews* **236**, 190-202, doi:10.1111/j.1600-065X.2010.00911.x (2010).
- 153 Jacobs, S. R., Michalek, R. D. & Rathmell, J. C. IL-7 is essential for homeostatic control of T cell metabolism in vivo. *Journal of immunology* **184**, 3461-3469, doi:10.4049/jimmunol.0902593 (2010).
- 154 Pua, H. H. & He, Y. W. Mitophagy in the little lymphocytes: an essential role for autophagy in mitochondrial clearance in T lymphocytes. *Autophagy* **5**, 745-746 (2009).
- 155 Lord, G. M. *et al.* Leptin modulates the T-cell immune response and reverses starvation-induced immunosuppression. *Nature* **394**, 897-901, doi:10.1038/29795 (1998).
- 156 Nicklin, P. *et al.* Bidirectional transport of amino acids regulates mTOR and autophagy. *Cell* **136**, 521-534, doi:10.1016/j.cell.2008.11.044 (2009).
- 157 Duvel, K. *et al.* Activation of a metabolic gene regulatory network downstream of mTOR complex 1. *Molecular cell* **39**, 171-183, doi:10.1016/j.molcel.2010.06.022 (2010).
- 158 Cunningham, J. T. *et al.* mTOR controls mitochondrial oxidative function through a YY1-PGC-1alpha transcriptional complex. *Nature* **450**, 736-740, doi:10.1038/nature06322 (2007).
- 159 Amiel, E. *et al.* Inhibition of mechanistic target of rapamycin promotes dendritic cell activation and enhances therapeutic autologous vaccination in mice. *Journal of immunology* **189**, 2151-2158, doi:10.4049/jimmunol.1103741 (2012).
- 160 Finlay, D. K. Regulation of glucose metabolism in T cells: new insight into the role of Phosphoinositide 3-kinases. *Frontiers in immunology* **3**, 247, doi:10.3389/fimmu.2012.00247 (2012).
- 161 Greiner, E. F., Guppy, M. & Brand, K. Glucose is essential for proliferation and the glycolytic enzyme induction that provokes a transition to glycolytic energy production. *The Journal of biological chemistry* **269**, 31484-31490 (1994).

- 162 Vander Heiden, M. G., Cantley, L. C. & Thompson, C. B. Understanding the Warburg effect: the metabolic requirements of cell proliferation. *Science* **324**, 1029-1033, doi:10.1126/science.1160809 (2009).
- 163 Marko, A. J., Miller, R. A., Kelman, A. & Frauwirth, K. A. Induction of glucose metabolism in stimulated T lymphocytes is regulated by mitogen-activated protein kinase signaling. *PloS one* **5**, e15425, doi:10.1371/journal.pone.0015425 (2010).
- 164 Juntilla, M. M., Wofford, J. A., Birnbaum, M. J., Rathmell, J. C. & Koretzky, G. A. Akt1 and Akt2 are required for alphabeta thymocyte survival and differentiation. *Proceedings of the National Academy of Sciences of the United States of America* **104**, 12105-12110, doi:10.1073/pnas.0705285104 (2007).
- 165 Kelly, A. P. *et al.* Notch-induced T cell development requires phosphoinositide-dependent kinase 1. *The EMBO journal* **26**, 3441-3450, doi:10.1038/sj.emboj.7601761 (2007).
- 166 Lochner, M., Berod, L. & Sparwasser, T. Fatty acid metabolism in the regulation of T cell function. *Trends in immunology* **36**, 81-91, doi:10.1016/j.it.2014.12.005 (2015).
- 167 Lo, Y. C., Lee, C. F. & Powell, J. D. Insight into the role of mTOR and metabolism in T cells reveals new potential approaches to preventing graft rejection. *Current opinion in organ transplantation* **19**, 363-371, doi:10.1097/MOT.0000000000000098 (2014).
- 168 Pearce, E. J. & Everts, B. Dendritic cell metabolism. *Nature reviews. Immunology* **15**, 18-29, doi:10.1038/nri3771 (2015).
- 169 Huang, J. & Manning, B. D. A complex interplay between Akt, TSC2 and the two mTOR complexes. *Biochemical Society transactions* **37**, 217-222, doi:10.1042/BST0370217 (2009).
- 170 Morelli, A. E. *et al.* Cytokine production by mouse myeloid dendritic cells in relation to differentiation and terminal maturation induced by lipopolysaccharide or CD40 ligation. *Blood* **98**, 1512-1523 (2001).
- 171 Ono, Y. *et al.* Graft-infiltrating PD-L1(hi) cross-dressed dendritic cells regulate antidonor T cell responses in mouse liver transplant tolerance. *Hepatology* **67**, 1499-1515, doi:10.1002/hep.29529 (2018).
- 172 Schwiebs, A. *et al.* Activation-Induced Cell Death of Dendritic Cells Is Dependent on Sphingosine Kinase 1. *Frontiers in pharmacology* **7**, 94, doi:10.3389/fphar.2016.00094 (2016).

- 173 Chen, M. *et al.* Dendritic cell apoptosis in the maintenance of immune tolerance. *Science* **311**, 1160-1164, doi:10.1126/science.1122545 (2006).
- 174 Yang, J., Huck, S. P., McHugh, R. S., Hermans, I. F. & Ronchese, F. Perforin-dependent elimination of dendritic cells regulates the expansion of antigen-specific CD8<sup>+</sup> T cells in vivo. *Proceedings of the National Academy of Sciences of the United States of America* **103**, 147-152, doi:10.1073/pnas.0509054103 (2006).
- 175 Garedew, A., Henderson, S. O. & Moncada, S. Activated macrophages utilize glycolytic ATP to maintain mitochondrial membrane potential and prevent apoptotic cell death. *Cell death and differentiation* **17**, 1540-1550, doi:10.1038/cdd.2010.27 (2010).
- 176 Pfeffer, S. R. How the Golgi works: a cisternal progenitor model. *Proceedings of the National Academy of Sciences of the United States of America* **107**, 19614-19618, doi:10.1073/pnas.1011016107 (2010).
- 177 Groenewoud, M. J. & Zwartkruis, F. J. Rheb and mammalian target of rapamycin in mitochondrial homeostasis. *Open biology* **3**, 130185, doi:10.1098/rsob.130185 (2013).
- 178 Ramanathan, A. & Schreiber, S. L. Direct control of mitochondrial function by mTOR. *Proceedings of the National Academy of Sciences of the United States of America* **106**, 22229-22232, doi:10.1073/pnas.0912074106 (2009).
- 179 Wieman, H. L., Wofford, J. A. & Rathmell, J. C. Cytokine stimulation promotes glucose uptake via phosphatidylinositol-3 kinase/Akt regulation of Glut1 activity and trafficking. *Molecular biology of the cell* **18**, 1437-1446, doi:10.1091/mbc.e06-07-0593 (2007).
- 180 Melser, S. *et al.* Rheb regulates mitophagy induced by mitochondrial energetic status. *Cell metabolism* **17**, 719-730, doi:10.1016/j.cmet.2013.03.014 (2013).
- 181 Schaller, M. D. & Parsons, J. T. Focal adhesion kinase: an integrin-linked protein tyrosine kinase. *Trends in cell biology* **3**, 258-262 (1993).
- 182 Cary, L. A. & Guan, J. L. Focal adhesion kinase in integrin-mediated signaling. *Frontiers in bioscience : a journal and virtual library* **4**, D102-113 (1999).
- 183 Johnson, S. E., Shah, N., Bajer, A. A. & LeBien, T. W. IL-7 activates the phosphatidylinositol 3-kinase/AKT pathway in normal human thymocytes but not normal human B cell precursors. *Journal of immunology* **180**, 8109-8117 (2008).
- 184 Laplante, M. & Sabatini, D. M. An emerging role of mTOR in lipid biosynthesis. *Current biology : CB* **19**, R1046-1052, doi:10.1016/j.cub.2009.09.058 (2009).

- 185 Guo, B., Huang, X., Lee, M. R., Lee, S. A. & Broxmeyer, H. E. Antagonism of PPAR-gamma signaling expands human hematopoietic stem and progenitor cells by enhancing glycolysis. *Nature medicine* **24**, 360-367, doi:10.1038/nm.4477 (2018).
- 186 Aronova, S. *et al.* Regulation of ceramide biosynthesis by TOR complex 2. *Cell metabolism* **7**, 148-158, doi:10.1016/j.cmet.2007.11.015 (2008).
- 187 Rosborough, B. R. *et al.* Adenosine triphosphate-competitive mTOR inhibitors: a new class of immunosuppressive agents that inhibit allograft rejection. *American journal of transplantation : official journal of the American Society of Transplantation and the American Society of Transplant Surgeons* **14**, 2173-2180, doi:10.1111/ajt.12799 (2014).
- 188 Fantus, D. *et al.* Influence of the Novel ATP-Competitive Dual mTORC1/2 Inhibitor AZD2014 on Immune Cell Populations and Heart Allograft Rejection. *Transplantation* **101**, 2830-2840, doi:10.1097/TP.0000000000001933 (2017).
- 189 Populo, H., Lopes, J. M. & Soares, P. The mTOR signalling pathway in human cancer. *International journal of molecular sciences* **13**, 1886-1918, doi:10.3390/ijms13021886 (2012).
- 190 Pardoll, D. M. The blockade of immune checkpoints in cancer immunotherapy. *Nature reviews. Cancer* **12**, 252-264, doi:10.1038/nrc3239 (2012).
- 191 Langdon, S. *et al.* Combination of dual mTORC1/2 inhibition and immune-checkpoint blockade potentiates anti-tumour immunity. *Oncoimmunology* **7**, e1458810, doi:10.1080/2162402X.2018.1458810 (2018).
- 192 Lamming, D. W. *et al.* Rapamycin-induced insulin resistance is mediated by mTORC2 loss and uncoupled from longevity. *Science* **335**, 1638-1643, doi:10.1126/science.1215135 (2012).
- 193 Dai, H. *et al.* Rictor deficiency in dendritic cells exacerbates acute kidney injury. *Kidney international* **94**, 951-963, doi:10.1016/j.kint.2018.06.010 (2018).
- 194 Liu, P. *et al.* PtdIns(3,4,5)P3-Dependent Activation of the mTORC2 Kinase Complex. *Cancer discovery* **5**, 1194-1209, doi:10.1158/2159-8290.CD-15-0460 (2015).
- 195 Zeng, H. & Chi, H. mTOR signaling in the differentiation and function of regulatory and effector T cells. *Current opinion in immunology* **46**, 103-111, doi:10.1016/j.coi.2017.04.005 (2017).
- 196 Ebner, M., Sinkovics, B., Szczygiel, M., Ribeiro, D. W. & Yudushkin, I. Localization of mTORC2 activity inside cells. *The Journal of cell biology* **216**, 343-353, doi:10.1083/jcb.201610060 (2017).